Development and Implementation of a Reliable Decision Fusion and Pattern Recognition System for Object Detection and Condition Monitoring

Von der Fakultät für Ingenieurwissenschaften,
Abteilung Maschinenbau und Verfahrenstechnik
der
Universität Duisburg-Essen
zur Erlangung des akademischen Grades
eines
Doktors der Ingenieurwissenschaften
Dr.-Ing.
genehmigte Dissertation

von

Lou'i Al-Shrouf, M.Sc.
aus
Hebron, Palästina

Gutachter: Univ.-Prof. Dr.-Ing. Dirk Söffker
Univ.-Prof. Dr.-Ing. Claus-Peter Fritzen
Tag der mündlichen Prüfung: 04. Juli 2014

Dedicated to

the memory of my father Ragheb Al-Shrouf,

my mother Fatima Al-Shrouf,

brothers and sisters,

and

my wife

Acknowledgement

First, I would like to thank Univ-.Prof. Dr.-Ing. Dirk Söffker for his powerful supervision during my work and for his helpful social support.

I am also thankful to Univ.-Prof. Dr.-Ing. Claus-Peter Fritzen for his effort as second supervisor.

I am also grateful to my colleagues at RWE Power AG, opencast mine garzweiler (Nina Szczepanski, Georg-Wilhelm Küppers, Adam Lebede, Ulrich Nies, Heinrich Ewerts, Frank Fliegen, Hermann-Josef Lugt, Bernd Steinbach, Patrick Schulz, Andreas Owsjannikow, and Christian Galyo) for their powerful and helpful support during the cooperation project "Feature-based multi sensor fusion system for object and stone recognition".

I would also like to thank my committee members of the chair of dynamics and control at University of Duisburg-Essen for their academical and social support; my thanks also for the students who worked with me in the project for their helpful contribution.

Special thanks to my family in my homeland Palestine, to my wife, and friends for their encouragement and support.

Duisburg, August 2014 Lou'i Al-Shrouf

Abstract

A monitoring task of production system (bucket-wheel excavator) is investigated for the development and realization of a multisensor-based monitoring system. The objective of the monitoring system is to obtain in real time reliable decisions on the presence of target objects (large stones) in the transported material during the production process to avoid disturbances or failures of the transportation process. Due to the complexity of the considered production system, different physical effects are used for the development of the multisensor-based monitoring system. The measured signals are acquired using different sensors (five acceleration sensors, two load cells, and a laser scanner). Due to the inevitable and varying time shift between the stimulations of the individual sensors, each signal is individually subjected to preprocessing, feature extraction, and classification process.

The proposed monitoring system consists of three modules: acceleration, laser scanner, and decision fusion modules. For the acceleration module which uses acceleration signals of five different acceleration sensors, two detection approaches are developed. The first approach (STFT-SVM) is based on Short-Time Fourier Transform (STFT) as feature extraction tool, Support Vector Machine (SVM) for the classification, and a novel decision fusion process to fuse the individual decisions. The second approach (CWT-SVM) is based Continuous Wavelet Transform (CWT) as feature extraction tool, Support Vector Machine (SVM) for the classification, and a rule-based decision fusion process to fuse the individual decisions. Both approaches are trained, validated, and tested using real industrial data. The developed approaches show strong improvements in detection and false alarm rates. Due to the implementation complexity and the high number of false alarms of the STFT-SVM approach in comparison to the CWT-SVM approach, the CWT-SVM-based approach is chosen for the development of the overall monitoring system.

The Laser scanner module which processes the laser scanner signal consists of prefiltering, filtering, validation, and classification process. The module is validated, and successfully tested on real industrial data.

The decision fusion module fuses the decisions of both detection modules in order to obtain a final reliable decision. Three fusion techniques are investigated, which are OR-logic, Bayesian Combination Rule (BCR), and the new developed decision fusion technique Basic Belief Fusion (BBF). Due to the characteristics of the considered application, the OR-Logic is chosen to perform the fusion task.

For the online realization, the weightometer module is added to avoid false alarms which could be caused by acceleration module. Additionally modifications and simplification processes are performed in order to overcome the hardware limitations

The proposed monitoring approach is developed for online and real time implementation, and it achieves high detection rate, with minimum false alarms rate, thus the production process disturbance is minimized.

Contents

List of figures

List of tables

Nomenclature

Symbol	Meaning
a	Scale parameter
b_0	Numeric parameter
Beg_{Ob}	Index of the scan profile, which is considered as the beginning of an object in the running direction of the transport belt
$bel(Neg.)$	Degree of belief that the decision is negative
$bel(Pos.)$	Degree of belief that the decision is positive
$bel(Z_1)$	Degree of belief that the decision is Z_1
$bel(Z_2)$	Degree of belief that the decision is Z_1
$bel(Z_3)$	Degree of uncertainty
C	Penalty parameter
C_1	Class 1
C_2	Class 2
cl^k	Classifier number k
CM^k	Confusion matrix of classifier k
D_1, D_2, D_3	Threshold values
End_{Ob}	Index of the scan profile, which is considered as the end of an object in the running direction of the transport belt
$f(t)$	Simplified cross-sectional area
$f_w(i)$	simplified cross-sectional area (transverse to the running direction of the transport belt) for the selected scan profiles
Fp	The index of the first relevant measurement point of the scan profile
FP	False positive
$g(t)$	Window function
h	Polynomial kernel of degree
h_1	Hypothesis 1 (specific event)
h_2	Hypothesis 2 (no specific event)
h_3	Hypothesis 3 (uncertain)
H_p	Average protruding height of the considered object relative to the average height of the neighboring area
H_p	Average protruding height of the considered object relative to the the laser scanner
i	Running index (describes the number of the measurement point within a scan profile and thus extends transverse to the running direction of the transport belt)
i_{Begin}	Index of the scan profile, which is considered as the beginning of the object transverse to the running direction of the transport belt
i_{End}	Index of the scan profile, which is considered as the end of the object transverse to the running direction of the transport belt
k	Classifier number
l	Total number of the support vectors

Symbol	**Meaning**
Lp	The index of the last relevant measurement point of the scan profile
M	Number of the considered classes
$m(cl_1^k)$	Degree of belief that the classified pattern x belongs to class 1 (C_1) if it is assigned by the classifier cl^k as class C_i
$m(cl_2^k)$	Degree of belief that the classified pattern x belongs to class 2 (C_2) if it is assigned by the classifier cl^k as class C_i
$m(cl_3^k)$	Degree of uncertainty
n	Number of the scan profiles within the sliding moving window
N	Window length
$S(t)$	The change of the simplified cross-sectional area vector (for length determination)
$S_s(t)$	The smoothed $S(t)$ vector
$S_w(i)$	The change of the simplified cross-sectional area vector (for width determination)
$S_{wr}(i)$	The change of the simplified cross-sectional area vector relative to the neighboring area
t	Running index (describes the serial number of the scan profiles, which extends longitudinally to the running direction of the transport belt, and can also be considered as time running index)
T_1, T_2	Threshold values
T_s	Required time for generating each scan profile by the laser scanner
TN	True negative
TP	True positive
V_{Belt}	The velocity of the transport belt
x	Data point (single pattern)
$x(t)$	Time series signal
x_j	Value of the hidden and output neurons j
X_i	Support vector
X^T	Unknown test data point
y	Class label
y_i	Class label
W	Weighting vector
w_{ji}	Weighting factor of the connection between the neurons i and j
$z(t,i)$	The vertical distance of the measurement point i of the scan profile t from the laser scanner (in Cartesian coordinates)
α_i	Numeric parameter
ω	Hypothesis set
$\psi(t)$	Wavelet function
σ	Standard deviation of the Gaussian window
τ	Time shift

Important abbreviations

Symbol	Meaning
Acc.	Acceleration/acceleration module
ANNs	Artificial Neural Networks
BBF	Basic Belief Fusion
BCR	Bayesian Combination Rule
BKS	Behavior Knowledge Space
CWT	Continuous Wavelet Transform
DB2	Daubechies wavelet 2
DB4	Daubechies wavelet 4
DST	Dempster-Shafer Theory
DWT	Discrete Wavelet Transform
ICA	Independent Component Analysis
k-NN	k-Nearest-Neighbor classifiers
Las.	Laser scanner module
Neg.	No specific event exists (negative decision)
NN	Neural Network
MLP	Multilayer Perceptron
MMH	Maximum Marginal Hyperplane
PCA	Principle Component Analysis
Pos.	Specific event exists (positive decision)
Re	Reliability
STFT	Short Time Fourier Transform
SVM	Support Vector Machine
LDA	Linear Discriminant Analysis
WVD	Wigner-Ville Distribution

1 Introduction

This chapter introduces the motivation and the objectives of this work. The description of the investigated production process and the related scope of the art are presented in this chapter.

During the progress of this work, parts of this chapter have been published in [ASSSS11, ASSSS12, ASSS13].

1.1 Motivation

Monitoring and supervision systems are essential for the automation of industrial processes. Individual process-related variables are usually considered and thresholds are defined and used to distinguish regular and abnormal operations. In addition, abnormal conditions need to be identified for fault detection and diagnostic tasks. Such methods are not generally applicable for highly complex systems because the multidimensionality and interrelations involved cannot be handled by low-dimensional approaches that use classical thresholds.

Model-based monitoring systems are often not suitable for complex systems because precise models of the mechanical system considered are required for reliable monitoring. Model-based methods usually require complex modeling of the process with detailed process parameters and additional information on changes in the system states.

Signal-based diagnostic methods are based on the analysis of measured (physical) signals. They are useful when the measured variables contain direct or implicit information about possible faulty behavior. Signal-based diagnostic methods are easy to use and are widely adopted to extract relevant process characteristics from analyzed sensor data in combination with further knowledge.

Feature extraction can be performed in either the time or frequency domain of the signal. The extracted features should be able to represent the regular state of the system, as well as non-regular behaviors. In other words, they should indicate changes in system state. Thus, signal-based methods when combined with machine learning techniques can be used to distinguish system states.

Depending on the machine and process complexity, suitable sensors have to be used to define suitable mappings between machine operating states and sensor data. Moreover, for specific complex systems, sensor signals have to be individually preprocessed and classified. Consequently, an individual decision is obtained for each sensor signal. Furthermore, for other specific applications, individual sensor signals are simultaneously subjected to different preprocessing and classification modules. Each module provides a decision statement about the system state. These various individual decisions (based either on different sensor signals or on a single sensor signal) have to be fused to obtain better classification performance over individual classifiers. Therefore, an appropriate decision fusion method should be developed or one of the appropriate and available fusion approaches has to be used in order to perform the fusion process to obtain the best possible fusion performance.

A complex production system (bucket-wheel excavator) is investigated in this work. Bucket-wheel excavators are used for lignite mining in some of the opencast mines (Fig. 1.1). These excavators are utilized to extract the coals and to remove the overburden that are located above the coal layers. The material excavated by the bucket-wheel are continuously discharged on a transport belt to be transported to another place. Stones of various sizes, as well as other objects, e.g. metallic objects are often included in the excavated overburden.

Fig. 1.1: Target production system (bucket-wheel excavator)

Large stones may cause damage to the transport belt, support rollers, drums and other components. Consequently, they could reduce the production capacity, and increase in the operating costs. These large stones are currently detected manually to be removed from the first transport belt before they are discharged on the next one to avoid the above mentioned problems.

The current manual detection process is based on the use of video signal supplied from an installed camera over the first transport belt. An operator observes transported material through this video camera and detects large stones that could cause serious problems and remove them away using a specific technique.

In this work, the production system that suffer from various drawbacks of approaches applied before [Nie09, PK05] is considered in order to develop an automated object detection system to detect target objects after being discharged on the transport belt. The presence of target objects has to detected to avoid resulting disturbances and failures during the continuous transportation process. The detection system should achieve the highest possible detection and lowest possible false alarms rates. In addition to these objectives, several scientific objectives have to be reached. New signal based pattern recognition approaches have to be developed as a solution for complex systems in general. The development process involves development of new pattern recognition approaches using available pattern recognition tools and the development of new fusion technique, which can be used for mutliclassifier pattern recognition tasks.

The term “target object” is used in this work to denote the stones that must be detected by the developed multisensor object detection system, which have minimum edge length of at least 600 mm (Fig. 1.2).

Fig. 1.2: Target object on the first transport belt

1.2 State of the art

This section introduces the state of the art of the investigated problem for the development of the new monitoring system. Moreover, several application examples of used feature extraction, classification, and fusion techniques for the development process of the monitoring system of interest will be introduced.

The production system (bucket-wheel excavator) is not deeply considered by researchers in aspect of developing intelligent and practical monitoring systems in order to improve its functionality and productivity. Therefore this system is investigated to develop a multisensor decision fusion monitoring system.

A few studies have been considered the development of monitoring systems for similar production processes. Petrich and Köhler [PK05] developed a monitoring system based on georadar to detect target objects in overburden before excavation. A detection rate of less than 60% was achieved. Their system was not able to distinguish non-critical objects such as frozen overburden from the target objects of interest. Such objects lead to false alarms, disturbing the production process. Their system could also not identify the position of target objects accurately. Petrich and Köhler also installed a radiometric measuring system above a transport belt to detect target objects in the material flow. A detection rate of less than 70% was achieved. Changes in the petrography and elemental composition of the overburden, other objects such as clay chunks, and small objects led to false alarms.

Nieß developed an automatic monitoring system to detect target objects in a material flow using acceleration sensors [Nie09]. Several acceleration sensors were mounted in the area of impact along the production line. The amplitude of the acceleration signals and vibration durations were considered to determine the presence of target objects. A detection rate of approximately 75% was achieved. However, the production process was often disturbed by false alarms for this system [SMS07].

The best achieved detection rate through the previously designed monitoring systems was 75%. Consequently, the production process was often disturbed through the high rate of false alarms. Therefore, the designed monitoring system should provide the highest possible detection rate and the lowest possible false alarm rate. For the development of the monitoring system of interest and to satisfy the objectives of this work, different physical effects are considered and being preprocessed, evaluated, and fused using different techniques.

In applications that involve vibrational signals such as the production system discussed in this work, these signal components are typically associated with a large variety of related frequencies. Thus, feature extraction should be based on a suitable domain-specific transform module such as Short Time Fourier Transform (STFT) or Continuous Wavelet Transform (CWT). The goal of such signal processing algorithms is to transform a time-domain signal into a suitable domain to extract those characteristics that are embedded in the time series which cannot be directly observed in the original form [BD12].

Short Time Fourier Transform (STFT) has been widely used as feature extraction tool according to its ability to display the time and frequency contents of the analyzed signal simultaneously and according to its low computational costs in comparison to other time-frequency signal processing tools.

Yella et al. [YGD09] proposed a condition monitoring approach of wooden railway sleepers. The approach based on the use of an impact acoustic signal of the wooden sleeper. The acquired signal is preprocessed and its relevant features are extracted using STFT and Discrete Wavelet Transform (DWT). This step is followed by dimensionality reduction process using Principal Component Analysis (PCA). The obtained feature vector using PCA is subjected to classification process using

Multi-layer Perceptron (MLP), Radial Basis Function Neural Network (RBFNN) and Support Vector Machine (SVM). The individual decisions of the three classifiers are fused using a further SVM-classifier to improve the system performance. In [SXC07] an online fault detection algorithm of induction machine was developed. The developed algorithm consists of feature extraction process using STFT of the quasi-steady vibration signals followed by classification process using Neural Network (NN) model. Haiharan et al. [HSY12] used STFT and General Regression Neural Network (GRNN) for normal and hypoacoustic infant cry signal classification. In this contribution, the developed approach performs STFT of the infant cry signal for analysis. Specific statistical features from the power spectrum are considered. These features are subjected to classification process using GRNN. The normal and pathological cries are effectively classified using GRNN in compare to Multilayer Perceptron (MLP) and Time-Delay Neural Network (TDNN). In [CGYI11] noninvsive microwave method was extended to monitor two important vital signs (heart rate and breathing) and the changes of lung water content using a single microwave transmission coefficient measurement. Heart rate and breathing were detected based on the STFT-analysis of the considered signal. The proposed method was tested using experimentally data generated by thorax phantom model. Yuyuan [YX10] used STFT for the fault detection of high voltage inverter. The output voltage waveform of the inverter was considered and subjected to STFT analysis using Hamming window. The faults of the inverter posses a significantly different power spectrum behaviors from the normal state power spectrum behavior.

Continuous Wavelet Transform (CWT) is an alternative method for generating a time–frequency representation of a time series signal. The wavelet transform allows for variable window sizes in analyzing different frequency components within the signal [Can10]. This allows good frequency resolution at low frequencies and good time resolution at high frequencies. Muralidharan [MS13] used the CWT as feature extraction tool to extract the relevant features of the vibrational signals in order to detect four different faults of a mono-block centrifugal pump. The vibrational signals were measured by an accelerometer integrated in the pump inlet. Eight different wavelet mother functions with different versions and for different levels were considered for the feature extraction. Each of the extracted features was subjected to classification process using J48 decision tree algorithm in order to find the appropriate wavelet mother function and wavelet level, which leads to the best classification accuracy. Li et al. [LZZ11] found that the CWT using Hermitian mother wavelet is suitable tool to diagnose the localized crack fault of gears. The CWT was performed using Hermitian wavelet for a vibration signal for a gear with localized crack fault. The analysis showed that the localized crack fault can be clearly detected based on the phase and amplitude of the Hermitian representation. On the other hand, no significant faulty signatures were detected based on the phase and amplitude of the Morlet representation. In [IDO10], the CWT has been used for the development of a new method for the tumor detection in the magnetic resonance (MR) brain image.

The CWT using Gaussian wavelets is performed to extract the characteristics of the tissues in MR head images. The extracted images are subjected to segmentation process using the incremental supervised neural network (ISNN), which segments the image into seven segments. These segments consist of six head tissues and the background. In the process, the symmetry of extracted head from the background is determined and the asymmetry of the six tissues is analyzed. The analysis leads to two vectors for the left and the right hand sides of the head symmetry axis. The existence of the asymmetry and the tumors are stated based on the distance between the two vectors. Konar et al. [KC11] developed a CWT-SVM-based approach for bearing fault detection of three-phase induction motors. The CWT is used to extract the features of the signals considered. Extracted features are classified using SVM-based classifier. For comparative purpose, a further classification approach based on DWT and ANN was developed. As a result, the CWT-SVM approach retains better results than DWT-ANN approach.

A Support Vector Machine (SVM) is used in this work for the classification. The first algorithm which is named "Support Vector Machine" was introduced in 1992 by Boser et al. [BGV92]. The algorithm suffered from the outliers problem. This problem was addressed by the introduced soft margin SVM classifier in 1995 by Cortes and Vapnik [Vap95].

Owing to the advantages of SVM over the traditional classifier techniques (see Section 2.1.2.4), SVM has been widely used in different pattern recognition areas. In [WWWL12] a pattern recognition system for the automated inspection of high speed conveyed objects was developed in order to provide an online detection and classification of the defects of transported objects. According to the classification results, specific tasks were necessary. The designed system consisted of preprocessing, segmentation, feature extraction, and SVM-based classification process to classify the defects of transported objects. A set of binary SVMs were used in [DRS+12] to develop a character recognition approach for the recognition of the handwritten Arabic, Bangla, Devangari, Latin and Telugu numerals. Principal Component Analysis (PCA), Modular PCA (MPCA) and Quad-Tree based Longest-Run (QTLR) were used to extract the relevant features. The combined features were subjected to classification process using a set of binary SVM classifiers. The SVM was utilized in [BDS+10] to develop an automatic mail sorting system. The mails are sorted based on the called numeric string ZIP (Zone Improvement Plan) or PIN (Postal Identification Number). The numeric postal code is subjected to specific feature extraction process followed by SVM-based classification process to classify the postal code to 25 classes. A 92.03% recognition accuracy was achieved by the developed system. In [LCZD05] a binary set SVM-based classifiers were used to develop a pattern recognition technique to detect the faults of the power transformers. The dissolved gasses ($H_2, CH_4, C_2H_6, C_2H_4$, and C_2H_2) in the transformer oil that obtained by dissolved gas analysis are subjected to specific feature extraction process. Six different features are extracted. Based on these features, multi-layer SVM-based classifier (consist of three SVM-based classifiers) is designed. The contribution [CMXC12] proposed four comparative approaches (Fisher-SVM, PCA-SVM, Fisher-ANN, and PCA-ANN model) to classify six different speech emotions (sadness, anger, surprise, fear, happiness, and disgust). Each approach consists of three levels which consist of five classifiers for the emotion classification. Classification process in each approach is based either on SVM or ANN. Fisher discriminator and PCA were used for the dimensionality reduction of the extracted features of the utterance. The results showed that, Fisher discriminator is better than PCA for dimensionality reduction and SVM showed better results than ANN in speaker independent recognition due to its high generalization ability. Li et al. [LZY$^+$13] found that SVM-based classifiers and the empirical mode decomposition (EMD) of ictal EEG signal are suitable to monitor the epilepsy. The intrinsic mode functions (IMFs) were decomposed using EMD. The coefficients of variation and fluctuation index of each IMF are determined to construct the feature vector of interest (the coefficients of variation and fluctuation index are used to measure the variations of the signal amplitude and the intensity of the signal change, respectively). The extracted features are subjected to classification process using SVM. In [IGL$^+$11] an SVM-based approach was developed to diagnose Alzheimers disease (AD). The main idea behind this approach is to factorize the single-photon emission computed tomography (SPECT) images to a set of small components and subjecting each component to a classification process using SVM-based classifiers. The binary decisions of the different SVM-based classifiers are combined together using either majority voting or relevance voting principle in order to state whether the Patient suffering from AD or not.

The Bayesian Combination Rule (BCR) is one of the widely used decision fusion methods in abstract level. Therefore, this method is used in this work as comparative fusion approach to approve the plausibility of the developed fusion approach. In [XKH11] a multi classifier bearing fault diagnosis approach based on PCA and Bayesian belief method (BCR) was developed. Six features for the investigated vibration signal were extracted. The correlation among extracted statistical features was eliminated using PCA. The first four principal components were selected and classified using six different classifiers. A correlation process was performed to find the optimal classifier sequence. Individual decisions of the selected classifiers were fused using Bayesian belief method. Niu et al. [NHYT07] developed a decision fusion-based monitoring system for motor fault diagnosis. Different physical phenomena were measured and considered for fault detection purpose. These signals were subjected to feature extraction and classification processes. The following methods were utilized to classify the extracted features: SVM, Linear Discriminant Analysis (LDA), k-Nearest-Neighbor (k-NN), learning mixture model (GMM) [HZBF10], and Improved Iterative Scaling (IIS) [Ber97]. A correlation measure was used to obtain the best combination sequence of the designed classifiers to achieve the best fusion performance with the least set of classifiers. Three different fusion techniques (majority voting, Bayesian belief method, and multi-agent method) were applied to fuse the decisions of the selected classifiers. Finally, multi-agent method has been used for the fusion due to its accuracy and robustness. Metallinou et al. [MLN10] proposed a multimodalities Bayesian fusion-based approach for emotion recognition. The face, the voice, and the head cues were individually modeled to provide an individual emotion recognition. Bayesian framework has been used to combine the decisions from the individual models. Fusion process led to significant recognition performance over the individual recognition models. Shin et al. [SJYH11] proposed a multi-classifier fusion based approach for WiFi-based positioning system. As introduced in this contribution, the performance of the previously individually used machine learning systems are strongly affected by the environmental conditions. These negatively environmental effects are reduced by the proposed approach which consists of three various classifiers (k-NN, Bayesian, and Histogram classifier) and a Bayesian combination rule to combine the decision statements of the various classifiers. The experimental results showed that, the developed approach led to better performance than the individual classifiers.

1.3 Structure of thesis

The remaining contents of this thesis are structured as follows:

Chapter 2 introduces a short overview about pattern recognition systems and their design. Moreover, it consists of brief introduction about decision fusion techniques and their importance. The novel developed decision fusion technique is introduced in Chapter 3. In this chapter, a numerical example is considered with the help of Bayesian combination rule to approve the plausibility of this approach. The designed monitoring system for target object detection is considered in Chapter 4. It includes a detailed description of the different detection modules and their individual detection performance as well as the final detection performance using different fusion techniques. Chapter 5 considers the modified monitoring system, which is implemented on the target production system. The performed modifications are described and the detection performance of the individual detection modules as well as the final detection performance are introduced. Finally, in Chapter 6 the thesis is summarized and the scientific contributions of this work are described. Moreover, several recommendations, which might be helpful for the future researches are given.

2 Background: Pattern recognition and decision fusion techniques

This chapter introduces a short overview about pattern recognition systems and decision fusion techniques.

During the progress of this work, parts of this chapter have been published/demonstrated in [ASSSS11, ASSSS12, ASSS13] and [Rot12].

2.1 Pattern recognition

This section introduces the definition of pattern recognition and the most widely used procedure for designing pattern recognition systems. In addition, feature extraction and classification tools that are used in this work will be described in detail.

2.1.1 Definition

Schalkoff defined pattern recognition in [Sch92] as "*the science that concerns the description or classification (recognition) of measurement*". In [TK08] "*pattern recognition is the scientific discipline whose goal is the classification of objects into a number of categories or classes*".

The discovery procedure of the hidden regularities and similarities in the considered data is the main objective of pattern recognition. This procedure is achieved by automatic computer-based algorithms to accomplish several tasks such as classification, rules association tasks, etc. [Kun04, Abe10].

2.1.2 Design steps

The most important goal during the design process of any pattern recognition system is to achieve the highest possible inference of patterns of interest [SMK01, SS07]. To fulfill this goal, the design process generally involves the following steps (as illustrated in Fig. 2.1): data acquisition, feature extraction, feature selection, classifier design, and system evaluation. The feed arrows (black colored arrows) in Fig. 2.1 denote the dependency between design steps. Therefore, the overall system performance depends on the performances of the individual steps. In other words, the overall system performance could be improved by redesigning and optimizing the earlier processes [TK08]. Design process steps are explained briefly in the following subsections.

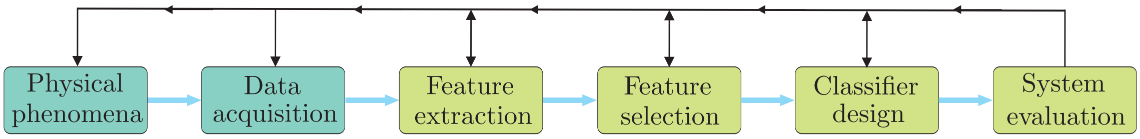

Fig. 2.1: Design procedure of pattern recognition system

2.1.2.1 Data acquisition

Data acquisition is defined in [AD12] as the process of capturing the real world physical effects and converting them to appropriate form to be processed by computing devices.

According to [Kun04], if the data of interest for a specific pattern recognition problem are not given, the problem should be deeply analyzed to identify the relevant physical effects (observations) to solve this problem. The observations, which do not have direct relation with the problem considered, should be at this step measured and analyzed. This is due to the fact that some observations are individually irrelevant but their fusion with other observations might be informative and helpful for problem solution. This point can be explained by the following artificial pattern recognition example. In this example, a specific fault in a production process has to be detected. There are several measurable and available signals, which are acceleration, pressure, force, and position signals. The first analysis of the problem considered showed that only the acceleration signal has a direct relation with the fault to be recognized. Simultaneously, the individual analysis of the other signals showed that these signals are individually not helpful for the recognition task. These signals have to be combined (using, e.g. PCA, LDA, Independent Component Analysis (ICA), etc.) with each other and be analyzed in order to find out specific relation(s) between them and the fault to be recognized. If a helpful relation(s) is founded, these signals have to be considered in the design process of the targeted pattern recognition system. Otherwise, these signals have to be neglected at this stage.

2.1.2.2 Feature extraction

Feature extraction is defined in [ZX09] as the transformation process of individual raw signals or combination of several signals into a new informative feature set. It is usually used to extract the representative and informative hidden features of the acquired data to obtain suitable mapping between the acquired data of the system of interest and its related possible classes. The clear mapping makes classification tasks easier as well as it improves the classification efficiency [GJN05, Kec05].

In pattern recognition problems that involve vibrational signals (such as the considered problem in this work), feature extraction should be based on a suitable domain-specific transform module such as STFT or wavelet transformation to extract the relevant components of these signals. In other words, the goal of such transformation processes is to transform a time-domain signal into a suitable domain to extract those characteristics that are embedded in the time series which cannot be directly observed in the original form [BD12, HYLW10, VLR+06]. Mathematically, this can be achieved by representing time-dependent signal $x(t)$ as a series of parameters and inner product coefficients according to comparison of the signal to a set of known template functions [BWR13, GY11, HVG11].

Short Time Fourier Transform (STFT)

For Fourier transforms, the similarity of a time series signal to a series of sine and cosine template functions is evaluated [AV13]. The Fourier transform represents only the average frequency information for the entire period of the signal analyzed and not the variation of its content over time, which makes it only useful for stationary signals [Ise06, MR05].

To overcome the limitations of Fourier transforms and to investigate the time-frequency behavior of the signal of interest, a fourier transform should be locally performed within sliding window. This kind of transformation is called Short Time Fourier Transform (STFT). As described in [MMOM96], the STFT method slices the signal using a short time window and breaking up the sliced signals to a set of sinusoidal functions with various frequencies. According to the fact that the considered signal could be slightly change in short time period (short slice), sliced signal parts can be considered as stationary signals and thus Fourier transform is suitable for the transformation of these slices [GY11].

As shown in Fig. 2.2, the STFT uses a window function $g(t)$ that is centered at τ (τ denotes the time shift), slides over the time axis to perform a localized window-based Fourier transform for each specific τ till the end of the time series signal $x(t)$. This leads to extract two dimensional time-frequency representation of the time series signal in which the variations of the frequency composition within the considered signal over time is obtained [GY11]. The STFT is mathematically described as [GY11]

$$STFT(\tau, f) = < x, g_{\tau,f} > = \int_{-\infty}^{\infty} x(t)g(t-\tau)e^{i2\pi ft}dt. \tag{2.1}$$

The subplot "raw signal" in Fig. 2.3 shows an acceleration signal in time domain. Whereas the subplot "spectrogram" in the same figure shows the corresponding power spectrum as time-frequency function, which is obtained by applying STFT. The colors present the power magnitudes.

Numerous types of window functions were developed in the last decades such as rectangular window, hamming window, Hanning window, three sample Blackman-Harris, etc. [Kul03]. Each window type is designed for certain type of applications [GY11]. The most commonly used window functions [GY11] are Hamming, Hanning, and Gaussian function, which are described briefly in the following.

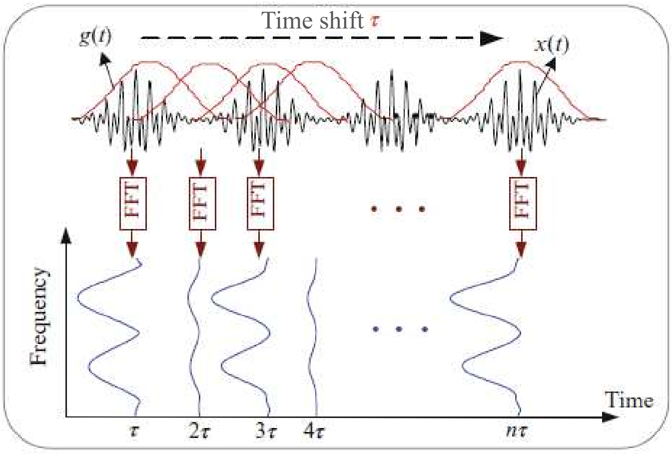

Fig. 2.2: Illustration of the STFT decomposition of a raw signal $x(t)$ [GY11]

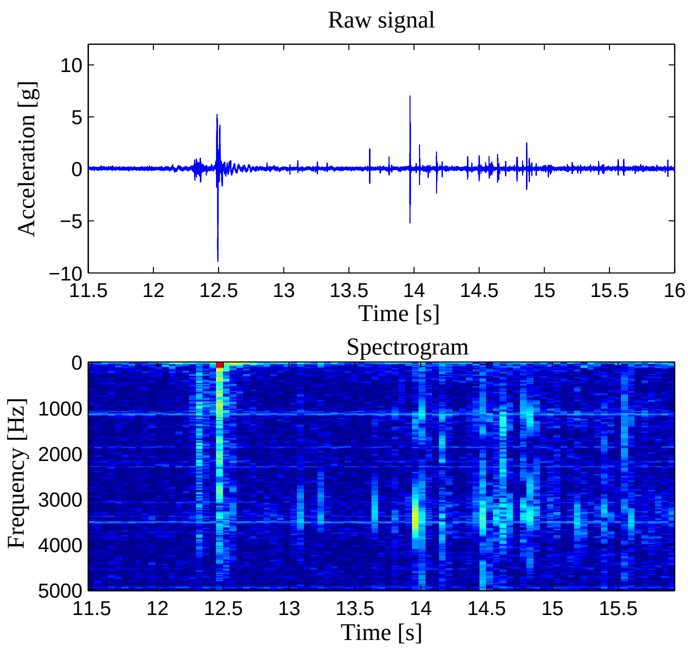

Fig. 2.3: Acceleration signal of sensor 1 [ASSSS11, ASSS13]

- Hann window function (Hanning window): it is named after Julius von Hann. As described e.g. in [Ste00], Hann window is defined mathematically as

  $$\omega(n) = 0.5(1 - cos(2\pi \frac{n}{N})), \tag{2.2}$$

  for $n = 0...N-1$, where N denotes the window length, in samples, of a discrete-time.

  Hanning window is appropriate for narrowband and random signals [GY11].

The solid line in Fig. 2.4 represents the Hanning windowing function in the time domain. Hanning window is useful for solving specific practical problems. For example, in [HXWC09], STFT analysis using Hanning windowing function was utilized for the series arc faults detection.

- Hamming window function: it is derived through the adjusting of the coefficients of the Hanning window in order to cancel the first sidelobe [Ste00]. Thus it has better selectivity for large signals than Hanning window [Vib13]. However, it is suffered from getting close to zero near the edges as Hanning window done [Ste00].

  Hamming function is described mathematically e.g. in [Eas10] as

  $$\omega(n) = 0.54 - 0.46cos(2\pi \frac{n}{N}), \tag{2.3}$$

  for $n = 0...N-1$, where N denotes the window length, in samples, of a discrete-time.

  Hamming window is appropriate for narrowband and random signals [GY11]. The blue dashed line in Fig. 2.4 represents the Hamming window in the time domain.

  The contribution [ASA$^+$12] showed that this window function is appropriate than the rectangular window function for the specific problem considered, which approved the fact that each window function is appropriate for certain type of applications. In this contribution, the STFT analysis, of the seismic electric signal (SES) acquired prior to an earthquake, using Hamming window provided better results than the analysis using the rectangular window.

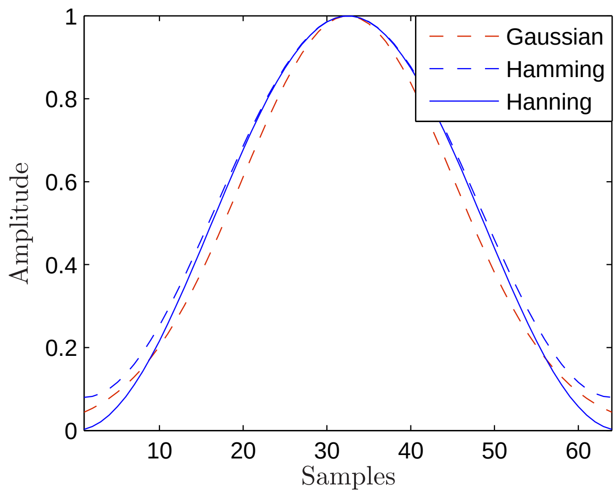

Fig. 2.4: Gaussian, Hamming, Hanning window

- Gaussian window function: it is defined mathematically as

  $$\omega(n) = e^{-(n-m)^2/2(\sigma N)^2}, \tag{2.4}$$

  for $n = 0...N-1$, where N is the window length, in samples, of a discrete-time, $m = (N-1)/2$, and σ the standard deviation of the Gaussian window.

  The red dashed line in Fig. 2.4 represents the Gaussian window in the time domain. This window is appropriate for the analysis of transient signal. Gaussian window is useful for solving specific practical problems. For example, in [YSL+13], an adaptive approach was developed to choose the appropriate window parameters of the Gaussian window function for the STFT analysis of Linear Frequency Modulated (LFM) signals. The goal was to obtain the optimal 3 dB Signal-to-Noise Ratio (SNR) with the right time-frequency resolution.

A disadvantage of STFT is once window function is chosen and its length is defined, the time and frequency resolutions over the entire time-frequency plane are fixed. Consequently, time and frequency resolutions cannot be simultaneously improved. In other words, a trade-off between the time and frequency resolution is existed [ABSC11].

Continuous Wavelet Transform (CWT)

The Continuous Wavelet Transform (CWT) is an alternative method for generating a time-frequency representation of a time series. It utilizes wavelets as basis functions instead of sinusoidal functions that used in STFT. In addition to the time variable, it involves a further variable (scale parameter). These variables are used together for the inner product transform [FLC13, Mal08].

The time series signals are broken up by Fourier transform into a set of sine waves of different frequencies; while wavelet transform breaks up the time series signals to scaled (stretched or squeezed) and shifted templates of the elementary wavelet mother function [MMOM96]. These scaled and shifted functions represent localized frequencies of varying durations of a sound signal or image details, for example [NTMB10, RR06].

The wavelet transform allows for variable window sizes in analyzing different frequency components within the signal [BWR12, Can10, LLK+99]. This allows good frequency resolution at low frequencies and good time resolution at high frequencies. The superiority of wavelets is more tangible in the case of non-stationary measurements and the existence of non-stationarities in time [LLK+99, SES+05].

The CWT of a signal $x(t)$ projected into a two-dimensional, time-scale plane is represented as [GY11]

$$wt(s,\tau) = <x, \psi_{s,\tau}> = \frac{1}{\sqrt{s}} \int_{-\infty}^{\infty} x(t)\psi^*(\frac{t-\tau}{s})dt, \tag{2.5}$$

where τ denotes the time shift (translation parameter) and s the scale parameter. These parameters are used for the shifting (translation) and dilation (scaling) of the wavelet mother function, respectively.

The wavelet mother functions should satisfy the following mathematical conditions:

- admissibility condition:

$$\int_{-\infty}^{\infty} \frac{|\Psi(f)|^2}{(f)} df < \infty, \quad \text{and} \tag{2.6}$$

- zero average value in time domain

$$\int_{-\infty}^{\infty} \psi(f) dt = 0. \tag{2.7}$$

These criteria are discussed in detail in [Add02]. Wavelet functions have limited duration in compare to the sinusoidal functions, which have infinite duration (Fig. 2.5) [MMOM96].

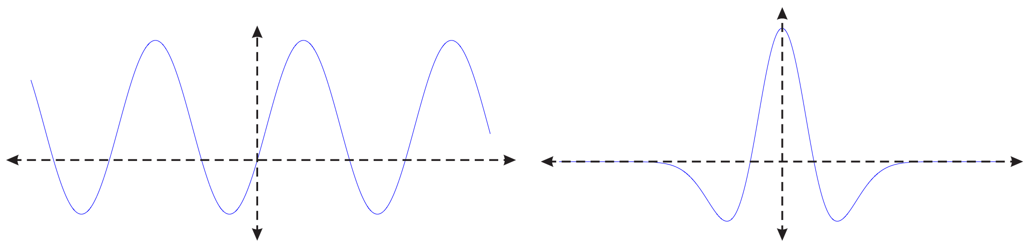

(a) Sine wave

(b) Mexican hat

Fig. 2.5: Sine wave and Mexican hat wavelet function

In contrast to Fourier transform, which has only sinusoidal function as mother function, wavelet transform has a large number of mother functions to be utilized for wavelet analysis such as Haar, Littlewood-Paley, Mayer, Battle-Lemare-spline, Daubechies, coiflet, etc. [Tan00].

It is important to mention that there is no best mother function for all applications. The best choice of the mother function mainly depends on the type of the signal to be analyzed and the analysis objective(s) [Add02].

Three of the most commonly used wavelet function for practical application [Add02] are briefly described in this sequel.

- Haar wavelet: Haar wavelet is the simplest wavelet function. It is mathematically defined by Haar in [Haa10] as

$$\psi(t) = \begin{cases} 1 & 0 \leq t < 0.5; \\ -1 & 0.5 \leq t < 1; \\ 0 & \text{otherwise.} \end{cases} \tag{2.8}$$

  Haar wavelet has good resolution in time domain but low frequency resolution in frequency domain because of its rectangular shape, which leads to estimate its related spectrum with slow decay characteristics [Tan00].

  The time domain behavior of the Haar wavelet is shown in Fig. 2.6(a). The application example in [GMGD13] showed that each mother function is suitable for a certain type of applications. In this contribution, the extracted features using Haar wavelet showed more promising results than other tested wavelet functions (Daubechies 2 (DB2), Daubechies 4 (DB4), and biorthogonal spline) for the design of automatic defect detection on hot-rolled flat steel products.

- Mexican hat: it is the normalized second derivative of the Gaussian distribution function $e^{-t^2/2}$. It is described mathematically as [Add02]

$$\psi(t) = (1 - t^2)e^{-t^2/2}. \tag{2.9}$$

  The time domain behavior of the Mexican hat is shown in Fig. 2.6(b). This type of mother functions is also suitable for a certain type of applications; for example, in [LH13] an improved Mexican hat mother wavelet function was used for development of a de-noising method for gear fault experiment.

- Morlet: it is mathematically defined in [VK95] as

$$\psi(t) = \frac{1}{\sqrt{\pi}} e^{-j\omega_0 t} e^{-t^2/2}, \tag{2.10}$$

  where ω_0 presents the center frequency. The factor $\frac{1}{\sqrt{\pi}}$ is addressed for the normalization so that $||\psi(t)|| = 1$.

  The time domain behavior of the Morlet wavelet function is shown in Fig. 2.6(b). Owing to its shape, which looks like mechanical shock signals, Morlet wavelet was successfully used together with Wigner-Ville Distribution (WVD) in [TLS10] to develop a wind turbine fault diagnosis approach. The CWT analysis using Morlet wavelet is performed to extract the features of the considered raw vibration signals.

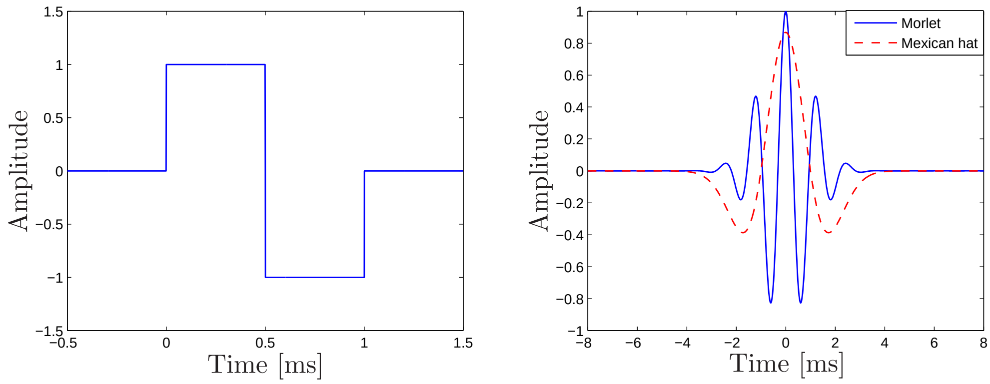

(a) Haar wavelet (b) Mexican hat and Morlet wavelet

Fig. 2.6: Haar wavelet, Mexican hat, and Morlet wavelet

2.1.2.3 Feature selection

The goal of feature selection process as introduced in [SW11] is to exclude irrelevant and/or redundant information (features or attributes) in order to obtain the useful features for the pattern recognition problem to be solved.

The main reason for applying the feature selection process is to select the minimum sufficient feature subset to solve the pattern recognition problem by eliminating irrelevant features. This can lead to significant improvement of the accuracy and generalization ability of the designed classification model. Eliminating irrelevant features leads also to reduce the computational complexity [CKLS07].

Feature selection approaches can be generally categorized into filter and wrapper approaches [CKLS07, SMABTS07]. Both categories are briefly described in the following subsections.

Filter approaches

The filter feature selection algorithm is used to filter the features in order to choose an optimum feature subset. Optimum features are chosen via their intrinsic properties. This process is performed independently from the classifiers, which can be used for the classification task [CKLS07].

Wrapper approaches

The wrapper feature selection approach involves a learning algorithm. The goal of this approach is to choose the feature subset, which obtains the best classification performance of the involved learning algorithm. Training and evaluation processes are performed for the learning algorithm in order to select the optimal feature subset [CKLS07, MW09].

2.1.2.4 Classifier design

Schalkoff defined pattern classification [Sch92] as "*the act of assigning a class label to an object, a physical process or an event*".

The classifier design step in supervised pattern recognition problems can be considered as learning process of a mapping function, $y = f(X)$, that can assign the associated class label y to a given pattern X. The mapping function can be generally expressed either through classification rules, decision trees, or mathematical formulas [HK05].

Several classification techniques have been developed in the last decades, such as decision tree classifiers, Bayesian classifiers, Artificial Neural Networks (ANNs), Support Vector Machine (SVM), k-Nearest-Neighbor classifiers (k-NN), etc. The most used techniques for classifiers design are introduced in this sequel.

Support Vector Machine (SVM)

Since early applications in fault diagnosis [ROG99], SVM has yielded better results than other techniques such as neural networks, decision trees, and model-based reasoning approaches [SLS12, Zan12]. The method introduced by Cortes and Vapnik [CV95] is based on statistical learning theory and is considered one of the best techniques for pattern recognition.

The SVM was used for classification because of its good generalization ability and its robustness to outliers. The SVM generalization ability can be improved using the concept of large margin classification [GE03]. Unlike typical classification methods, SVM uses information on the separating margin while learning from a data set, which leads to improved separability between classes. The SVM is developed to maximize the margin, and thus the generalization ability is better under conditions such as scarce training data. Moreover, SVM training always finds a global solution, in contrast to NNs, for example, for which many local minima usually exist [Abe10, AnC09, Bur98]. The SVM training also appears to be easier and requires less parameter tuning. Moreover, geometric interpretation of the separating hyperplane in the SVM feature space provides better transparency and interpretability of the results than NNs do.

For signal fusion tasks, the SVM feature space is used as a tool to realize a complimentary transformed description in which a combination of signals provides better insight into the problem and therefore better accuracy than direct consideration of individual signals. Another advantage of SVM is its robustness to outliers. Proper setting of the penalty parameter C, which controls the misclassification error, can suppress outliers and reduce the effect of increased noise. In NNs, outliers need to be eliminated before training [Abe10].

The importance of the SVM robustness to outliers is more emphasized by high-dimensional data sets with large number of features. The performance of traditional classification methods such as NNs often decreases as the number of features increases, which is referred to as the curse of dimensionality. To deal with this problem, dimensionality reduction and feature subset selection techniques are often applied as a data preprocessing step prior to classification. In case of SVM, the learning complexity is independent of the dimensionality of the input space [Kec05]. Therefore, dimensionality reduction methods do not significantly increase SVM accuracy. A support vector machine (SVM) classifier with a small number of support vectors has good generalization ability, even in very high-dimensional spaces [Kec05].

For linearly separable data, SVM solves the classification problem by finding the maximum marginal hyperplane "MMH". Actually, there is an infinite number of hyperplane that could be used to separate the attributes relating to class 1 from attributes relating to class 2 (Fig. 2.7). The goal is to obtain the optimal hyperplane, which increase the generalization ability [HK05].

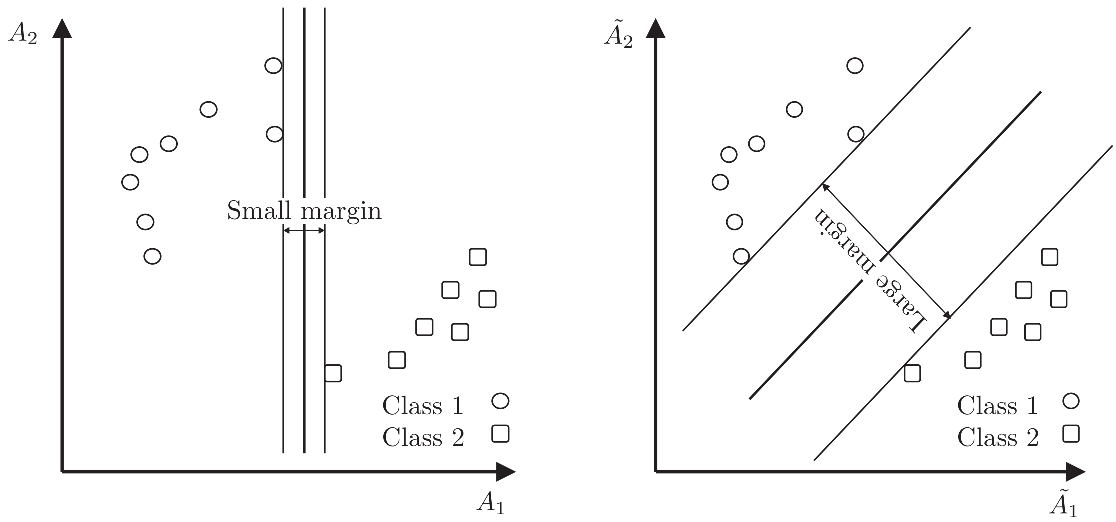

(a) Hyperplane with small margin (b) Hyperplane with large margin

Fig. 2.7: Two possible hyperplanes for a 2-D training data

In the following the mathematical background is repeated as developed and given in [HK05]. A separating hyperplane can be mathematically described as

$$WX + b = 0, \tag{2.11}$$

where W represents the weighting vector, $W = w_1, w_2, w_3, ..., w_n$, n is the number of attributes, b is a scalar representing the bias term of the separating hyperplane, and X the training attributes vector; namely $X = x_1, x_2, x_3, ..., x_n$; $x_1, x_2, x_3, ..., x_n$ are the attributes values.

For the demonstrated 2-D training data in Fig. 2.8, any point being upper the hyperplane (circle points) fulfills

$$b + w_1x_1 + w_2x_2 > 0. \tag{2.12}$$

Correspondingly, the points being under the hyperplane (rectangle points) fulfills

$$b + w_1x_1 + w_2x_2 < 0. \tag{2.13}$$

The hyperplanes which define the margin sides can be mathematically described by adjusting the weights. Consequently, they can be written as

$$H_1 : b + w_1x_1 + w_2x_2 \geq +1 \text{ and} \tag{2.14}$$

$$H_2 : b + w_1x_1 + w_2x_2 \leq -1, \tag{2.15}$$

where H_1 and H_2 are the upper and lower margin sides, respectively.

The Eq. 2.14 and Eq. 2.15 can be rewritten as

$$y_i(b + w_1x_1 + w_2x_2) \geq 1, \tag{2.16}$$

where, y_i is the class label; $y_i = +1$ for class 1 and $y_i = -1$ for class 2. The general mathematical form of Eq. 2.16 is written as [Abe10]

$$y_i(w^T x_i + b) \geq 1 \quad \text{for} \quad i = 1, 2, ..., n. \tag{2.17}$$

Any training point lies on the hyperplanes H_1 or H_2 and fulfills Eq. 2.16 is named support vector. Support vectors are the circle and rectangle points with black background (Fig 2.8).

The Maximum Marginal Hyperplane (MMH) and the support vectors can be found by rewriting Eq. 2.16 to become a constrained quadratic optimization problem. This optimization problem can be solved using for example Karush-Kuhn-Tucker conditions (KKT) [GT51] to find out the problem solution (MMH and support vectors). Once the support vectors and MMH are determined, an SVM-based classifier has been ready designed. It can be used to classify linear separable test data [HK05].

Since the support vectors are determined, MMH can be rewritten as the boundary decision function [HK05]

$$d(X^T) = \sum_{i=1}^{l} y_i \alpha_i X_i X^T + b_0, \tag{2.18}$$

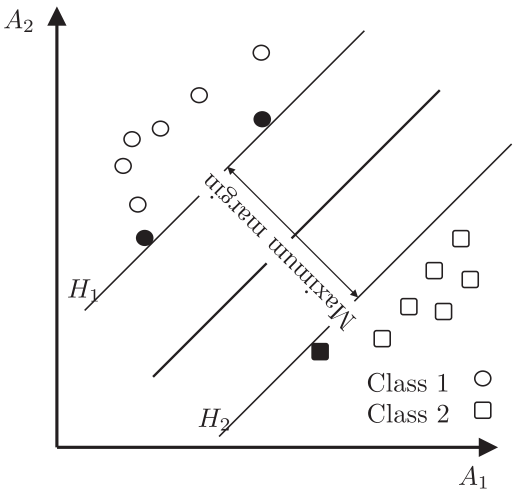

Fig. 2.8: Support vectors and MMH

where X_i denotes the support vector, y_i the class label of the support vector (where $i = 1, 2, ..., l$), l the total number of the support vectors, X^T an unknown test data point, and α_i and b_0 represent numeric parameters.

Any unknown test data point X^T can be classified by inserting its related attributes values in Eq. 2.18. Positive $d(X^T)$ result denotes that X^T belongs to class 1; while negative one denotes that X^T belongs to class 2 [HK05].

For the non-linear separable data, no straight line can be obtained to separate the classes (Fig. 2.9). Consequently, the designed linear SVMs would not be able to provide a practical solution for non-linear separable data [HK05].

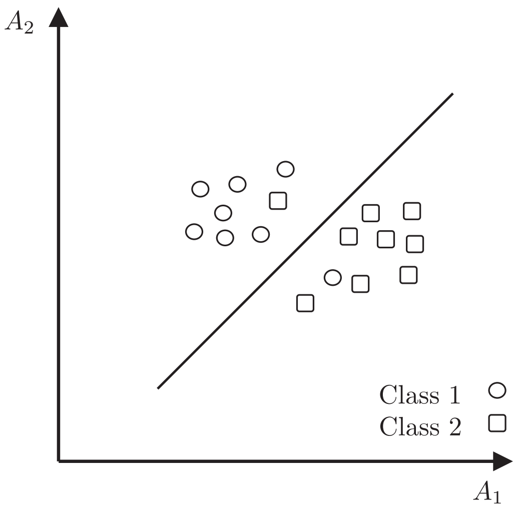

Fig. 2.9: Non-linear separable data

This problem is resolved by extending the previously demonstrated approach for linear SVMs in order to design a non-linear SVMs that could be able to classify non-linear separable data. The extended process involves two steps. As first step, a non-linear mapping is utilized to transform the original data from its current dimensional space to a higher dimensional space. Second step, a linear separating hyperplane for separating the classes in the new space is searched. A dot product should be performed several times in training phase using the higher dimensional space till the MMH is founded. This process needs heavy computational costs. To avoid this costly dot product, specific kernel functions are used and applied on the original data [HK05].

The possible kernel functions that could be used are: polynomial kernel of degree h, Gaussian Radial Basis Function kernel (RBF), and sigmoid kernel. There are no rules that can be used to specify which kernel function can lead to the most accurate SVM-based classifiers. In addition, the difference of the resulting accuracies using the various kernel functions is generally not large [HK05].

The binary classification using SVMs is described above. However, SVMs can be used to solve multiclass problems. This can be done by combining K binary classifiers to classify K classes. Each classifier k is learned to classify class k as positive and the rest as negative. Each test data point X^T should be classified through the K classifiers. Each classifier obtains a decision value for X^T (either positive or negative). The test point X^T is assigned the class which has the largest positive decision value [HK05].

Artificial Neural Networks (ANNs)

Haykin defined the artificial neural networks (ANNs) in [Hay98] as "*a neural network is a massively parallel distributed processor made up of simple processing units, which has a neural propensity for storing experimental knowledge and making it available for use. It represent the brain in two respects:*
1. Knowledge is acquired by the network from its environment through a learning process.
2. Interneuron connection strength, known as synaptic weights, are used to store the acquired knowledge".

Neural network algorithms are based on the use of the concept of the brain for processing a task of interest. Numerous types of neural networks models have been developed. The common properties between them, that they consist of units (neurons) and the connections in between. The connections between the neurons are weighted with a specific weighting factor. The behavior of the neural network is determined based on its neurons and the interconnection in between including the corresponding weighting factors.

The choice of the appropriate network type to be used for solving a specific task is predicated on the task itself [RLD+97].

Backpropagation algorithm is the most commonly used neural network [Ert11]. According to [Cha11], backpropagation neural networks are widely used in pattern recognition field. It is composed of the following layers:

- One input layer: it consists of n neurons. The number of neurons in the input layers is defined based on the number of the individual signals/features to be fed in the NN. Input layer propagate the signals/features to the next layer (first hidden layer) (Fig. 2.10) [HK05].

- One hidden layer at least: backpropagation networks could have one or more hidden layers. The number of the neurons in each hidden layer is defined experimentally by the user [RLD+97]. The neurons of the hidden layers combine and transform the propagated signals/features to the output layer [HK05].

- One output layer: it consists of N neurons for the N classes of interest. It combines and transforms the coming data from the last hidden layer to generate the output of the network [HK05].

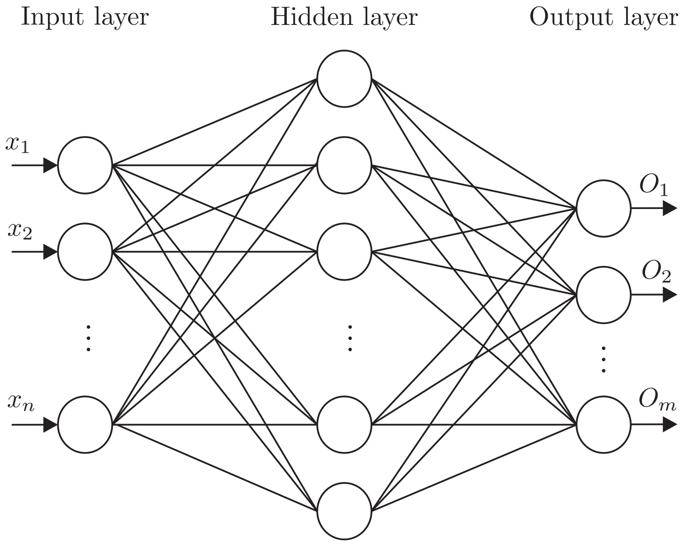

Fig. 2.10: Schematic structure of a multi-layer NN

The weights are randomly defined at the first time. The value of each weight is adjusted during the training process of the network in order to construct a suitable input-output mapping. The value x_j of the hidden and output neurons j (Fig.2.11) are determined as [RLD+97]

$$x_j = \sum_{i=1}^{l} w_{ji} x_i, \tag{2.19}$$

where x_i is the previous value of the neuron i in the layer before, l the number of neurons in the previous layer, and w_{ji} the weighting factor of the connection between the neurons i and j.

The usually used activation function of neurons is the sigmoid function [RLD+97]

$$f(x_j) = \frac{1}{1 + exp^{(-x_j)}}. \tag{2.20}$$

Other function such as threshold, Gaussian, and piecewise linear function can be used as activation functions [Hay98].

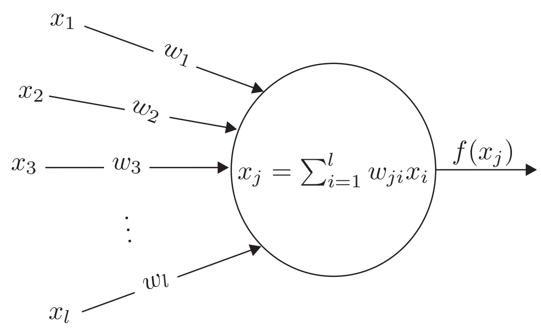

Fig. 2.11: Neuron model

The backpropagation algorithm is able to be learned using training data. The goal of the learning process is to find a suitable mapping between the input and output of the network. As mentioned before, a random weight factor is associated to each connection between two neurons. During the training process, sequential iterations are performed to determine the optimal values the various weights. The difference between the desired output and actual determined output for the given training is estimated in each iteration. This error difference is propagated back on the weights between the neurons in order to adjust these weights. Iteration process is continued as far as the difference error is greater than a negligible value [RLD+97].

k-Nearest-Neighbor (k-NN)

This method was developed in the beginning of the 1950s. It is commonly used first at 1960s because of the computing power limitations [HK05].

Nearest-neighbor classifiers are pattern-based learning classifiers. The training patterns are arranged and stored in a pattern space. For an unknown testing pattern, k-NN compares this pattern with the stored training patterns in the pattern space to find the training patterns that are most similar to the unknown pattern. The k-NN classifiers have a simple architecture. However, the classification time is usually increased by increasing the number of training pattern in the stored pattern space [Abe10].

The Euclidean distance are commonly used to determine the similarity (the closeness) of unknown pattern to any training pattern in the pattern space [Mit10]. The

Euclidean distance between two points ($X = x_1, x_2, ..., x_n$ and $Y = y_1, y_2, ..., y_n$ is determined from [Abe10] as

$$d(X,Y) = \sqrt{\sum_{i=1}^{n}(x_i - y_i)^2}. \tag{2.21}$$

Other methods such as the Manhattan distance [Abe10]

$$d(X,Y) = \sum_{i=1}^{n}|x_i - y_i| \tag{2.22}$$

can be used for the closeness determination.

According to [HK05], the appropriate value of k to obtain good classification result is experimentally determined. The user can start with $k = 1$ and tests the classifier performance using a test data. The process is repeated several times and k value should be increased by each repetition. The k value which leads to the lowest classification error is might be finally chosen.

2.1.2.5 System evaluation

The evaluation of the designed pattern recognition system is carried out by testing the designed system using test data set(s) followed by the calculation of the system performance. System performance for the problem considered in this work can be determined by calculating the detection and false alarm rates of the designed recognition system. The detection rate defines the ability of the system to recognize the pattern of interest; whereas the false alarms rate defines detection reliability of the pattern of interest. It could be defined as the ratio of the number of patterns that are wrongly assigned as pattern of interest to total number of patterns that assigned as pattern of interest.

If the recognition or false rates of the designed pattern recognition system does not fulfill the design goals, the previous design steps should be improved.

2.2 Decision fusion techniques

Decision fusion techniques are widely used in last decades to develop reliable multiclassifier systems. This section presents a brief review about the importance of decision fusion, type of sensor fusion, and decision fusion techniques.

2.2.1 Definition and importance of decision fusion

Fauvel et al. defined decision fusion in [FCB06] as "*the process of fusing information from several individual data sources after each data source undergone a preliminary classification*".

Sensor fusion of a multisensor system can be generally performed at three levels: data (observation) fusion, feature fusion, and decision fusion [Das91].

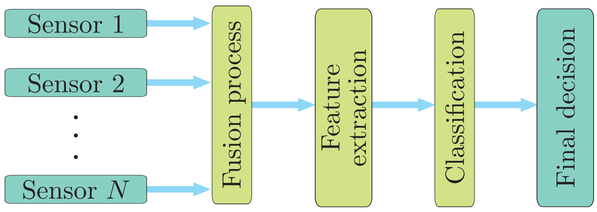

(a) Data (observation) fusion

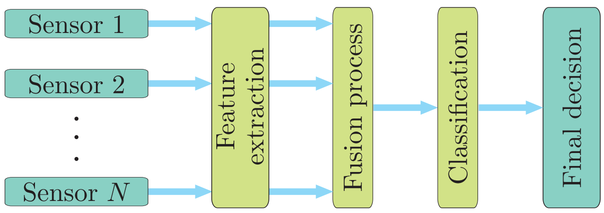

(b) Feature fusion

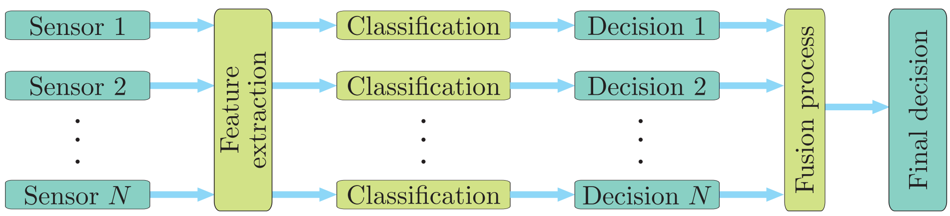

(c) Decision fusion

Fig. 2.12: Schematic representation of sensor fusion levels

At observation fusion level, the raw data of the different information sources are directly combined together. Fused data are subjected to feature extraction process to extract the relevant features. This process is followed by classification process to recognize the target of interest (Fig. 2.12(a)). This kind of fusion is appropriate to combine data of different information sources, which measure the same physical phenomena, such as fusing the data of several acceleration sensors [HL09].

At feature fusion level, the representative features of the data of the different information sources are individually extracted. After that, the extracted features are fused together. Fused features are subjected to classification process to recognize the target of interest (Fig. 2.12(b)). This kind of fusion can be used to combine the features of different information sources, which measure different physical phenomenon. In this case, a normalization process of feature is needed before being combined and subjected to classification by the appropriate classifier [XKS92].

There are numerous methods, which can be used to perform the fusion task at observation and feature level, such as PCA, LDA, ICA, non-negative matrix factorization, etc. These methods are clearly explained in [Mit07, TK08].

An accurate synchronization of the data of the different information sources is necessary in the previous fusion levels, which could be impossible to apply in multisensor system with inevitable varying time shift between the different information sources. Additionally, lumping a lot of data in one very high-dimentional vector could increase the computational costs as well as lead to implementation and accuracy problems [XKS92].

At decision fusion level, the data of the different information sources are subjected to individual processing and classification processes. The obtained decisions througth the individual classifiers are fused to obtain accurate recognition result about the target of interest (Fig. 2.12(c)).

Decision fusion techniques are important due to several aspects:

First aspect: Different physical effects can be investigated to recognize specific patterns. However, the investigated signals have various types of features with widely diversified representation, therefore, it is not appropriate to fuse these features using either observation or feature fusion techniques. To solve this problem, the signals with different feature types have to be individually classified. After that, the obtained individual decisions from the individual classifiers have to be fused using an appropriate decision fusion technique in order to obtain accurate pattern recognition [XKS92].

Second aspect: The impossibility to achieve a reliable inference/detection for specific pattern recognition problems based on only one type of the known classification algorithms [XKS92].

Numerous classification algorithms are known and can be realized to solve pattern recognition problems in the application areas of pattern recognition. These algorithms have different methodologies and based on different mathematical theories. Therefore, it could happen that the individual classification results of the realized classification algorithms for a recognition problem are not good enough. On the other hand, each classifier could obtain a partial solution of the problem which is not obtained by other classifiers. Thus, the fusion of their results could lead to sufficient recognition performance [XKS92, NHYT07].

Third aspect: The inevitable varying time shift between the different information sources.

This problem could lead to difficulties and complexities in the synchronization process of the data of the different information sources. It could be avoided by implementing specific complex synchronization algorithms, which could increase the computational time and delay the decision making process. Even, if this problem could be solved by implementing very complex synchronization algorithms, it is still better to process/classify the data of the different information sources individually and a simple synchronization process could be then utilized to match the decisions of the individual classifiers to be fused in order to obtain a final reliable decision.

2.2.2 Decision fusion methodologies

According to the previously mentioned aspects, the promising results for many pattern recognition problems achieved by using different decision fusion techniques, and the growing interest of realizing distributed systems for complex multiclassifier systems, many decision fusion methodologies are developed and implemented in the last decades [Das91, NWS+08, ODDA10, XKH11].

Owing to the fact that fusion processes consist of several inputs and one output, they could be considered as a pattern recognition problem [SL00]. Consequently, many classification algorithms such as SVM, ANNs, etc. can be realized to perform the fusion process of the individual decisions of the multiclassifier-based pattern recognition problems [SL00].

There are no decision fusion techniques that can provide a best fusion performance for all applications. Many of the developed methods are based on diversified mathematical rules. This diversity allows specific fusion method to provide better fusion performance for particular applications than the other ones. It could be concluded that the best achieved fusion performance for a particular application does not depend on the realized fusion method only, but also on the nature of the considered pattern recognition problem.

Decision fusion techniques can be categorized according to the type of the obtained outputs from the classifiers to be combined. Classifier outputs are usually categorized to three levels [Kun04, MF08]:

- Abstract level: This level deals with classifiers, which output a unique label for each classified input pattern. In this level, no information is provided about the confidence of the obtained class. Many abstract level-based fusion techniques have been developed in the last decades such as majority vote, weighted majority vote [RNJ06, HL09, Mit07], Behavior Knowledge Space (BKS) [Pol06], Dempster-Shafer Theory (DST) of evidence [YKF94, KC03], Bayesian Combination Rule (BCR) [JFR07, Mit07, NWS+08], etc.

- Rank level: Each classifier obtains (assigns) for each classified pattern (sample) a set of possible classes ranked in decreasing order of confidence; i.e. a list of so called n-best classes is obtained for each classified pattern. The most likely class is listed at first in the list (top of the list). Consequently the most unlikely class is listed at the end of the list (foot of the list). In the rank level, classifiers do not assign confidence values for the obtained n-best classes. Their likelihood is only denoted through their position in the obtained n-best list [CDSM10, Kun04, MF08]. Several ranking-based fusion methods were developed such as the Borda count [MF08, Wu12], the Condorcet voting [Wu12], the weighted Condorcet voting [Wu12], etc.

- Measurement level: Each classifier obtains (assigns) a confidence value for each target class, for each classified pattern (sample). The form of the assigned values for the target classes can be rational or irrational numbers depending on the utilized classification architecture [MF08, SL00]. Many fusion techniques were developed for this kind of output level such as basic combination operators [SL00], weighted operators on measurement level outputs [SL00], artificial neural networks (ANNs), etc.

Each of the realized classifiers for the considered pattern recognition problem in this work outputs a unique class for each classified pattern; i.e. these classifiers can be categorized as abstract level classifiers. For a successful fusion of the classifier outputs, an abstract level-based decision fusion technique should be either realized or developed to obtain the best final fusion performance.

This work involves development of a novel approach to combine abstract level classifiers (chapter 3). The developed approach is basically based on the combination of the basic belief values of the classifier statements. The assigned values of the classifier statements are determined based on the performance of the individual classifier. Bayesian Combination Rule (BCR) is utilized to approve the plausibility and the performance of the developed decision fusion method. It is chosen from the numerous number of the decision fusion techniques because it is based on the classifier performance. The BCR is introduced in the following section.

2.2.3 Bayesian Combination Rule (BCR)

In contrary to majority voting method, which considers the obtained labels by each classifier for the combination, BCR considers the classifiers performance of each possible class. A training data set is necessary to determine the classifier performance of each class. Based on this data set, a confusion matrix CM^k (where k is the classifier number, with $k = 1, 2, 3, ..., K$) is obtained for each classifier (cl^k). It gives an indication about the classifier performance for each class [SL00]. The confusion matrix of each classifier is described as

$$CM^k = \begin{bmatrix} n^k_{11} & n^k_{12} & ... & n^k_{1M} & n^k_{1(M+1)} \\ n^k_{21} & n^k_{22} & ... & n^k_{2M} & n^k_{2(M+1)} \\ . & . & . & . & . \\ . & . & . & . & . \\ . & . & . & . & . \\ n^k_{M1} & n^k_{M2} & ... & n^k_{MM} & n^k_{M(M+1)} \\ \end{bmatrix} . \quad (2.23)$$

The confusion matrix CM^k is a "$M \times (M+1)$" matrix. The parameter M denotes the number of the considered classes for the pattern recognition problem of interest. Each row $i = 1, 2, 3, ..., M$ in CM^k accords to the class C_i and each column $j = 1, 2, 3, ..., M, M+1$ accords to classifier events (statement) $cl^k = j$.

The parameter n^k_{ij} indicates the number of patterns with real class i, which is assigned by the classifier cl^k as class j (for all $j \leq M$). The parameter n^k_{ij} denotes the number of rejected patterns if $j = M+1$.

The total number of patterns, belonging to each class C_i in the used training data set, can be determined from [XKS92]

$$n^k_i = \sum_{j=1}^{M+1} n^k_{ij} \, , \quad (2.24)$$

whereas the number of patterns that is assigned as class j (C_j) by classifier cl^k can be determined as [XKS92]

$$n^k_j = \sum_{i=1}^{M} n^k_{ij} \, . \quad (2.25)$$

The conditional probability that a pattern x relates in reality to class i (C_i), given that classifier cl^k assigns it to class j, can be determined as [XKS92]

$$P(x \in C_i | cl^k(x) = j) = \frac{n^k_{ij}}{\sum_{i=1}^{M} n^k_{ij}} \, . \quad (2.26)$$

If the classifier cl^k assigns class i (C_i) to a pattern x, then the term in Eq. 2.26 represents its related degree of accuracy.

The combined belief value that a pattern x relates to class i, given that K classifiers assigned it to class j ($cl^k(x) = j_k$, for $1 \leq k \geq K$), can be defined as [SL00, XKS92]

$$bel(i) = P(x \in C_i | cl^1(x) = j_1, ..., cl^K = j_K). \quad (2.27)$$

By assuming that the considered classifiers are independent and by applying the Bayes formula, Eq. 2.27 is approximated as [SL00]

$$bel(i) \doteq \frac{\prod_{k=1}^{K} P(x \in C_i | cl^k(x) = j_k)}{\sum_{i=1}^{M} \prod_{k=1}^{K} P(x \in C_i | cl^k(x) = j_k)}. \tag{2.28}$$

Consequently, the class which possesses the highest combined belief value $bel(i)$ presents the final classification decision [XKH11].

Numerical example

A multiclassifier system consists of four independent classifiers (A, B, D, and E) is assumed. Each classifier outputs either positive (Pos.) or negative (Neg.) statement. Positive statement denotes the existence of specific event (class 1), whereas negative one denotes no specific event exists (class 2). To combine these classifiers using BCR, the performance of the individual classifiers of each class must be calculated. A training data set includes 400 patterns is used for this purpose (includes 180 real specific event). The confusion matrix for each classifier is obtained, based on its classification result of the considered training data set, as

$$CM^A = \begin{bmatrix} 160 & 20 & 0 \\ 40 & 180 & 0 \end{bmatrix}, \quad CM^B = \begin{bmatrix} 180 & 10 & 0 \\ 20 & 190 & 0 \end{bmatrix},$$

$$CM^D = \begin{bmatrix} 140 & 30 & 0 \\ 60 & 170 & 0 \end{bmatrix}, \quad CM^E = \begin{bmatrix} 160 & 160 & 0 \\ 40 & 40 & 0 \end{bmatrix}.$$

For example, the first element (160) in CM^A denotes the number of patterns that are actually positive and are correctly classified by classifier A as positive patterns. The element (40) denotes the number of patterns that are actually negative but wrongly classified by classifier A as positive patterns (misclassified negative patterns). The element (20) denotes the number of patterns that are actually positive and are wrongly classified by classifier A as negative patterns (misclassified positive patterns). The element (180) denotes the number of patterns that are actually negative and correctly classified by classifier A as negative patterns. Zero elements denote that, there are no rejected (not classified) patterns by classifier A. All other confusion matrices are constructed in the same manner.

The conditional probabilities were determined based on the confusion matrices. For example, conditional probabilities of classifier A are

$P(x \in C_{Pos.} | cl^A(x) = Pos.) = bel(Pos.) = 80\%$,

$P(x \in C_{Neg.} | cl^A(x) = Pos.) = bel(Neg.) = 20\%$,

$P(x \in C_{Pos.} | cl^A(x) = Neg.) = bel(Pos.) = 10\%$, and

$P(x \in C_{Neg.}|cl^A(x) = Neg.) = bel(Neg.) = 90\%$.

There are 16 alternative combination scenarios that can happen by fusing four binary classifiers. The fusion result for each possible combination scenario for the introduced example are demonstrated in Table 2.1.

Table 2.1: Fusion results of independent classifiers (A, B, D, and E) using BCR. The term $bel(Pos.)$ denotes the degree of belief that the classified pattern x belongs to positive class if it is assigned by the classifier cl^k as class C_i [Rot12].

Case	A : $bel(Pos.)\%$	B : $bel(Pos.)\%$	D : $bel(Pos.)\%$	E : $bel(Pos.)\%$	bel(Pos.)%
1	Pos.(80)	Pos.(90)	Pos.(70)	Pos.(80)	99.70
2	Neg.(10)	Pos.(90)	Pos.(70)	Pos.(80)	90.32
3	Pos.(80)	Neg.(05)	Pos.(70)	Pos.(80)	66.27
4	Pos.(80)	Pos.(90)	Neg.(15)	Pos.(80)	96.21
5	Pos.(80)	Pos.(90)	Pos.(70)	Neg.(20)	95.45
6	Neg.(10)	Neg.(05)	Pos.(70)	Pos.(80)	5.18
7	Neg.(10)	Pos.(90)	Neg.(15)	Pos.(80)	41.38
8	Neg.(10)	Pos.(90)	Pos.(70)	Neg.(20)	36.84
9	Pos.(80)	Neg.(05)	Neg.(15)	Pos.(80)	12.94
10	Pos.(80)	Neg.(05)	Pos.(70)	Neg.(20)	10.94
11	Pos.(80)	Pos.(90)	Neg.(15)	Neg.(20)	61.36
12	Neg.(10)	Neg.(05)	Neg.(15)	Pos.(80)	0.41
13	Neg.(10)	Neg.(05)	Pos.(70)	Neg.(20)	0.34
14	Neg.(10)	Pos.(90)	Neg.(15)	Neg.(20)	4.23
15	Pos.(80)	Neg.(05)	Neg.(15)	Neg.(20)	0.92
16	Neg.(10)	Neg.(05)	Neg.(15)	Neg.(20)	0.03

In Table 2.1 only the final belief for the positive class (Pos.: specific event exists) is given. Belief value for negative class (Neg.: no specific event exists) is the complement of the positive one. The class with highest final belief value is assigned as the final fusion result.

3 Basic Belief Fusion (BBF) method

In this chapter, the novel developed decision fusion method is introduced.

During the progress of this work, parts of this chapter have been published/demonstrated in [ASS11] and [Rot12].

3.1 Introduction

Mutliple classifiers systems are widely used in last decades to solve complex pattern recognition problems [BBST13, ODDA10]. Each individual classifier provides a preliminary decision about the system state. To fuse these individual preliminary decisions, numerous decision fusion methodologies were developed to obtain a final decision about the system state. The most important goal of these methods is to achieve better inference/detection over individual preliminary decisons [LKH09, YS09].

The individual decisions of the designed monitoring system in this work are independent from each other. This fact is concerned by the development process of the new decision fusion technique (Basic Belief Fusion (BBF) method); i.e. the developed approach should be appropriate to combine independent classifiers. Moreover, the degree of accuracy of different classifier classes is less than one (not fully evident). Thus, it is probable that a pattern "x" with actual "class 1" is wrongly classified by a one classifier as "class 2". Such kind of classifiers decisions can be assigned to a set of hypotheses.

The hypotheses set is defined for binary classifiers as

$$\omega = \{h_1, h_2, h_3\} = \{\text{class 1 } (C_1), \text{ class 2 } (C_2), \text{ uncertain}\}. \tag{3.1}$$

Each decision statement (each class) that obtained by the classifier has its own hypotheses set ω.

A specific value $m(cl_l^k)$ is assigned to each hypothesis in ω. This value is named "basic belief value". The parameter $l = i + 1$ and denotes the hypotheses numbers in ω, and i the number of the considered classes for the targeted pattern recognition problem; whereas $i = 2$ for binary classifiers.

The assigned basic belief values for the given hypotheses set in Eq. 3.1 are

- the basic belief $m(cl_1^k)$: the degree of belief that the classified pattern x belongs to class 1 (C_1) if it is assigned by the classifier cl^k as class C_i,
- the basic belief $m(cl_2^k)$: the degree of belief that the classified pattern x belongs to class 2 (C_2) if it is assigned by the classifier cl^k as class C_i, and

- the basic belief $m(cl_3^k)$: represents the degree of uncertainty.

The basic belief value $m(cl_3^k)$ is assumed to be zero in this work. Consequently, the belief values $m(cl_1^k)$ and $m(cl_2^k)$ are assumed to be equal to the conditional probabilities, which are determined based on the confusion matrices of the classifiers considered. Owing to the assumption that $m(cl_3^k)$ is equal to zero, $m(cl_2^k)$ is the complement of $m(cl_1^k)$. Consequently, the summation of

$$m(cl_1^k) + m(cl_2^k) = 1. \tag{3.2}$$

3.2 Combining an odd set of independent classifiers using BBF

The basic idea of the developed approach is based on using the majority rule to combine the basic belief of the different classifiers statements (classes). Each combination results either hypothesis h_1 or h_2.

Odd set of independent classifiers denotes multiclassifier systems, which consist of odd number (3, 5, 7, etc.) of independent classifiers.

Table 3.1 shows the resulted hypotheses through the basic belief combination of three classifiers (A, B, and D) (for the explanation purposes, an example with three independent classifiers is introduced here). In the demonstrated example, the classification task of each classifier is to check whether a specific event exist. The considered classes of this pattern recognition problem are: “specific event exist”(class 1) and “no specific event exist”(class 2). Each classifier statement (each class $C_i, i = 1, 2$) is assigned to two hypotheses $\omega = \{h_1, h_2\}$={specific event, no specific event} (h_3 is assumed to be zero).

The realized combination process leads to 2^n hypotheses (n is the number of the combined independent classifiers), which belong to the general hypotheses set $\omega = \{h_1, h_2, h_3\}$ for such considered binary classifiers. The realized majority combination rule checks whether the number of $m(cl_1^k)$ is greater than the number of $m(cl_2^k)$ for each possible combination. The fulfillment of this condition leads to the hypothesis “h_1: specific event exists”. Otherwise, it leads to the hypothesis “h_2: no specific event” (Table 3.1).

The assigned belief values for the resulting hypotheses (h_1, and h_2) in the combination shown in Table 3.1 are determined by multiplying their related basic belief values. For example, the combination of the basic beliefs $m(A_1), m(B_1)$, and $m(D_2)$ using majority rule leads to hypothesis h_1. The assigned belief value for this hypothesis is determined as

$$m(h_1) = m(A_1)m(B_1)m(D_2). \tag{3.3}$$

Table 3.1: Basic belief combination of three independent classifiers

	$m(A_1)$		$m(A_2)$	
	$m(D_1)$	$m(D_2)$	$m(D_1)$	$m(D_2)$
$m(B_1)$	h_1	h_1	h_1	h_2
$m(B_2)$	h_1	h_2	h_2	h_2

The combined basic belief for the class for the C_1 "specific event" is calculated by the summation of the basic belief values for the hypothesis h_1 over all possible combinations

$$m(C_1) = \sum m(h_1), \text{ therefore} \tag{3.4}$$

$$\begin{aligned} m(C_1) = m(A_1)m(B_1)m(D_1) \\ +m(A_1)m(B_1)m(D_2) \\ +m(A_1)m(B_2)m(D_1) \\ +m(A_2)m(B_1)m(D_1). \end{aligned} \tag{3.5}$$

The final degree of belief for the class C_1 "specific event" is determined by [Kay07] as

$$bel(C_1) = m(C_1). \tag{3.6}$$

Hence, the proposed fusion process does not lead to any uncertainties in the final decision for the odd classifiers sets. Thus, the degree of uncertainty $m(C_3) = 0$. From Eq. 3.2, the combined basic belief value for the second class C_2 "no specific event" is

$$m(C_2) = 1 - m(C_1). \tag{3.7}$$

Consequently, the degree of belief for the class C_2 is calculated by [Kay07] as

$$bel(C_2) = m(C_2). \tag{3.8}$$

Alternatively, the combined basic belief for the class C_2 can be determined as follows

$$m(C_2) = \sum m(h_2), \text{ therefore} \tag{3.9}$$

$$\begin{aligned} m(C_2) = m(A_2)m(B_1)m(D_2) \\ +m(A_1)m(B_2)m(D_2) \\ +m(A_2)m(B_2)m(D_1) \\ +m(A_2)m(B_2)m(D_2). \end{aligned} \tag{3.10}$$

The value of the basic belief for the class C_1 "specific event" is determined as

$$m(cl_1^k) = \begin{cases} P(x \in C_1/cl^k(x) = 1), \\ P(x \in C_1/cl^k(x) = 2). \end{cases} \tag{3.11}$$

The value of the basic belief for the class C_2 "no specific event" is the complement of $m(cl_1^k)$. Alternatively, $m(cl_2^k)$ can be determined as

$$m(cl_2^k) = \begin{cases} P(x \in C_2/cl^k(x) = 1), \\ P(x \in C_2/cl^k(x) = 2). \end{cases} \tag{3.12}$$

The demonstrated example in Section 2.2.3 is considered in order to simplify the explanation of the developed fusion method as well as to approve its plausibility. The plausibility is approved by the comparison of the fusion results of BBF method with fusion results of the BCR. Here only the first three classifiers (A, B, and D) are taken into account in order to approve the BBF method for odd classifier sets. If case 2 ($A : Neg., B : Pos., D : Pos.$) is considered in detail, the related belief values for each classifier for the considered case are determined using Eq. 3.11 and Eq. 3.12. The determined belief values are given in Table 3.2.

Table 3.2: Basic belief values for the classifiers A, B, D (case number 2)

Classifier	Decision	$m(cl_1^k)$ [%]	$m(cl_2^k)$ [%]
A	Neg.	10	90
B	Pos.	90	10
D	Pos.	70	30

The combination of the basic beliefs for the considered scenario (case 2) using the proposed decision fusion method leads to a final degree of belief for the existence of the specific event $bel(Pos.) = 66.6\%$. The degree of belief against the existence of the specific event (second class) is the complement, $bel(Neg.) = 23.4\%$. The final decision for case 2 is "Pos.: specific event exist" because the degree of belief for the existence of specific event is greater than the degree of belief against the existence of specific event ($bel(Pos.) > bel(Neg.)$).

The decision fusion process of any three independent classifiers leads to eight different decision probabilities (scenarios). Fusion results using BCR and BBF method for the probable decision scenarios of the three classifiers (A, B, and D in the demonstrated example in Section 2.2.3)) are shown in Table 3.3.

The results in Table 3.3, which are graphically demonstrated in Fig 3.1 indicate the following:

Table 3.3: Fusion results of BBF method and BCR for three independent classifiers [Rot12]. Green color denotes the best fusion performance of BBF over BCR. Red color denotes the best fusion performance of BCR over BBF.

Case	A : $m(A_1)$ [%]	B : $m(B_1)$ [%]	D : $m(D_1)$ [%]	BBF $bel(Pos.)$ [%]	BCR $bel(Pos.)$ [%]
1	Pos. (80)	Pos. (90)	Pos. (70)	90.20	98.82
2	Neg. (10)	Pos. (90)	Pos. (70)	66.40	70.00
3	Pos. (80)	Neg. (05)	Pos. (70)	57.90	32.94
4	Pos. (80)	Pos. (90)	Neg. (15)	75.90	86.40
5	Neg. (10)	Neg. (05)	Pos. (70)	10.30	1.35
6	Neg. (10)	Pos. (90)	Neg. (15)	21.30	15.00
7	Pos. (80)	Neg. (05)	Neg. (15)	15.55	3.58
8	Neg. (10)	Neg. (05)	Neg. (15)	02.60	0.1

- The developed approach leads to plausible final decisions for all cases.
- The plausibility of BBF method is ensured by the comparison with fusion results using BCR.
- For case three, BBF method leads to a final positive decision. On the other hand, BCR leads to final negative decision. However, the fusion result of the BBF method seems more plausible than the result predicted by BCR. Owing to the human experts (senses), the combination should lead to final positive decision. This is because two classifiers (A, D) provide positive decisions with relatively high degree of accuracy and only one classifier (B) provides a negative decision with a high degree of accuracy.

3.3 Combining an even set of independent classifiers using BBF

The fusion of odd number of independent classifiers is introduced in the previous section. This section presents the developed BBF method for reliable decision making of an even set of independent classifiers.

Even set of independent classifiers denotes multiclassifier systems, which consist of even number (2, 4, 6, etc.) of independent classifiers.

Majority rule is successfully applied for the basic beliefs combination of the individual classifiers decisions in case of the odd set of independent classifiers. This is because for any alternative basic belief combination of the different classifiers classes, the numbers of the combined basic beliefs for one class be always greater than the other. However, majority rule can not be used successfully for combining even sets of independent classifiers. To approve this claim, the rule is used to combine four independent classifiers (the demonstrated example in Section 2.2.3). The rule can successfully combine the basic beliefs for the elements in which the numbers of basic beliefs for one class is greater than the other (for the element in which the number of $m(cl_1^k)$ is greater than the number of $m(cl_2^k)$ or vice versa). Thus the combination leads either to hypothesis h_1 or h_2 (Table 3.4). In case of the equality of the numbers of basic beliefs for the different classes (for the element in which the number of $m(cl_1^k)$ is equal to the number of $m(cl_2^k)$), the combination leads to the hypothesis h_3 (Table 3.4).

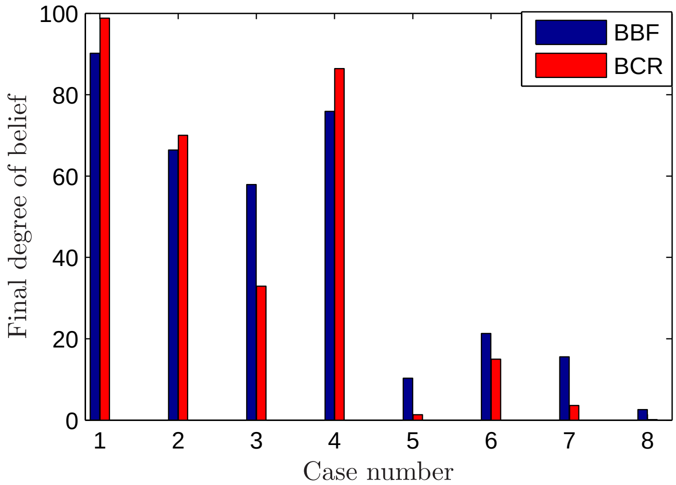

Fig. 3.1: Fusion results of BBF method and BCR for three independent classifiers

Table 3.4: Basic belief combination of four independent classifiers using majority rule

		$m(A_1)$		$m(A_2)$	
		$m(D_1)$	$m(D_2)$	$m(D_1)$	$m(D_2)$
$m(B_1)$	$m(E_1)$	h_1	h_1	h_1	h_3
	$m(E_2)$	h_1	h_3	h_3	h_2
$m(B_2)$	$m(E_1)$	h_1	h_3	h_3	h_2
	$m(E_2)$	h_3	h_2	h_2	h_2

The BBF method is adapted by integrating a further combination rule (beside the majority rule) to obtain an appropriate combination for the elements in the combination table, for which the numbers of basic beliefs for the different classes are equal.

The integrated rule checks whether the summation of the basic belief values for class 1 (specific event) n_1 is either greater than, smaller than, or equal to the summation of the related basic belief values for class 2 (no specific event) n_2. Hypothesis h_1 is supported if the $n_1 > n_2$; whereas hypothesis h_2 is supported if $n_1 < n_2$. Otherwise hypothesis h_3 is supported.

To demonstrate the combination process using BBF method for even set of independent classifiers, case 10 ($A : Pos., B : Neg., D : Pos., E : Neg.$) in the presented example in Section 2.2.3 is considered. Their related belief values are determined using Eq. 3.11 and Eq. 3.12. The determined belief values are given in Table 3.5.

Table 3.5: Basic belief values for the classifiers A, B, C, D (case number 10)

Classifier	Decision	$m(cl_1^k)$ [%]	$m(cl_2^k)$ [%]
A	Pos.	80	20
B	Neg.	5	95
D	Pos.	70	30
E	Neg.	20	80

As a next step, the basic belief combination table is formed based on the majority rule and the integrated combination rule. Table 3.6 shows the resulted hypotheses by the combination of the basic beliefs for the considered case. For example, the basic belief combination of $m(A_1), m(B_1), m(D_2)$, and $m(E_2)$ leads to hypothesis h_2. This is because

$$n_1 = m(A_1) + m(B_1) = 0.85, \tag{3.13}$$

$$n_2 = m(D_2) + m(E_2) = 1.10, \tag{3.14}$$

consequently, $n_1 < n_2$.

Table 3.6: Basic belief combination of four independent classifiers (case number 10)

		$m(A_1)$		$m(A_2)$	
		$m(D_1)$	$m(D_2)$	$m(D_1)$	$m(D_2)$
$m(B_1)$	$m(E_1)$	h_1	h_1	h_1	h_2
	$m(E_2)$	h_1	h_2	h_2	h_2
$m(B_2)$	$m(E_1)$	h_1	h_2	h_2	h_2
	$m(E_2)$	h_2	h_2	h_2	h_2

The combined basic belief for the existence of a specific event is calculated by applying Eq. 3.4

$$\begin{aligned} m(Pos.) = & m(A_1)m(B_1)m(D_1)m(E_1) \\ & +m(A_1)m(B_1)m(D_1)m(E_2) \\ & +m(A_1)m(B_1)m(D_2)m(E_1) \\ & +m(A_1)m(B_2)m(D_1)m(E_1) \\ & +m(A_2)m(B_1)m(D_1)m(E_1). \end{aligned} \tag{3.15}$$

The final degree of belief for class 1 $bel(Pos.)$ is determined using Eq. 3.6.

Hence, the resulted uncertainty in the final decision for the considered case is equal to zero (the combination of the basic beliefs did not lead to hypothesis h_3 (Table 3.6)).

The final degree of belief for class 2 $bel(Neg.)$ is the complement of $bel(Pos.)$. The combination leads to the final degree of belief of class 1 and 2, $bel(Pos.) = 13.8\%$ and $bel(Neg.) = 86.2\%$, respectively. Class two is assigned as the final fusion result.

The following points can be concluded from the introduced example:

- The combination of the basic beliefs for any four independent classifiers leads to the same hypotheses in case of the inequality of the number of combined basic beliefs for the different classes regardless of their basic belief values; i.e. the results h_1 and h_2 in Table 3.4 for the combination of any four independent classifiers does not change and still as they are demonstrated in this table.

- The combination of the basic beliefs in case of the equality of the numbers of the combined basic beliefs for the different classes can lead to different results from one combination case to another depending on the basic belief values of the combined elements; i.e. the results h_3 in Table 3.4 can varied from one decision scenario to another depending on the values of the combined elements. The combination can lead either to h_1, h_2, or h_3 depending on the values of n_1 and n_2.

The decision fusion process of any four independent classifiers leads to sixteen different decision probabilities (scenarios). Fusion results using BCR and BBF method for the probable decision scenarios of the four classifiers (A, B, D, and E in the demonstrated example in Section 2.2.3)) are shown in Table 3.3.

The results in Table 3.7, which are graphically demonstrated in Fig 3.2 indicate the following:

- The developed BBF method leads to plausible final decisions for all cases.

- The plausibility of BBF method is ensured by the comparison with the fusion results using BCR.
- Both methods leads to the same final decision for all considered decisions scenarios, although the resulted degree of belief of both methods is differed from each other in several decision scenarios.
- The divergence of the final degree belief of both methods is less than 3% in the 16 considered decision scenarios except the scenarios 3, 7, 8, and 11. In these mentioned scenarios, the divergence is between 18% to 23%. However, this divergence does not affect the final decision.
- The fusion results of the developed BBF method in case three seems more plausible than the result predicted by BCR.

  The reliability of the different decisions statements in this case is high. Although the reliability of the negative decision is higher than the other three positive decisions, but it stills only one negative decision against three positive ones. Therefore, the belief of the final positive decision should be very high. The BBF method provided a higher degree of belief than the BCR.
- The fusion results of BCR in case 7, 8, and 11 seem more plausible than the results predicted by BBF method.

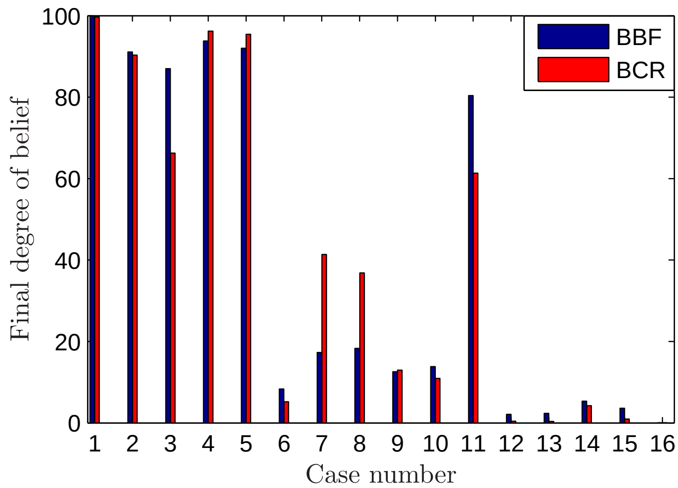

Fig. 3.2: Fusion results of BBF method and BCR of four independent classifiers

Table 3.7: Fusion results of BBF method and BCR for four independent classifiers [Rot12]. Green color denotes the best fusion performance of BBF over BCR. Red color denotes the best fusion performance of BCR over BBF.

Case	$A:$ $m(A_1)$ [%]	$B:$ $m(B_1)$ [%]	$D:$ $m(D_1)$ [%]	$E:$ $m(E_1)$ [%]	BBF $bel(Pos.)$ [%]	BCR $bel(Pos.)$ [%]
1	Pos.(80)	Pos.(90)	Pos.(70)	Pos.(80)	99.88	99.70
2	Neg.(10)	Pos.(90)	Pos.(70)	Pos.(80)	91.12	90.32
3	Pos.(80)	Neg.(05)	Pos.(70)	Pos.(80)	87.02	66.27
4	Pos.(80)	Pos.(90)	Neg.(15)	Pos.(80)	93.82	96.21
5	Pos.(80)	Pos.(90)	Pos.(70)	Neg.(20)	92.04	95.45
6	Neg.10	Neg.(05)	Pos.(70)	Pos.(80)	8.31	5.18
7	Neg.10	Pos.(90)	Neg.(15)	Pos.(80)	17.31	41.38
8	Neg.(10)	Pos.(90)	Pos.(70)	Neg.(20)	18.32	36.84
9	Pos.(80)	Neg.(05)	Neg.(15)	Pos.(80)	12.56	12.94
10	Pos.(80)	Neg.(05)	Pos.(70)	Neg.(20)	13.82	10.94
11	Pos.(80)	Pos.(90)	Neg.(15)	Neg.(20)	80.38	61.36
12	Neg.(10)	Neg.(05)	Neg.(15)	Pos.(80)	2.10	0.41
13	Neg.(10)	Neg.(05)	Pos.(70)	Neg.(20)	2.34	0.34
14	Neg.(10)	Pos.(90)	Neg.(15)	Neg.(20)	5.34	4.23
15	Pos.(80)	Neg.(05)	Neg.(15)	Neg.(20)	3.59	0.92
16	Neg.(10)	Neg.(05)	Neg.(15)	Neg.(20)	0.02	0.03

4 Experimental realization and validation of a multisensor-based monitoring system

This chapter introduces the developed monitoring system for detecting target objects within the material transported during a production process.

During the progress of this work, the most parts of this chapter have been published/demonstrated in [ASSSS10, ASSSS11, ASS12, ASSSS12, ASSS13] and [Rot12, Win11].

4.1 Concept and elements of the designed system

Owing to the complexity and variety of detection schemes in production processes, the task cannot be solved satisfactorily using only one sensor technique. Moreover, due to the complexity of the transportation process, no single sensor technique can achieve the task directly. Thus, different physical effects are considered to solve this pattern recognition task, described as follows:

- Force which induces impact responses during transportation of target objects. These responses should be measured by sensors (five acceleration sensors here) in the impact area along the transport belt.
- Topographic of the transport belt including the transported overburden and the target objects. This surface topographic is reconstructed based on a laser scanner.

In Fig. 4.1 the locations of different sensors along the transport belt are shown. Due to the geometrical distribution of the used sensors and the behavior of the discharged target objects on the transport belt, an inevitable and varying time shift between the stimulations of the individual sensors exist. This makes the fusion in the observation and feature levels difficult. Therefore, signal preprocessing, feature extraction, and classification for the individual signal sources (five acceleration signals and a laser scanner signal here) are used. Each type of the considered physical effects are proceeded in an individual detection module. Each detection module outputs a decision statement. These decisions are combined using a fusion process to obtain a final decision about the system state (target object present yes/no).

The developed object monitoring system consists of the following modules (Fig. 4.2)

- Acceleration module,
- Laser scanner module, and
- Decision fusion module.

Each module is described and discussed in the following sections.

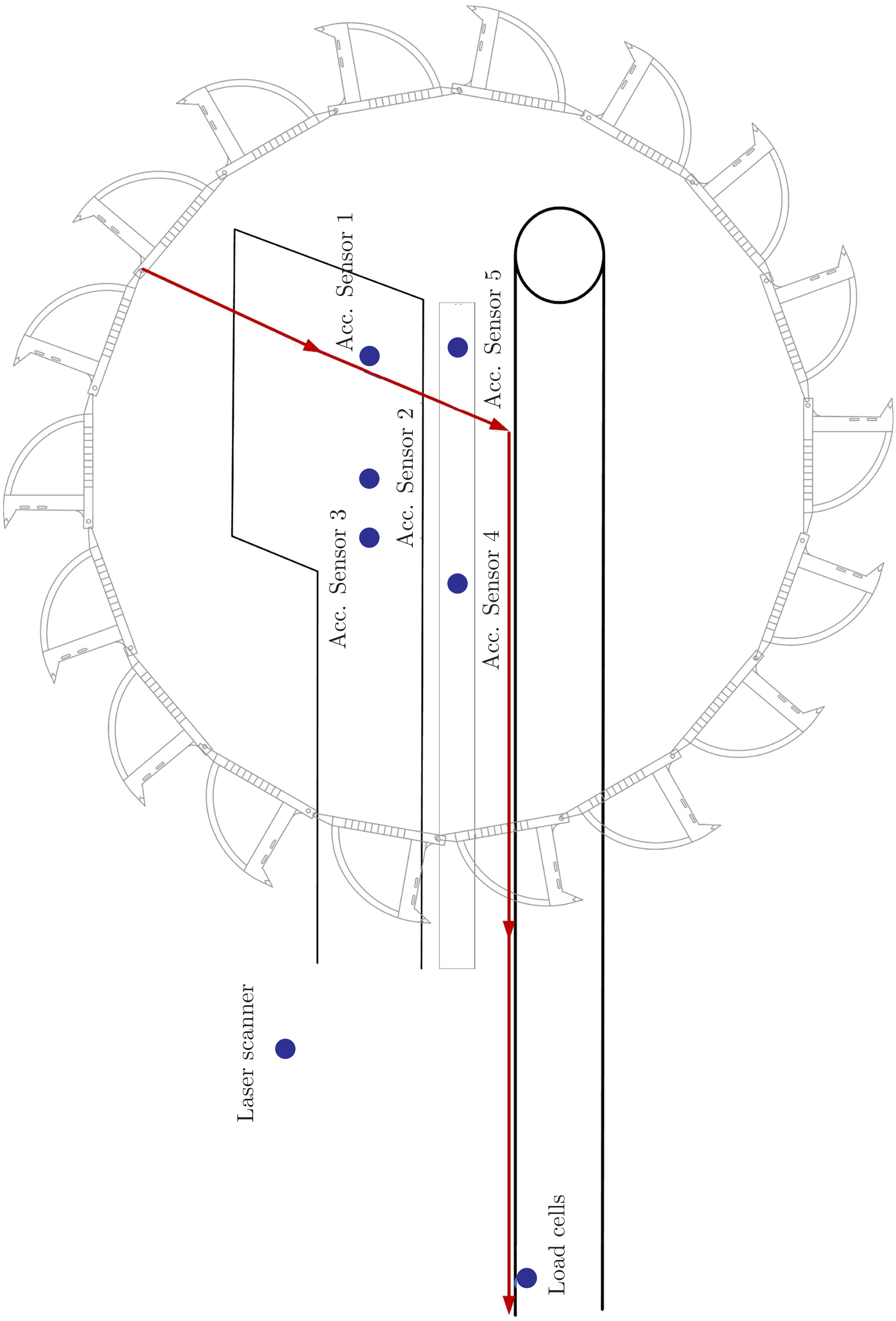

Fig. 4.1: Position of the different sensors along the transport belt [ASS12]

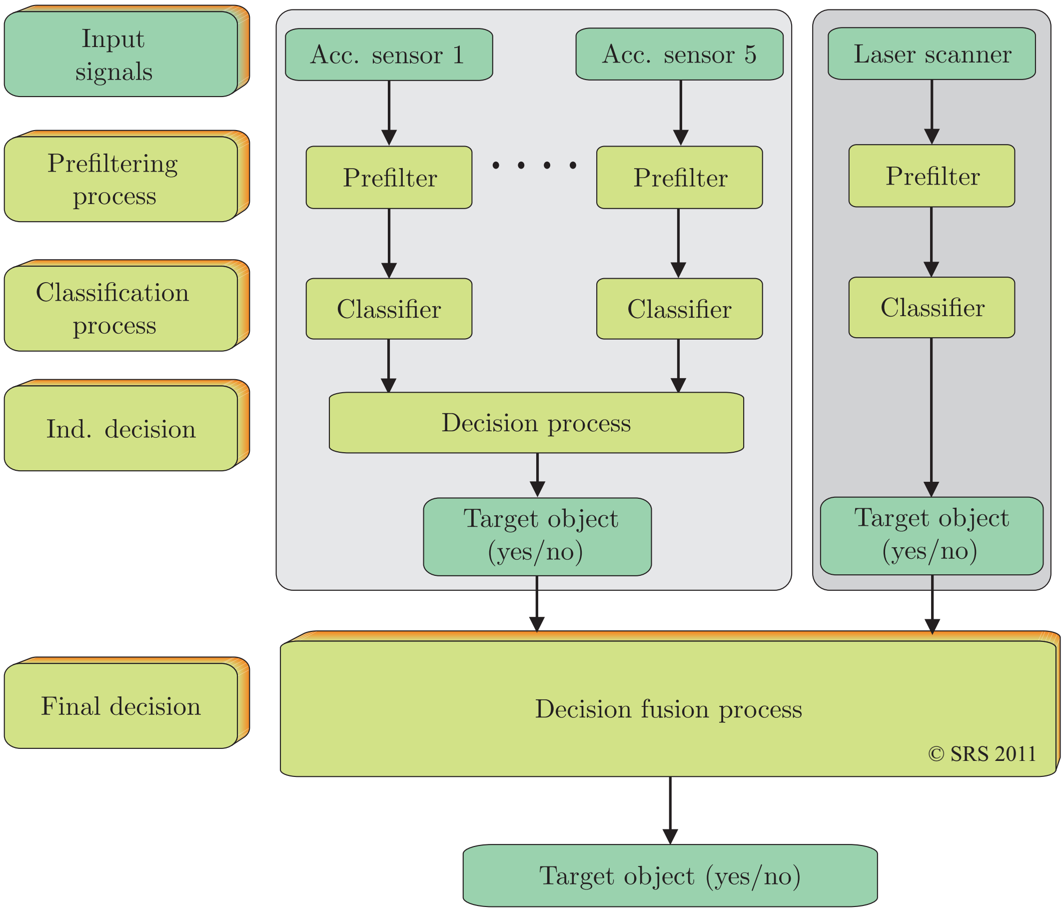

Fig. 4.2: Monitoring system for target object detection

4.2 Acceleration module

Two different detection approaches for the intended acceleration module were developed and compared. Signals from the acceleration sensors were considered first. Owing to the mentioned inevitable time shift between the object impact stimulations of the individual sensors, signal preprocessing, feature extraction, and classification, were applied to the individual acceleration sensors. Then a decision fusion process based on specific decision criteria is applied to combine the preliminary individual decisions of different classifiers (target object present yes/no) (Fig. 4.3).

Two different detection approaches for the acceleration module were investigated. The first uses STFT as a prefilter and SVM as a classifier. The second approach uses CWT as a prefilter and SVM as a classifier. The decision fusion process in both approaches is realized using different criteria. Both approaches are described and discussed in the following sections.

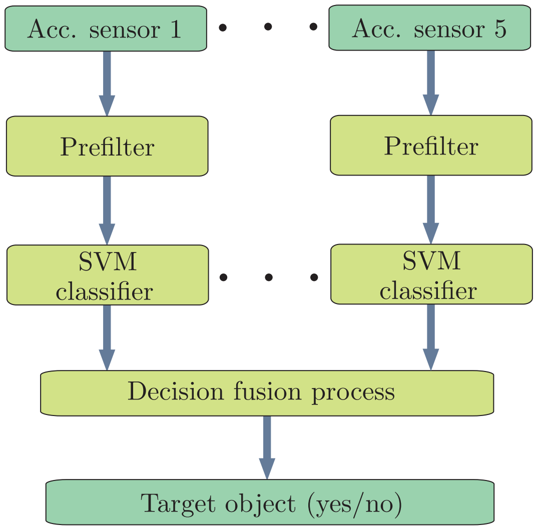

Fig. 4.3: Detection approaches based on STFT-SVM and CWT-SVM [ASSS13]

4.2.1 Approach I: Detection system based on STFT and SVM

In the STFT-SVM approach, STFT is used to extract relevant information from the signals obtained from different acceleration sensors. The SVM is then used to classify the extracted features. In addition, a specific fusion process based on SVM and experimentally-based decision rules is developed and applied to combine the preliminary decisions of the individual sensors. The signals are individually prefiltered with STFT (Fig. 4.3 and Fig. 4.4). This prefiltering process is used to extract relevant features of the acceleration signals (Section 4.2.1.1). A set of supervised classification filters, denoted SVM I, is developed to classify the features extracted from each sensor signal. An adjustable decision fusion process is developed to combine the preliminary individual decisions of the different classifiers (Section 4.2.1.3). Feature extraction, classification, and decision fusion processes are described in detail below.

4.2.1.1 Feature extraction based on STFT

The STFT extracts relevant information on system states. It serves to classify the information related to a single information path based on previously observed phenomena for a sensor signal. Fig. 4.5(a) (raw signal) shows a raw sample acceleration signal during the production process. At 12.5 s, a target object was manually classified. The impact of this object results in strong acceleration signal amplitudes. The other peaks in the signal are caused by other unknown events and are not object-induced signal changes. From the raw acceleration signals in the time domain it is very difficult to distinguish target object's effect from other unknown events. The different events can be classified on the basis of features extracted using prefilters

(STFT). As shown by the spectrogram in Fig. 4.5(a), the target object causes strong excitation of low frequencies. By contrast, higher frequencies are excited more by unclassified or unknown events. This effect is used to distinguish events due to target objects from those related to other events.

4.2.1.2 Classification process

Three classification modules are included in the detection system (Fig. 4.4). The SVM-based algorithms are used to detect the system states. The Libsvm algorithm [CL11] is used to realize the SVM classifiers.

The module SVM I

Due to the inevitable time delay between the excitation of the sensors which is constantly varying as a result of the structural dynamical behavior between the impact's and the sensor's locations. This affects the feature vectors. A classifier based on the SVM algorithm (SVM I) is developed for each individual acceleration signal. Data clearly indicating the presence of target objects are used to train SVM I. This should limit the false alarm rate, which is directly affected by the strength and intensity of the indicators used for training. Weak indicators lead to a higher rate of false alarms and vice versa. The decision functions of the individual classifiers generated by SVM I are input as preliminary decisions into subsequent stages to confirm the assumed system state.

The module SVM II

When SVM I does not provide sufficient information, the decision on the presence of target objects is uncertain. In such a case, and in the cases mentioned in the third classification module (SVM III), a more local and precise investigation is necessary. Data with weak indications of the presence of target objects are used to train module SVM II; the limited area of application of the signal allows more flexible detection criteria.

The SVM II is trained with data consisting of two states. State 1, "target object present", is represented by training data with weak indications of the presence of target objects. State 2, "uncertain", is represented by training data with all other indications except state 1. The output statement of SVM II is either "target object present" or "uncertain".

The module SVM III

A classification process based on SVM III is performed in cases for which SVM II provides an uncertain output statement. The SVM III provides further data classification for uncertain output statements. The SVM III is trained using data with clear indication of no target objects (state 1) and data with uncertain indications (state 2). The output statement of SVM III is either "target object not present" or "uncertain".

The SVM II and SVM III classifiers are used for more accurate trained classification locally in cases where further assessment of unclear decisions is required.

4.2.1.3 Adjustable decision fusion process

A new decision fusion process is developed to combine individual preliminary decisions and generate a final decision on the system state. The decision method is based on knowledge derived from analysis of experimental data from different acceleration sensors. It is designed to obtain the highest possible detection rate for the lowest possible false alarm rate. Therefore, tuning parameters are used to systematically adjust the fusion process.

The decision fusion filter consists of two rule-based filter levels and classification levels SVM II and SVM III (Fig. 4.4).

Classification level SVM I provides preliminary decision functions for the individual classifiers (Section 4.2.1.2). Depending on the individual preliminary decisions, the final decision of the acceleration module could be met by either rule-based filter I or by rule-based filter II.

The rule-based filter I consists of predefined rules that govern the final decision of the acceleration module. When it is impossible to achieve a reliable final decision from the acceleration module based on current values of the individual preliminary decision functions, a specific rule to trigger further classification levels (SVM II and SVM III) is included in rule-based filter I. The rules for rule-based filter I are as follows:

- *Rule I*: At least two simultaneous positive individual decisions lead to a final decision of "positive: target object present".
- *Rule II*: Weak individual positive decisions with a decision value less than the experimentally defined threshold value T_1 are ignored, leading to a final decision of "negative: no target object present".

  Experimental evidence shows that weak individual positive decisions (with decision values less than T_1) are generally caused by events denoted as non-target objects. Therefore this kind of decision is ignored and not considered as an indicator of a target object.
- *Rule III*: Individual positive decision with a decision value greater than the experimental threshold T_2 ($T_2 > T_1$) leads to a final decision of "positive: target object present".

- *Rule IV*: Individual positive decision with a decision value greater than T_1 and less than T_2 triggers further classification levels.

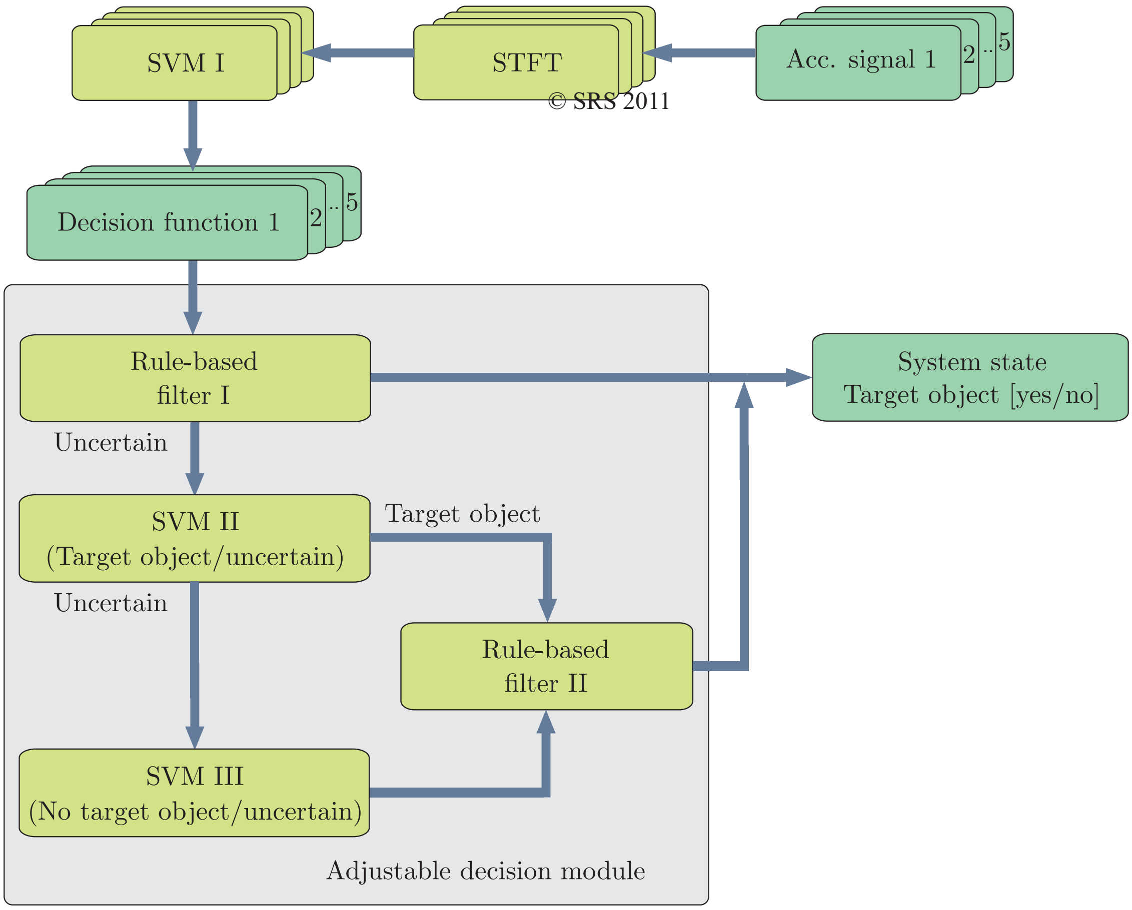

Fig. 4.4: Adjustable decision fusion process [ASSSS11, ASSS13]

As mentioned before, classification levels SVM II and SVM III are activated if rule IV is fulfilled. When an individual positive decision has a decision value greater than T_1 and less than T_2, the other four acceleration signals that provide negative decision values (parallel to the single individual positive decision) are subjected to more accurate evaluation using either SVM II alone or both SVM II and SVM III. Further classification is performed locally on neighboring areas of the corresponding acceleration signals to confirm or disprove the correctness of the single individual positive decision.

The acceleration signals are first evaluated using SVM II. The SVM II output statement is either "target object present" or "uncertain". Thus, SVM II confirms the presence of target objects. The SVM III evaluation is performed for acceleration signals that yield an uncertain output statement from SVM II. These acceleration signals are evaluated for the presence of events denoted as "no object". The output statement of SVM III is either “target object not present” or “uncertain”. Thus, SVM III confirms the absence of the target object.

The single individual preliminary decision from SVM I and the other four decisions provided by SVM II, SVM II and SVM III, or SVM III are combined using rule-based filter II. The rules for rule-based filter II are as follows:

- *Rule I*: If the number of output statements “target object present” is greater than the number of “uncertain” statement provided by SVM II and SVM III, the final decision is “positive: target object present” (majority rule).
- *Rule II*: An individual output statement “target object not present” from SVM III leads to a final decision of “negative: no target object”.

The decision generated by the fusion module depends on re-evaluation of individual partial decisions. Owing to the complexity of the system to be monitored, it is difficult to provide these benefits using classical fusion techniques. The main reason for using the proposed method for fusion is the inevitable and varying time shift between the object impact stimulation of the individual sensors, and the fact that the effect of noise and disturbance signals to the system and sensors (both individual and group sensors) is inevitable. Therefore, the importance of individual decisions is retained by combining and comparing them with other decisions that do not necessarily coincide in time. This data handling requires a floating decision window, which increases the computational load.

The improvement in quality resulting from the developed fusion technique over single-stage SVM classifiers demonstrates the validity of the approach. This multi-stage technique with additional stages focuses mainly on classes that cannot be identified with suitable reliability, and therefore have to be considered separately and in detail.

It should be noted that the floating window and decision re-evaluation require buffer savings for the range of data considered. These buffer savings should cover the processing window and transformed data for the different channels and their decisions, as well as decisions generated by the fusion module. These buffer savings increase the memory requirements of the system and the time required for the final decision owing to the inefficient buffering time.

In spite of the complexity of the detection system, the main requirement is that the final decision should at least be faster than subsequent events to provide enough time to isolate target objects that are detected. This requirement is fulfilled according to the implementation results presented below.

4.2.1.4 Industrial implementation and results

The STFT algorithm is used as a prefilter to extract relevant features from acceleration signals. The spectrograms generated (Fig. 4.5(a) and Fig. 4.5(b)) show the features extracted (frequencies in the range up to 3250 Hz) as functions of time. The impulse intensities for each feature are represented by a suitable color map. The feature vector is based on 511 features, one for each acceleration signal.

The spectrogram in Fig. 4.5(a) reveals that frequencies between 1 and 200 Hz are dominant at 12.5 s (red) owing to the impact of a target object. The specific behavior depends on the structural dynamic characteristics of the contact surface on which the sensor is mounted and on the impact position. Higher frequencies at 12.5 s show less energy (light blue) than frequencies below 200 Hz.

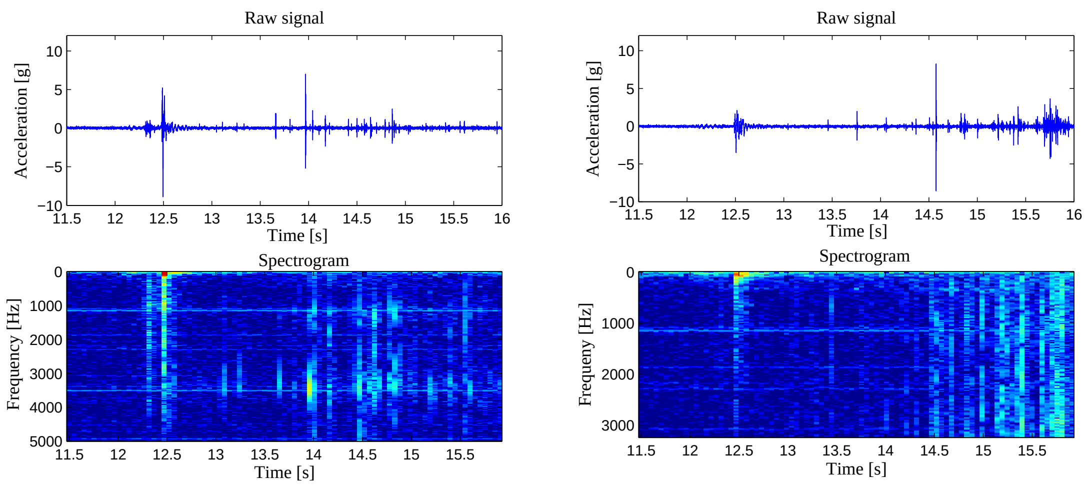

(a) Acceleration signal for sensor 1 (b) Acceleration signal for sensor 2

Fig. 4.5: Acceleration signal for sensors 1 and 2 [ASSSS11, ASSS13]

The amplitude behavior of the acceleration signal at 13.95 s (Fig. 4.5(a)) in the raw time-domain signal is in principle similar to that at 12.5 s; however the range of frequencies excited in the STFT features is different (2560–4200 Hz). Thus, it is experimentally observed that the machine structure reacts differently to target object events and allows a statement about the presence of objects. Therefore, target objects and other events can be detected, classified, and separated. If the resonance properties of the structure at the collision point, taking into consideration the sensor position, are known and are considered to allow reliable distinction between relevant frequency ranges and related impact power, the distinction is considered reliable.

In the raw signal in Fig. 4.5(b), the event observed at 12.5 s and the disturbance effects between 15.6 and 16 s show similar amplitudes and behavior in the time domain. It is expected that the excited structural dynamics at 12.5 s responds differently (in the frequency domain 0–200 Hz (Fig. 4.5(b))).

The approach was tested using an experimental set of real industrial data. The results for preliminary application to the system are summarized in Table 4.1. The best individual detection accuracy is 58.3% (classifiers 1 and 4). Classifier 5 leads to the lowest accuracy and false alarm rates, although it has the smallest number of support vectors, indicating comparatively low levels of noise. This result demonstrates a typical compromise: an increase in the detection rate leads to an increase in the false alarm rate (Table 4.1).

Table 4.1: Classification results for the STFT-SVM approach [ASSS13]

Sensor/classifier	1	2	3	4	5
Training data					
Target objects	17	19	17	17	16
No. of support vectors	193	210	177	158	79
SVM kernel			Linear		
Individual results for the test data					
Target objects			36		
Objects detected	21	20	19	21	16
Accuracy [%]	58.3	55.5	52.8	58.3	44.4
False alarms	18	14	7	4	2
Fusion results for the test data					
Objects detected			27		
Accuracy [%]			75		
False alarms			7		
False alarms/number of objects [%]			19.4		

The accuracy of the system based on fused decisions for the acceleration sensor network is 75%, which represents an improvement of at least 16.7% over the individual accuracy rates. This improvement in accuracy indicates that the individual sensors have different views, depending on their mounting position and their relation to the materials transported, including target objects. This means that each individual classifier can detect target objects that possibly went undetected by other classifiers. The rate of false alarms can be compromised, however, because the false alarms for individual sensor paths are not necessarily identical. The fusion approach not only improves the detection rate, but also leads to a strong reduction in the number of false alarms (Table 4.1). During development of the detection system, and considering the requirements of the mechanical system, a compromise between accuracy and rate of false alarms must be achieved.

4.2.2 Approach II: Detection system based on CWT and SVM

The CWT-SVM approach uses CWT to extract relevant information from acceleration signals for the different sensor channels. The SVM is used to classify the features extracted. A fusion process is applied to combine the individual decisions of the different SVM classifiers (Fig. 4.3).

The individual sensor signals are prefiltered separately using CWT (Fig. 4.3). The features extracted for individual sensors are subjected to multistage filtering. The feature extraction and decision fusion processes are described below.

4.2.2.1 Feature extraction based on CWT

As an example, Fig. 4.6(a) shows the acceleration signal for sensor 1. To illustrate the solution concept and for the purpose of comparison, the signal was filtered using STFT (Fig. 4.6(b)) and CWT (Fig. 4.6(c)). The signal has two events, denoted as objects 1 and 2 at time points 4000 and 8500, respectively, that were manually classified as target objects. These events appear at time points 30 and 70 in the STFT extracted feature space (Fig. 4.6(b)) and at time points 4000 and 8500 in the CWT extracted feature space (Fig. 4.6(c)). A third event resulting from an unknown disturbance is evident at time point 37000 in Fig. 4.6(a). Since this event was not classified manually, it cannot denote a target object. It is also evident in the STFT and CWT extracted feature spaces.

The object at time point 8500 and the event at time point 37000 can be clearly recognized in the STFT and CWT results. In the STFT results the two events seem to be similar, whereas in the CWT results they appear to be different. In the case of CWT, the higher scales (low frequencies) for the second object are excited more strongly than the lower ones, while the lower scales (higher frequencies) are more strongly excited in the case of the disturbing event.

Unlike the case in which a target object is present, the higher scales (lower frequencies) of the disturbance are related to lower energy than the lower scales (higher frequencies). The reason is that the range of the activated frequency and accordingly the center of frequency, which coincides with the energy peak are different for the disturbance and target object. This advantage of the CWT approach is used as a base rule for further filtering steps.

To illustrate this, consider the first target object in the sample data (object 1 at time 4000) that cannot be clearly distinguished from the time series signal (Fig. 4.6(a)). The object is difficult to detect because of its impact on the mechanical structure, which is obviously dampened by the accompanying materials (overburden). In the STFT results (Fig. 4.6(b)), the presence of the object is characterized by weak excitation of low frequencies. In the CWT results (Fig. 4.6(c)), the object can be better recognized and characterized by a longer band of high scales (low frequencies) of a specific shape. The effects of objects 1 and 2 are evident in Fig. 4.6(c) and are magnified in Fig. 4.6(d).

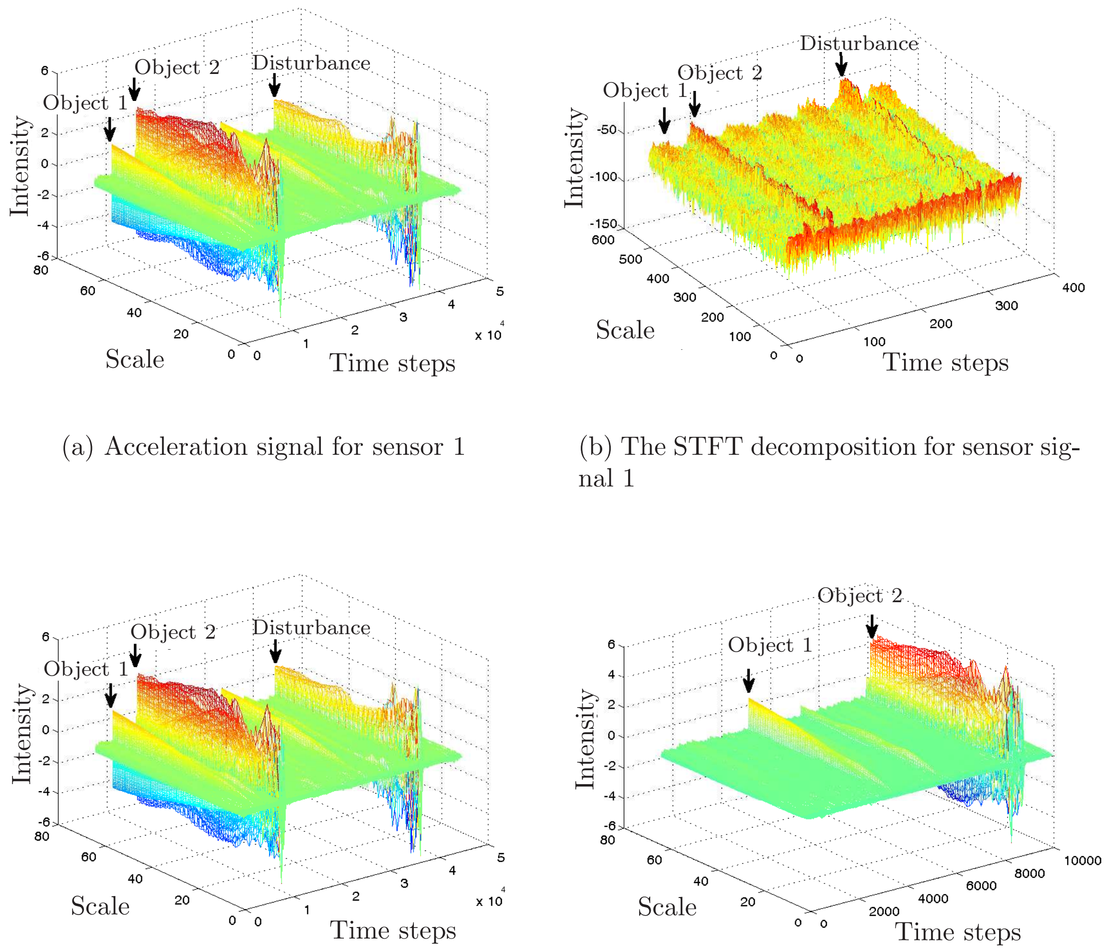

(a) Acceleration signal for sensor 1

(b) The STFT decomposition for sensor signal 1

(c) The CWT decomposition for sensor signal 1

(d) First part of the CWT decomposition

Fig. 4.6: Comparison of STFT and CWT [ASSSS12]

Several noise and disturbance sources are involved in this complex and unstable production process. These lead to difficulties in recognizing target objects. The disturbance can be stationary background noise or non-stationary noise, with large or rapid spectral changes over time, and can therefore resemble events resulting from target objects.

In Fig. 4.7(a) an acceleration signal resulting from CWT as a function of time and frequency is shown. The signal includes different events. The marked event is the only one that needs to be detected. All other events are caused by different noise events.

For efficient learning and reliable classification, further filtering is applied to reduce the data complexity. This filtering eliminates known noisy events, as described below.

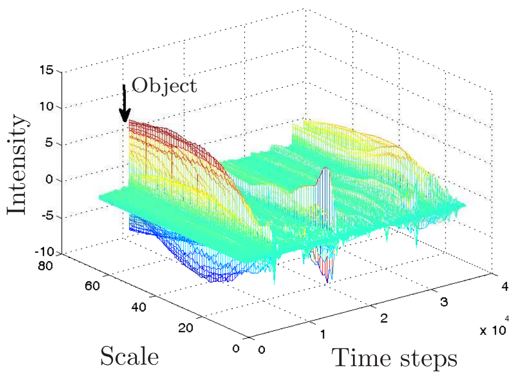

(a) The CWT decomposition of an acceleration signal

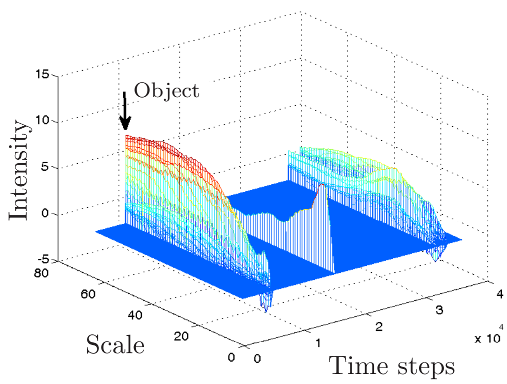

(b) The CWT decomposition of the acceleration signal after applying first prefiltering rule

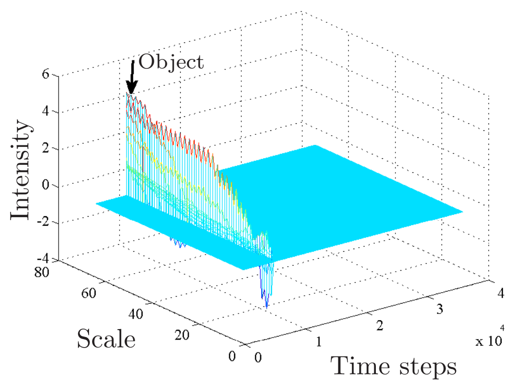

(c) The CWT decomposition of the acceleration signal after applying second prefiltering rule

Fig. 4.7: Prefiltering results of prefilter I and II [ASSS13]

Prefilter I: Prefiltering the background noise

An acceleration signal contains permanent background noise in both the time and frequency domains (Fig. 4.7(a)). The presence of events in the training data set complicates SVM training. This complexity results due to difficulty in labeling training data because of the interpenetration of the different events. Inaccurate labeling of the training data affects the classifier performance. The aim of prefilter I is to eliminate stationary background noise from the extracted features to avoid this problem and simplify SVM classifier training. This involves eliminating events in the acceleration signals for time points at which the maximum intensity of low-frequency excitation is less than an experimental threshold according to the prefiltering rule. If this condition is fulfilled, the intensity for all frequencies at such time points is set to zero (Fig. 4.7(b)).

Prefilter II: Prefiltering specific known noise behavior

The distinguishing characteristics are used to filter process-related non-stationary disturbances. The main characteristics differ for detection cases and for disturbances related to gradients and event forms. The gradient from the low-frequency to the high-frequency domain is estimated at each time point and compared to an experimental threshold. The frequency intensity is set to zero at those time points for which the gradient does not exhibit the same behavior as target events. In addition, the relative signal intensity for the low scales is checked and compared to the behavior of the target events. Experimental evidence has shown that certain behaviors for the starting scales can be known as they do not belong to target objects but to specific noise events. This characteristic was confirmed using manual classification of the target objects to be removed.

It should be noted that event strength is not necessarily a reliable characteristic for distinguishing between events to be detected and disturbances owing to the nature of the production process. Some target objects cause weaker effects than those caused by disturbances. Therefore, scale-invariant recognition based on the event form is more reliable and effective.

An example data set filtered using prefilter II is presented in Fig. 4.7(c). The second condition checks whether the gradient at each time point exhibits the behavior of the target object events.

4.2.2.2 Classification process

The Libsvm algorithm [CL11] is used for numerical realization of the SVM classifiers. An experimental data set was prepared using wavelet-based prefilters to build the training data set. The SVM classifier model is then built based on this set and used for classification of the five different acceleration signals.

4.2.2.3 Decision fusion process

The decision fusion process based on experimental data combines individual preliminary decisions to reach a final reliable decision. The decision fusion filter is a rule-based filter. The rules are as follows:

- *Rule I*: At least two simultaneously positive individual decisions lead to a final decision of "positive: target object present".
- *Rule II*: Several strong positive decisions from at least one of the five classifiers within a specific floating decision window lead to a final decision of "positive: target object present". Several relatively strong positive decisions imply that the number of positive peaks within the floating decision window is greater than an experimental threshold. In addition, the decision value should be greater than an experimental threshold.

4.2.2.4 Industrial implementation and results

Results for CWT-based detection are summarized in Table 4.2. The best individual accuracy is 58.3% (classifiers 1 and 2), but this corresponds to a higher rate of false alarms. It should be noted that decreases in the training accuracy for individual classifiers will lead to improvements in the detection accuracy; the rate of the false alarms would also increase accordingly. During development and depending on the system requirements, a compromise between detection accuracy and false alarms must be achieved.

The individual and fused results reveal that classifier fusion leads to a reduction in the false alarm rate by approximately 89%. The final detection rate is approximately 6% better than for the best individual classifier.

4.2.3 Discussion and comparison of approaches

The efficiency of any monitoring system is generally evaluated according to the detection accuracy and the false alarm rate. The challenge for any detection approach is to achieve the highest possible detection rate with the lowest possible false alarm rate. The complexity of the monitoring system should also be considered in evaluations. Complicated systems involve more unexpected defects and flaws than simple ones because of the unpredictable nature of disturbances which is not rigorously perceptible. In addition, implementation of more complicated systems usually requires more effort to realize and can involve greater difficulties in real-time applications.

According to the results in Tables 4.1 and 4.2, which use the same test data set to realize the testing phase, the STFT-SVM approach detects at least 10% more target

Table 4.2: Classification results for the CWT-SVM approach [ASSS13]

Sensor/classifier	1	2	3	4	5
Training data					
Target objects			16		
No. of support vectors			1197		
SVM kernel			RBF		
Individual results for test data					
Target objects			36		
Objects detected	21	21	20	18	13
Accuracy [%]	58.3	58.3	55.5	50.0	36.1
False alarms	7	11	12	6	1
Fusion results for test data					
Objects detected			23		
Accuracy [%]			63.9		
False alarms			4		
False alarms/number of objects [%]			11		

objects compared to the CWT-SVM approach. The detection rate is 75% for the STFT-SVM approach and only 64% for the CWT-SVM approach. This does not necessarily mean that the STFT-SVM approach is better than CWT-SVM, because the highest number of false alarms for STFT-SVM is approximately double that for CWT-SVM. It should be noted that the sensitivity of the training process affects the rate of detection and the rate of false alarms in various ways. Increasing the sensitivity of the model can increase the rate of detection, as well as the number of false alarms. In fact, a trade-off exists in the relationship between detection and false alarms. This means that both approaches have the same improvement potential with respect to detection and false alarm rates.

Other important issues regarding realization and implementation are as follows. In the first approach (STFT and SVM) a number of 7 SVM classifiers (5 of them in parallel) are developed in order to realize the proposed detection module, whereas in the second one (CWT and SVM) only one SVM classifier is developed and used for the five individual preliminary classifiers in the system. Moreover, the two sets of multiple rules required for STFT-SVM and the backward evaluation scheme are more complicated than the simple combination rules for the CWT-SVM approach. These are strong factors in judging whether the CWT-SVM approach is more efficient and reliable for real-time applications. The STFT-SVM approach is indeed difficult to design and develop and much processing effort is required for implementation. In spite of the comparable results for detection and false alarm rates, the CWT-SVM approach is more convenient to realize and implement and more appropriate for real-time applications.

For the two approaches, it is evident that the system was successful in isolating the required objects from noise events. After processing and transformation, many noise events acquire different shapes and become visually different from the target object; however, some noise events do not. Such noise events might be detected simultaneously by many sensors, which can lead to false alarms. Such noise events cannot be avoided. They are usually caused by objects that are similar to the targets but smaller in size (small stones).

Since the object size does not necessarily coincide with the event intensity, it is difficult to differentiate these smaller objects by simple adjustment of the system sensitivity, which could lead to deterioration in the performance and detection rate.

It should be noted that the accuracy achieved is not always that targeted for the intended monitoring system. These accuracies represent individual accuracies for the acceleration sensors among other detection module (laser scanner module). For this reason and according to the comparison of the false alarms rates and realization and implementation issues of both approaches, the CWT-SVM approach is chosen for the development of the overall monitoring system in combination with laser scanner and decision fusion module.

4.3 Laser scanner module

A laser scanner has been installed above the transport belt to estimate the volume of the transported material. It provides sequential cross-sectional scan profiles of the moving transport belt including overburden (Fig. 4.8). These sequential scan profiles are used in this work to reconstruct the topographic surface of the transport belt including the transported material (overburden, target objects, etc.) in order to develop a detection module for the transported target objects.

Protruding target objects from overburden cause sudden changes in the reconstructed surface topography; i.e. the beginning and the end of these objects cause sudden changes in the area under the related scan profiles. A sudden negative change between the areas of the previous and the current scan profile leads to specify the beginning of the protruding object. A sudden positive change is an indication to the end of the protruding object.

The developed detection module consists of prefiltering, filtering, validation, and classification process (Fig. 4.9). These processes are described in the following subsections.

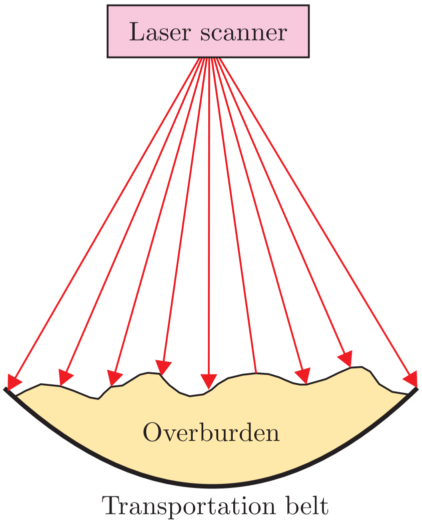

Fig. 4.8: Schematic representation of the cross-sectional scanning of the transport belt including overburden

4.3.1 Prefiltering process

The analysis of the measured data showed that some individual measurement points of the laser scanner profiles are extremely varied from their neighboring measurement points. These individual measurement points have either extremely high or extremely low values in comparison to their neighboring points (Fig. 4.10).

To eliminate such kind of measurement errors, laser scanner profiles are analyzed individually. The average height of the neighboring points for each single measurement is determined. The prefilter checks whether the difference between the individual measurement points and the average height of their neighboring points is greater than experimentally defined threshold value. If this condition is fulfilled, the height of the single point is replaced by the average height of its neighboring points.

The prefiltered scan profiles are subjected to coordination transformation process to transform them from polar to Cartesian coordinate. The goal of this process is to set laser scanner signals in a new representative and helpful form for the further filtering and evaluation processes.

4.3.2 Filtering process

The goal of this step is to extract the geometrical features of protruding objects from the overburden; i.e. to determine the length, the width, and the height of these objects.

A protruding object from the overburden can lead to sudden change in the cross-sectional area of the transported material longitudinally as well as transversely to the

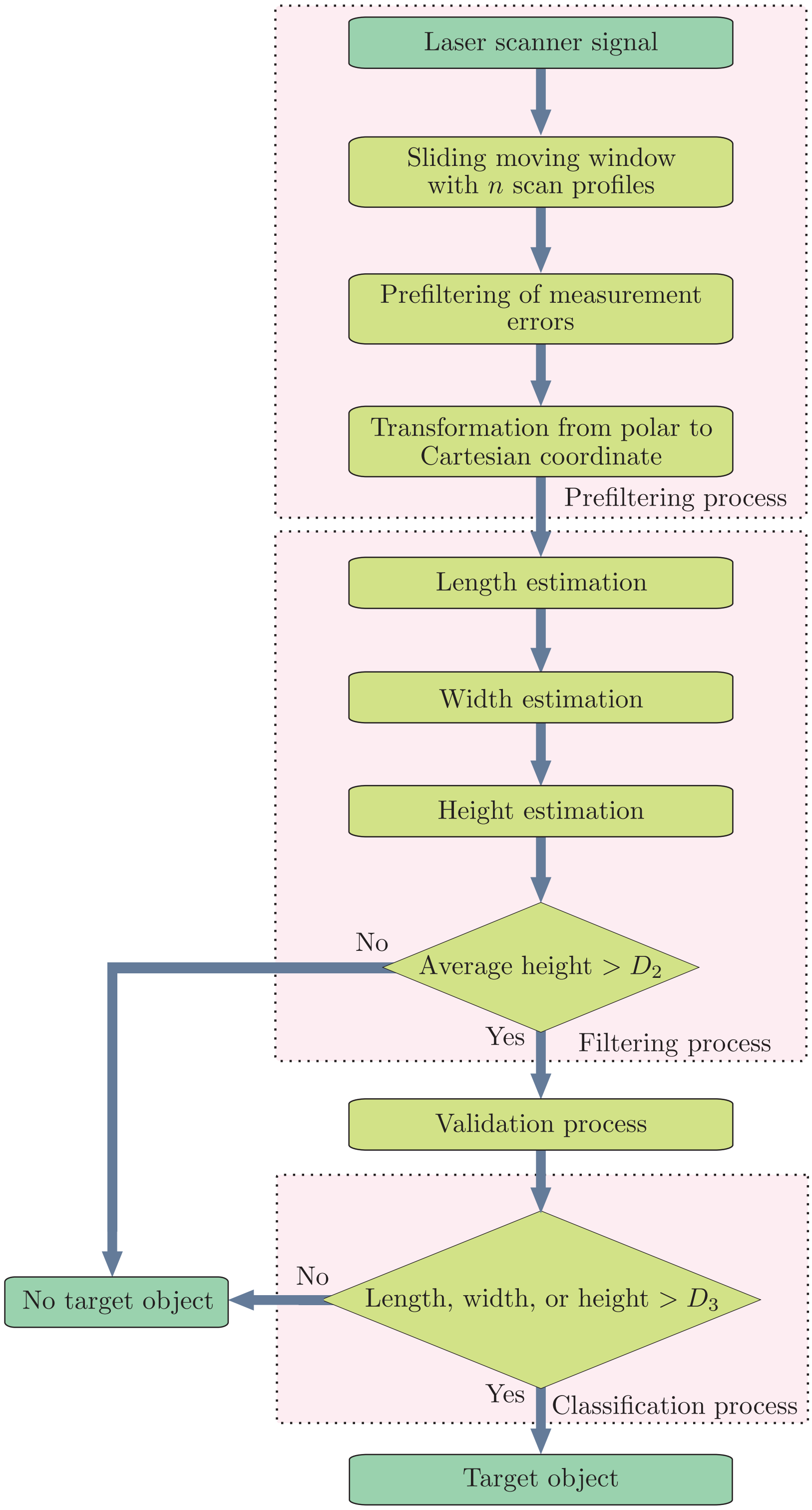

Fig. 4.9: Schematic representation of laser scanner module

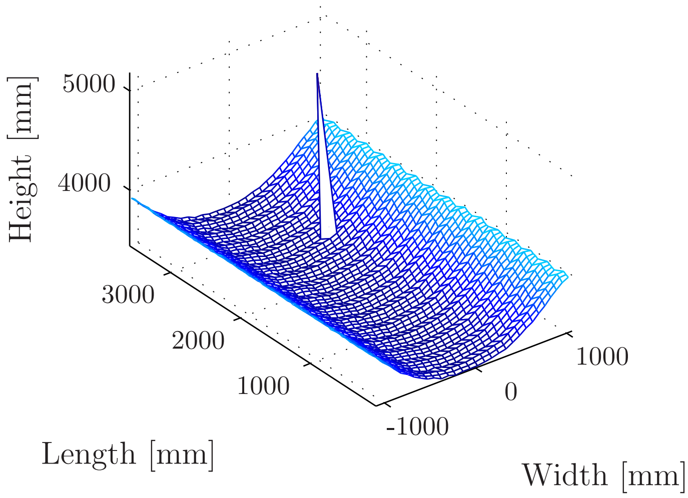

Fig. 4.10: Measurement errors in the laser scanner signal (a point with extremely high value) [Win11]

running direction of the transport belt. The consideration of these two phenomena leads to state the presence of protruding objects from the transported material.

The length of the transported object can be determined according to the time interval between the sudden negative change in the cross-sectional area along the transport belt running direction and the subsequent sudden positive change. The consideration of the distance between the sudden negative change in the cross-sectional area transverse to the transport belt and the subsequent sudden positive change allows the estimation of the object width.

The experimental analysis approved that the consideration of a simplified cross-sectional area $f(t)$ is sufficient for the length and width determination instead considering the real cross-sectional area. Once the length and width of the transported object are determined, the height of this object can be estimated.

A semi online determination of the geometrical features is performed by considering an overlapped sliding moving window with n scan profiles at each evaluation process. The determination of the geometrical features (length, width, and height) of the transported objects are described in this sequel.

4.3.2.1 Length determination of the transported object

The simplified cross-sectional area for each scan profile within the sliding moving window can be determined as

$$f(t) = \sum_{i=Fp}^{Lp} z(t,i), \tag{4.1}$$

where Fp and Lp represent the index of the first and last relevant measurement points of the scan profile, respectively. The index i is a running index, which describes the number of the measurement point within a scan profile and thus extends transverse to the running direction of the transport belt. The index t is running index, which describes the serial number of the scan profiles, which extends longitudinally to the running direction of the transport belt, and can also be considered as time running index. The parameter $z(t,i)$ denotes the vertical distance of the measurement point i of the scan profile t from the laser scanner (in Cartesian coordinates).

The change of the simplified cross-sectional area vector,

$$S(t) = f(t) - f(t+1), \tag{4.2}$$

is determined to identify the beginning and the end of a possible protruding object. The vector $S(t)$ is subjected to smoothing process to eliminate the sudden changes, which might be caused by the transported material. The Fig. 4.12 shows the smoothed vector $S_s(t)$ for the object shown in Fig. 4.11.

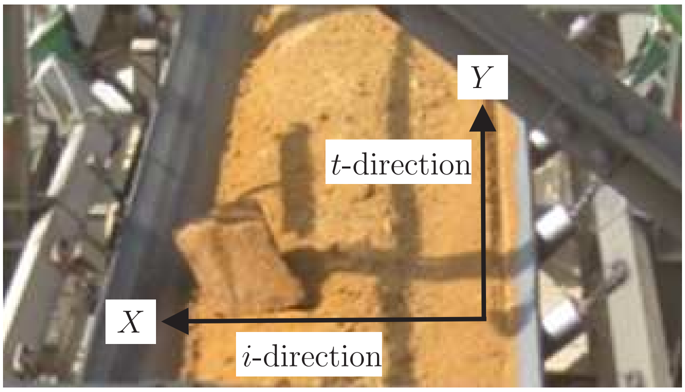

Fig. 4.11: Target object on the transport belt [Win11, ASS12]

The scan profile, which identifies the beginning of an object is defined through the high negative change of the $S_s(t)$ values. On the other hand, the scan profile, which identifies the end of an object is defined through the high positive change of the $S_s(t)$ values. If a high negative value falls below an experimentally defined negative threshold value, the index of the related scan profile Beg_{Ob} is recognized and considered as the beginning of an object in the running direction of the transport belt. After that, the related end point (assumed object end) of the recognized beginning point (considered object beginning) is searched. This process (recognition of the assumed object end) is performed as follows: First, the algorithm checks whether a point of the $S_s(t)$ has a value greater than experimentally defined positive threshold value. Second, if this condition is fulfilled, the next four points of the vector $S_s(t)$ are analyzed to check whether they posses values greater than the defined threshold value. Third, the index of the related scan profile End_{Ob} of the last point, which exhibits a change greater than the threshold value is recognized and considered as the end of the analyzed object.

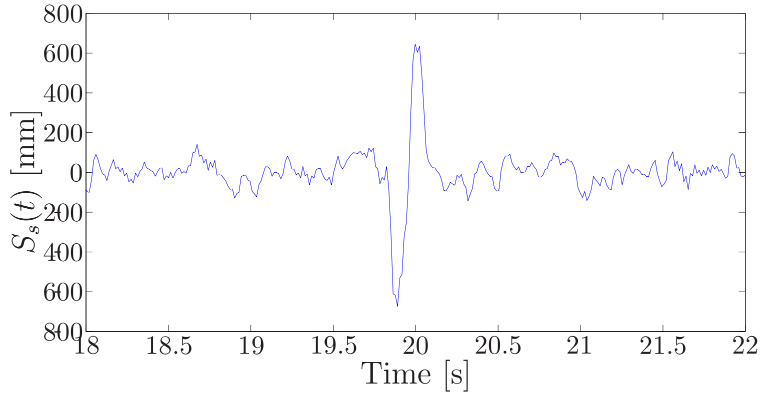

Fig. 4.12: The smoothed vector $S_s(t)$ of the object shown in Fig. 4.11 [Win11]

Second step are performed in order to ensure that the real end of analyzed object is found. Once the indices of the related scan profiles of both the beginning and end of the object are specified, the length of this object can be determined from

$$L = (End_{Ob} - Beg_{Ob})T_s V_{Belt} \,, \tag{4.3}$$

where T_s is the required time for generating each scan profile by the laser scanner and V_{Belt} the velocity of the transport belt.

The determination of the other geometrical features can be done after performing the length determination process. Owing to the analysis results of the experimental data, all objects, which have a length less than three scan profiles, are neglected and no further geometrical determination is performed.

4.3.2.2 Width determination of the transported object

The width of the objects can be determined analogous to the length of the object. This task is performed by considering the change of the simplified cross-sectional area transverse to the running direction of the transport belt.

The transported material (overburden) is strongly convexed transverse to the direction of the transport belt compared with the longitudinal direction. Therefore, there is a risk that, the transition from the left belt side to the overburden beginning (transverse to the transport belt) is considered as the beginning of an object. Analogous the transition from the end of the overburden to the right side of the transport belt is considered as the end of an object (Fig. 4.8). These risks can be avoided in two ways, which will be explained below.

The first way to avoid the above mentioned risks is to perform the width determination process after length determination and for specified sets of the scan profiles within the sliding window. Each set includes the scan profiles in between the recognized beginning and end of an object (Beg_{Ob} and End_{Ob}, respectively). The simplified cross-sectional area (transverse to the running direction of the transport belt) for the selected scan profiles is determined as

$$f_w(i) = \sum_{t=Beg_{Ob}}^{End_{Ob}} z(t,i). \tag{4.4}$$

After that, the change of the cross-sectional area can be determined from

$$S_w(i) = \frac{f_w(i) - f_w(i+1)}{End_{\mathrm{Ob}} - Beg_{Ob}}, \tag{4.5}$$

that is scaled by the division through ($End_{Ob} - Beg_{Ob}$) in order to be independent from the length of the considered object.

The second way to avoid the above mentioned risks is to consider the related neighboring areas of the object considered. This is performed by taking into account the simplified cross-sectional area of selected sets of the scan profiles before and after the determined beginning Beg_{Ob} and end End_{Ob} of the considered object. A new vector $S_{wr}(i)$ is obtained by this process.

The beginning of an object transverse to transport belt is specified through the high negative change of $S_{wr}(i)$ values. On the other hand, the end point of this object is specified through the high positive change of $S_{wr}(i)$ values. If a high negative value falls below an experimentally defined negative threshold value, the related index i_{Begin} of this point is recognized as the beginning of the object transverse to the running direction of the transport belt. After that, the end point of the object is searched. This process (recognition of the assumed object end) is performed as follows: First, the algorithm checks whether a point of $S_{wr}(i)$ has a value greater than experimentally defined positive threshold value. Second, if this condition is fulfilled, the next four points of $S_{wr}(i)$ are analyzed to check whether they posses values greater than the threshold value. Third, the related point i_{End} of the last point, which exhibits a change greater than the threshold value is recognized and considered as the end point of the analyzed object (transverse to the running direction of the transport belt).

The coordination of the determined index i_{Begin} and i_{End} in the x-direction is considered to determine the actual width

$$W = x(i_{\mathrm{End}}) - x(i_{\mathrm{Begin}})\,. \tag{4.6}$$

of the considered object.

4.3.2.3 Height determination of the transported object

The average height of the considered object relative to the laser scanner can be determined from

$$H = \frac{\sum_{t=Beg_{Ob}+1}^{End_{Ob}-1} \sum_{i=i_{Begin}+1}^{i_{End}-1} z(t,i)}{(End_{Ob} - Beg_{Ob} - 1)(i_{End} - i_{Begin} - 1)}. \tag{4.7}$$

This can be done after specifying the coordination in the xy-plan of the considered object. The average protruding height of the considered object (H_p) can be determined by subtracting the average height of the neighboring areas (before and after the transported object in the running direction of transport belt) from the average height of considered object.

After identifying the third geometrical feature (height) of the considered object, a validation process should be performed before the classification is performed.

4.3.3 Validation process

Two different validation tests have been implemented to find out the relationship between the calculated geometrical features in order to state whether the identified features belong to the same object.

First test estimates the number of the measurement points, which belong to the considered object and their height is greater than (H). According to the experimental experience, at least 40% of the measurement points should have a height greater than (H). Otherwise, the detected object is considered as non-real object and ignored.

Second test determines the geometrical spread of the measurement points, which have a height greater than (H_p). The underlying idea is that by the real objects, the considered points should be located closely to each other. In other words, they should have little geometrical spread due to the fact that the real object located in the middle of the interval from Beg_{Ob} to End_{Ob} and from i_{Begin} to i_{End}. The geometrical spread should be less than an experimentally defined threshold value. Otherwise, the analyzed object is considered as non-real object and ignored.

4.3.4 Classification process

A knowledge-based classifier is implemented to classify the identified objects. An object is classified as target object if it has an edge length greater than an experimentally defined threshold value "D_3" (here, $D_3 = 600mm$). The classifier checks whether at least one of the three object geometrical features is greater than the defined threshold value. If this condition is fulfilled, then the object is classified as target object.

4.3.5 Experimental results

Results for laser scanner module are summarized in Table 4.3. The detection accuracy for the tested data set is about 83%, whereas no false alarms are obtained by this module. The detection rate is affected by the position of the target object on the transport belt relating to the overburden; i.e. the detectable objects are these objects, which have one protruding edge at least that protrudes from the overburden. Target objects that lie under overburden are not detectable through this module. If several non-target objects lie close to each other above the overburden, they could be recognized as one object and they lead to a false alarm if the classification criterion is fulfilled.

Table 4.3: Classification results of laser scanner module

Target objects	40
Objects detected	33
Accuracy [%]	82.5
False alarms	0

4.4 Decision fusion module

The task of the decision fusion module is to combine the decisions of the detection modules to obtain a final decision with better inference (classification performance) over the individual decisions of the different detection modules. In other words, the goal of the fusion process is to improve the detection and false alarm rates of the overall monitoring system.

Different decision fusion approaches were realized to perform the combination process in order to obtain the highest detection and lowest false alarm rates. The realized fusion approaches are

- Basic Belief Fusion (BBF) method (Chapter 3),
- Bayes Combination Rule (BCR) (Section 2.2.3), and
- OR-logic.

For the fusion using either BBF method or BCR, the performance of the individual classifiers for each class should be determined using a training data set in order to obtain the corresponding conditional probabilities (Section 2.2.3) and the assigned belief values (Section 3.2) for the classifiers statements. The classifiers statements (decisions) are either positive (Pos.: target object present) or negative (Neg.: no target object).

Owing to the characteristics of the investigated production process, all available data sets are unbalanced data sets; i.e. number of excavated target objects (positive class) in comparison to the overburden (negative class) is extremely low in any considered data set. It could happened that less than 30 target objects are excavated in two hours. This data set consists of 30 positive decisions and 14370 negative decisions (if the the decision time is considered to be 0.5 s). Moreover, the number of excavated target objects within the overburden varies according to the variation of the overburden components. These two issues (unbalanced data, varied target object rate in the overburden) make the selection of representative training data set very difficult. Consequently, no representative conditional probabilities or basic belief values can be determined especially for the negative classifiers statements. To resolve this problem an artificial training data set consists of 40 events of target objects and 40 overburden events is constructed. The confusion matrix for each classifier has to be determined based on the artificial training data set. The general structure of the confusion matrix of this application is introduced in Table 4.4.

Table 4.4: General structure of the confusion matrix

	Classified as Pos.	Classified as Neg.
Pos. (actual)	True Pos. (TP)	False Neg. (FN)
Neg. (actual)	False Pos. (FP)	True Neg. (TN)

The confusion matrices of acceleration ($Acc.$) and laser scanner ($Las.$) modules are $CM^{Acc.} = \begin{bmatrix} 21 & 19 \\ 4 & 36 \end{bmatrix}$ and $CM^{Las.} = \begin{bmatrix} 36 & 4 \\ 2 & 38 \end{bmatrix}$, respectively.

The conditional probabilities and the basic belief values are determined based on the confusion matrices using the following equations,

$$P(x \in C_{Pos.}|cl^k(x) = Pos.) = m(cl_1^k) = \frac{TP}{TP + FP}, \tag{4.8}$$

$$P(x \in C_{Neg.}|cl^k(x) = Pos.) = m(cl_2^k) = \frac{FP}{TP + FP}, \tag{4.9}$$

$$P(x \in C_{Neg.}|cl^k(x) = Neg.) = m(cl_2^k) = \frac{TN}{TN + FN}, \text{ and} \tag{4.10}$$

$$P(x \in C_{Pos.}|cl^k(x) = Neg.) = m(cl_1^k) = \frac{FN}{TN + FN}. \tag{4.11}$$

In Table 4.5 and 4.6 the determined conditional probabilities and the assigned belief values for the positive and negative decisions of both detection modules are shown.

The performance of each realized fusion method are described in detail in the following section.

Table 4.5: Conditional probabilities and the assigned belief values for the positive statement of both detection modules

Module	$P(x \in C_{Pos.}/cl^k(x) = Pos.)$ $m(cl_1^k)$	$P(x \in C_{Neg.}/cl^k(x) = Pos.)$ $m(cl_2^k)$
Acceleration	84.00%	16.00%
Laser scanner	94.74%	5.26%

Table 4.6: Conditional probabilities and the assigned belief values for the negative statement of both detection modules

Module	$P(x \in C_{Pos.}/cl^k(x) = Neg.)$ $m(cl_1^k)$	$P(x \in C_{Neg.}/cl^k(x) = Neg.)$ $m(cl_2^k)$
Acceleration	35%	65.00%
Laser scanner	9.52%	90.48%

4.5 Experimental results and discussion

An experimental set of real industrial data was used to determine the performance of the overall monitoring system using previously mentioned fusion techniques (Section 4.4). The used data set contains 40 target objects. The detection and false alarm rates for the individual detection modules as well as the fusion results using the different fusion techniques are summarized in Table 4.7.

Fusion process using BCR and BBF method do not improve the detection rate of the overall monitoring system and lead to similar detection rate to laser scanner module. An improvement of the final false alarm rate using BCR and BBF is occurred and is similar to the false alarm of laser scanner module. This conclusion is obtained based on the demonstrated fusion results of the industrial data set in Table 4.7. The BCR and BBF lead to 90% detection rate and 2 false alarms, which are similar to the detection rate and number of false alarm of laser scanner module. The similarities of the fusion results using both methods with the classification results of laser scanner module could be explained by considering the fusion process of the different possible decision scenarios of both detection modules using both methods. In fact, there are four possible decision scenarios that can happen during monitoring process. These scenarios are

- both detection modules output negative decisions (Neg., Neg.),
- acceleration module outputs a negative decision and laser scanner module a positive one (Neg., Pos.),

- acceleration module outputs a positive decision and laser scanner module a negative one (Pos., Neg.), and
- both detection modules output positive decisions (Pos., Pos.).

Table 4.7: Classification results of the overall monitoring system using different fusion techniques

Module name	Acceleration	Laser scanner
Target objects	40	
Results of each module		
Objects detected	21	36
Accuracy [%]	52.5	90.0
False alarms	4	2
Fusion results using BCR		
Objects detected	36	
Accuracy [%]	90.0	
False alarms	2	
Fusion results using BBF		
Objects detected	36	
Accuracy [%]	90.0	
False alarms	2	
Fusion results using OR-logic		
Objects detected	37	
Accuracy [%]	92.5	
False alarms	5	

The fusion results for each possible decision scenario using BCR and BBF method are demonstrated in Table 4.8 and Table 4.9, respectively. The following results are concluded from these tables:

- The resulted degree of belief of both methods are close to each other for the various decision scenarios except the third scenario, in which the divergence of the final degree belief of both methods is about 28%. However, both methods obtained the same decision for this scenario.
- Bayesian combination rule and BBF method obtain similar decisions for all possible combination scenarios.

- The similarity of the final decisions of both methods for all possible decision scenarios explains the similarity of the detection and false alarms rate of both methods in Table 4.7.
- The final decision becomes positive if and only if a positive decision by laser scanner module is obtained regardless of the obtained decision by acceleration module; i.e. acceleration do not affect the final result for the given configuration. This result explains the similarity of the fusion results using both methods with the results of laser scanner module.

Table 4.8: Fusion results of possible scenarios using Bayesian combination rule

Case	Acc. module	Las. module	BCR method	
	$bel(Pos.)$[%]	$bel(Pos.)$[%]	$bel(Pos.)$[%]	Final decision
1	Neg.(35)	Neg.(9.52)	5.36	Neg.
2	Neg.(35)	Pos.(94.74)	90.65	Pos.
3	Pos.(84)	Neg.(9.52)	35.58	Neg.
4	Pos.(84)	Pos.(94.74)	98.95	Pos.

The dominance of the decision of laser scanner module is according to the significant highly reliability of laser scanner statement (either positive or negative) in comparison to the statement of acceleration module (either positive or negative).

Fusion result using OR-logic leads to better detection rate than the detection rate of the other used fusion methods. On the other hand, the resulted number of false alarms is higher than the number of false alarms of the other used methods.

Table 4.9: Fusion results of possible scenarios using BBF method

Case	Acc. module	Las. module	BBF method	
	$bel(Pos.)$[%]	$bel(Pos.)$[%]	$bel(Pos.)$[%]	Final decision
1	Neg.(35)	Neg.(9.52)	3.33	Neg.
2	Neg.(35)	Pos.(94.74)	96.62	Pos.
3	Pos.(84)	Neg.(9.52)	8.0	Neg.
4	Pos.(84)	Pos.(94.74)	99.16	Pos.

According to the following aspects, OR-logic was chosen to combine the decision of both detection modules:

- The OR-logic fusion leads to improve the final detection rate, whereas the resulted false alarms rate stills in the acceptable range.

- The impossibility to obtain a representative conditional probabilities or belief values especially for the negative statements of both classifiers for such kind of complex unbalanced data, makes the use of conditional probabilities-based fusion methods not effective.

- Detection and false alarms rates extremely depend on the nature of the excavated material including the target objects, their behavior during the excavation and transportation process, and weather conditions. Therefore, the detection rate of both modules could be changed and an OR-logic-based combination is necessary to achieve the requested detection rate.

  It can be happened that all transported target objects at specific time period are protruded from the overburden. These objects can be easily detected only by laser scanner module, which will provide an extremely high detection rate for this time period. However, laser scanner module detection rate will be low for another time period in which the most of target objects are covered with the overburden (lie under overburden).

  The detection rate of the acceleration module is also changeable. It can be happened that all transported target objects at specific time period cause significant impacts in the impact area. These impacts will be measured through the mounted acceleration sensors and can be easily detected through the acceleration module, which leads to high detection rate of this module. It can be also happened that many of the transported target objects do not cause any measurable vibrational events. Such kind of objects are not detectable by the acceleration module and lead to low detection rate of this module.

- Owing to the low false alarm rates of both detection modules, fusion process using OR-logic leads to limited false alarms rate. Simultaneously it leads to the maximum possible detection rate.

The experimental results show that the designed monitoring system fulfills the requested detection rate and the number of false alarms stills in the acceptable range. It should be noted that the most of the false alarms obtained by the acceleration modules are caused by objects similar to target objects to be detected but their sizes are relatively smaller than the defined size of target object (stones with maximum edge length that is smaller but close to the critical edge length of target objects).

5 Modification and experimental realization on the target system

This chapter introduces the modifications that are performed on the developed object detection system in the previous chapter to be applied on the target production system.

During the progress of this work, most parts of this chapter have been published/ demonstrated in [ASS12, ASSS13].

5.1 Introduction

The developed object detection system must be realized in real-time using the available hardware to have an online detection of the target objects to be removed before they lead to serious problems in the production line. However, the hardware implementation of the developed object detection system (Chapter 4) encounter several difficulties according to the capability of the available hardware and its ability to support the developed algorithms. To overcome this implementation problem, simplification processes of the developed algorithms are performed and an additional module is integrated. These changes are explained in the following sections.

5.2 Elements of the modified detection system

The modified object detection system consists of the following modules (Fig. 5.1)

- Acceleration module,
- Laser scanner module,
- Weightometer module, and
- Decision fusion module.

Implementation process of the acceleration module encounter difficulties by the realization of CWT-based prefilters and SVM-based classifiers because of the capability limitations of available hardware and the complexity of these classifier models. According to this problem, a simplification process of acceleration module is performed in order to develop an implementable acceleration module.

The developed laser scanner module has been successfully realized on the available hardware. Therefore, it does not subjected to any kind of changes.

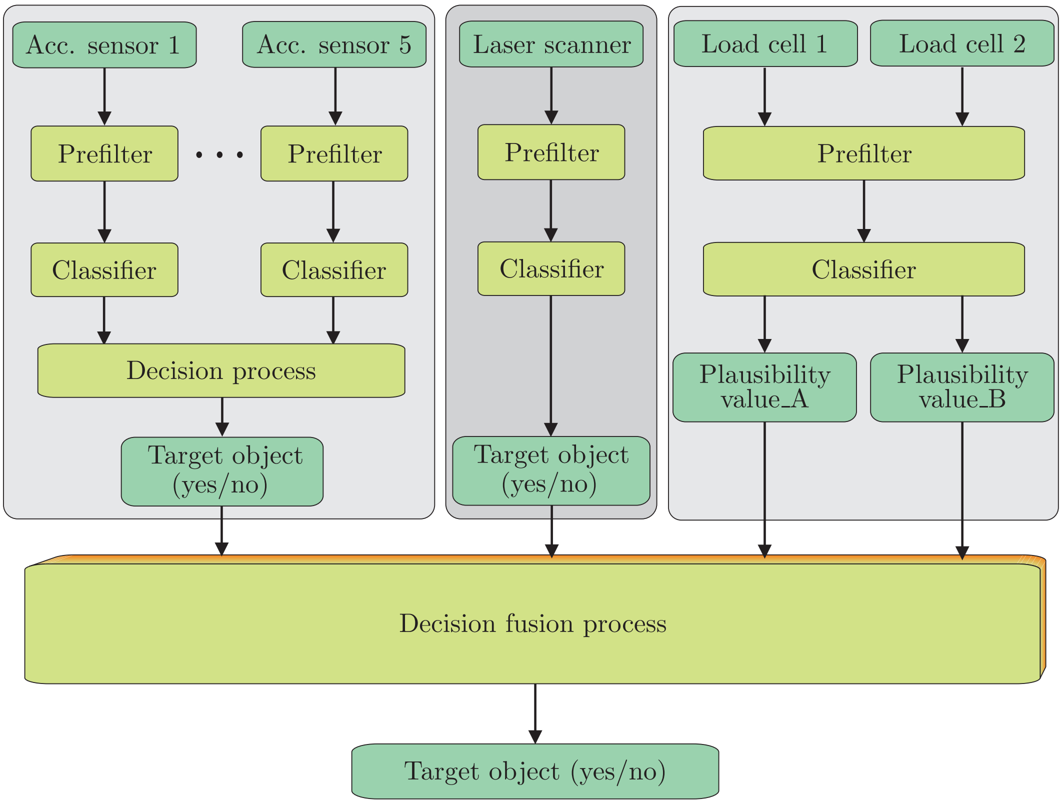

Fig. 5.1: Monitoring system for object detection [ASS12]

The additional integrated module (weightometer module) is based on the use of the weightometer signals. It consists of two load cells, which have been mounted in a specific way to provide a continuous weight measurement of the transported materials (overburden, target objects, etc.).

Weightometer module is realized to check plausibility of the positive decisions of the simplified acceleration module. The goal of the plausibility test is to reduce the false alarms rate by avoiding a specific kind of the false that can be caused by the simplified acceleration module.

Decision fusion method is realized to combine the output statements of laser scanner, acceleration, and weightometer module to meet a reliable decision about the presence of target objects.

Modified and new integrated modules are described in the following sections.

5.3 Acceleration module

As mentioned in Section 4.1, signal preprocessing, feature extraction, and classification process are applied to the individual acceleration sensors followed by a decision fusion process (Fig. 5.2). These processes are modified to overcome the hardware limitations. The modified processes are illustrated in the following subsections.

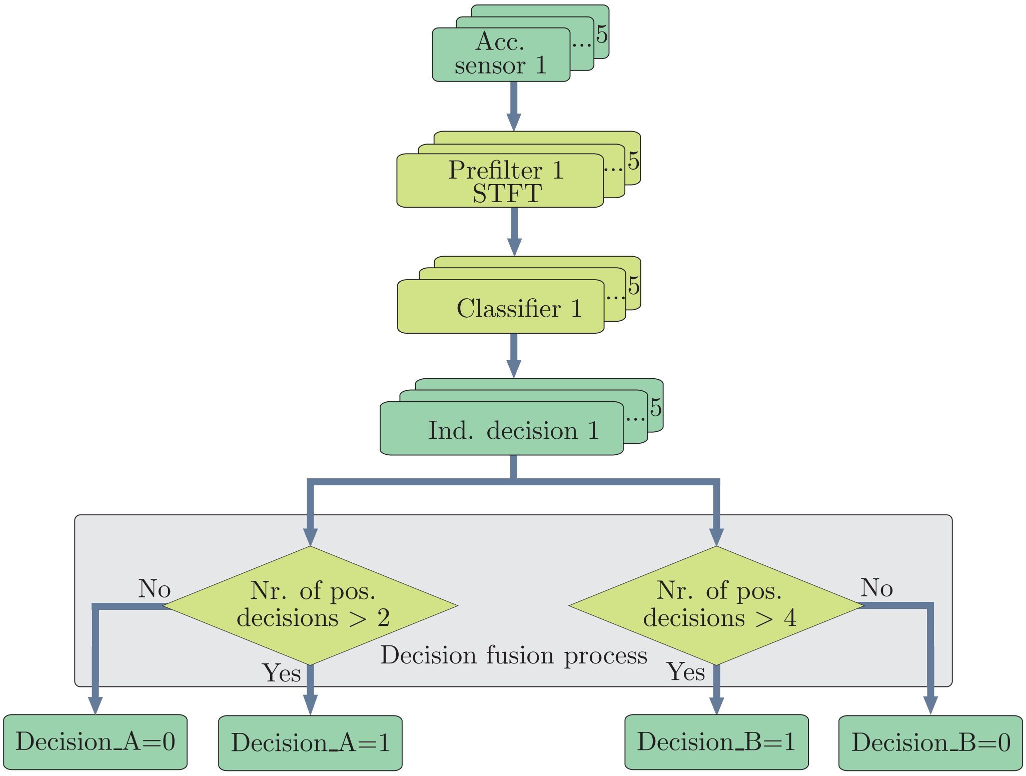

Fig. 5.2: Modified acceleration module [ASS12]

5.3.1 Feature extraction based on STFT

Short Time Fourier Transform (STFT) is realized as prefilter to extract the relevant information about system states (Section 4.2.1.1). The resolution parameters of the STFT-prefilter is changed to increase the time resolution and to obtain the representative feature vector for each classifier, which consists of the lowest possible number of attributes. The feature vector is based on 32 features, one for each acceleration signal (Section 4.2.1.4).

The experimental analysis shows that the 32 attributes are enough to provide classifiable feature space representation of target objects to be classified. Even, if the classifiability might be increased by increasing the dimension of the feature vector, the further evaluation costs and time are increased, which should be avoided in the real time realization.

As mentioned in Section 4.2.1.1 and shown in Fig. 5.3, the target object causes strong excitation of low frequencies. By contrast, higher frequencies are more excited by unclassified or unknown events. This phenomenon is used to distinguish target objects events from other unknown events.

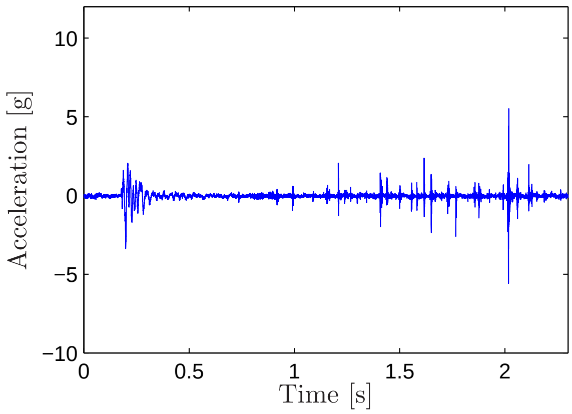

(a) Acceleration signal for sensor 2 in time domain

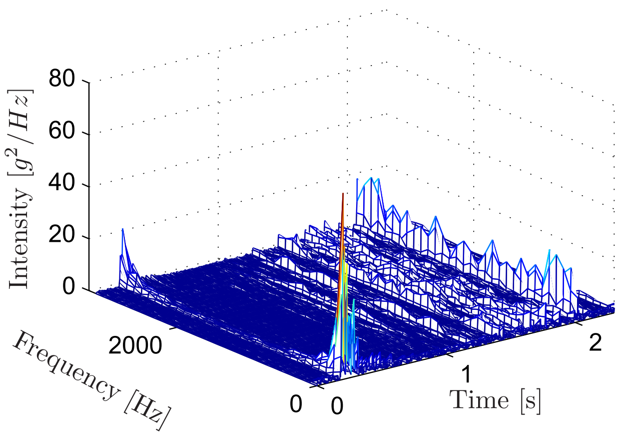

(b) The STFT spectrogram for sensor signal 2

Fig. 5.3: Acceleration signal for sensor 2. Target object event exists at 0.25 s. Other events are unknown events [ASS12].

5.3.2 Knowledge-based classification process

The developed knowledge-based classifier investigates the above mentioned phenomenon to classify the events related to target objects from the unknown/unclassified events, which result from the various sources of noise and disturbances. It involves five classification rules. These rules are derived based on the analysis of the experimental data.

As mentioned in Section 4.2.2.1, several noise and disturbance sources are involved in this complex production process. These lead to difficulties in recognizing target objects. The disturbance can be stationary or non-stationary noise, with large or rapid spectral changes over time, and can therefore resemble events resulting from target objects.

The obtained spectrogram by the feature extraction process consists of 32 attributes, which represent the particular frequencies from 1 Hz to 3250 Hz for each particular time window (Fig. 5.3(b)). The 32 attributes are split to several parts in order to realize the knowledge-based classifier. The number of parts, the number of considered attributes in each part, and the related boundaries of each part are experimentally defined. Part A consists of the first four attributes (from 1 to 4). Part B consists of the attributes between the 10th attribute and the 25th attribute. Part C consists of the last four attributes (from 28 to 32).

The first four rules are realized to classify and eliminate the disturbances, which appear over time in the spectrogram of the acceleration signals. The remain events should be the target object events and the event similar to target object events. Rule five checks whether the number of the remain events within a specific sliding window enough to ensure the presence of the target objects. These rules are introduced in detail in this sequel.

Rule I

As mentioned in Section 4.2.2.1, an acceleration signal contains permanent stationary noise in time and frequency domains. These noise events are classified through the first rule as non-target objects events. Rule I performs this task by eliminating all events in the acceleration signals for time points at which the maximum intensity of low-frequency excitation is less than an experimental defined threshold value. If this condition is fulfilled, the intensity for all frequencies at such time points is set to zero (Fig. 5.4).

Rule II

The acceleration signals in time as well as in frequency domain involves non-stationary noise events. This kind of noise appears in its feature space (spectrogram) as a strong excitation for the high attributes (high frequencies) compared to the low attributes (low frequencies). Based on the experimental experience, this kind of behavior is related to non-target objects. The task of the second rule is to classify out this kind of non-target object behavior. Rule II performs this task by eliminating all events of the acceleration signals at each time point where the ratio of the maximum intensity of the low frequency domain (part A) to the maximum intensity of the high frequency domain (part C) is less than a specific experimentally defined threshold value. If this condition is fulfilled, the intensity for all frequencies at such time points is set to zero.

As shown in Fig. 5.4, the non-target object event at 2.1 s stills remaining in the spectrogram of the acceleration signal after applying first classification rule. This non-stationary noise is classified as non-target object event and eliminated by applying second classification rule (Fig. 5.5).

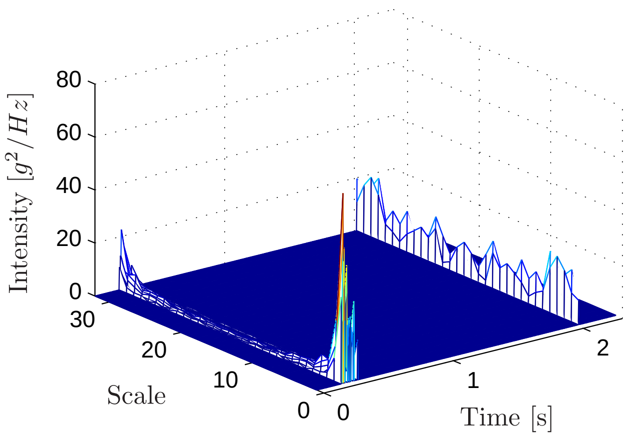

Fig. 5.4: The STFT spectrogram of the signal shown in Fig. 5.3 after applying rule I [ASS12]

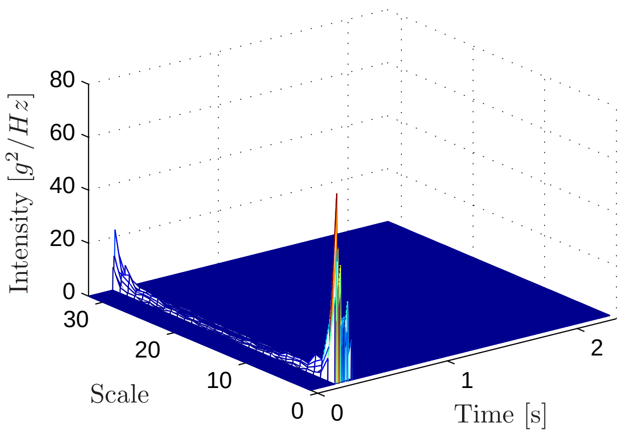

Fig. 5.5: The STFT spectrogram of the signal shown in Fig. 5.4 after applying rule II [ASS12]

Rule III

The analysis of the extracted features of the acceleration signals shows that the middle frequency domain (part B) is strongly excited compared to the low frequency domain (part A) through specific noise events. Rule III is developed to classify these noise events as non-target object events. Rule III performs this task by eliminating all events of the acceleration signals at each time point where the ratio of the maximum intensity of the low frequency domain (part A) to the maximum intensity of the middle frequency domain (part B) is less than a specific experimentally defined threshold value. If this condition is fulfilled, the intensity for all frequencies at such time points is set to zero.

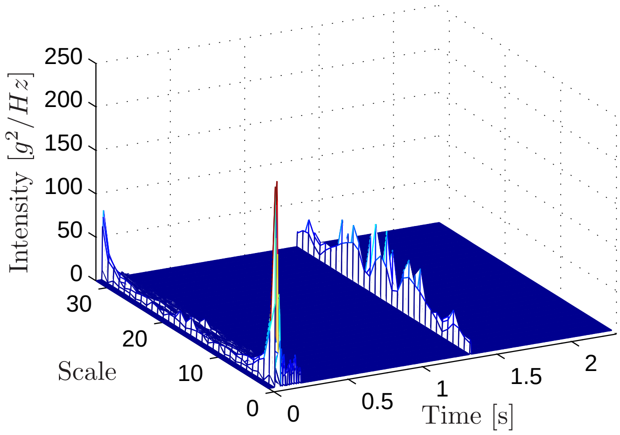

(a) The STFT spectrogram of an acceleration signal after applying rule I

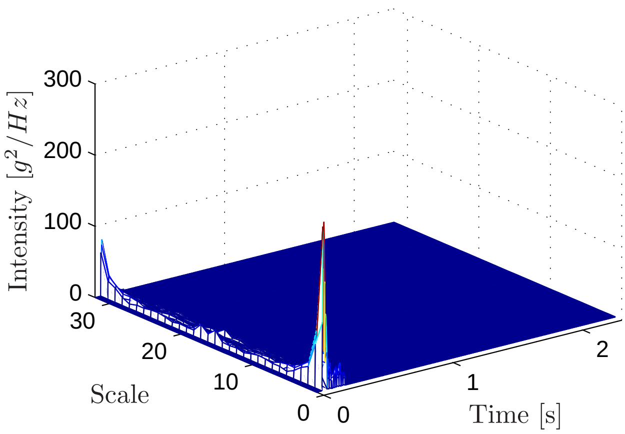

(b) The STFT spectrogram shown in Fig. 5.6(a) after applying rule III

Fig. 5.6: Classification results of rule III [ASS12]

In Fig. 5.6(a) the spectrogram of an acceleration signal after applying rule I is presented. The events at 0.2 s are resulted from a manually classified target object. The events at 1.4 s are caused by specific noise event. The events at 1.4 s are classified as non-target object events by applying the third classification rule (Fig. 5.6(b)).

Rule IV

Rule IV deals with the intensities of the low frequency domain (part A). The analysis of the target object events shows that the lowest frequency scale (first attribute) has the highest intensity and the intensity of the next three frequency scales falls quickly down. This behavior is investigated to classify out the non-target object events which do not posses this behavior.

This task is performed by estimating the mean value of the gradients between the first four frequency scales (the first four attributes). Rule IV checks whether the estimated mean value is less than a specific experimentally defined threshold value. If this condition is fulfilled, the intensity for all frequencies at such time points is set to zero. In other words, the related events are classified as non-target object events.

The spectrogram of an acceleration signals after applying the first classification rule is presented in Fig. 5.7(a). It involves two different kind of events. The first kind of events (at 0.1 s) is caused by a manually classified target object. The second kind of events (at 1.5 s) is resulted from unknown noise event. It is clearly that the gradient of the first four attributes of the non-target objects events are relatively low compared to the gradients of the first four attributes of the target object event. Such kind of non-target object events is classified out by realizing rule IV (Fig. 5.7(b)).

Rule V

All detectable and classifiable non-target objects events are eliminated by the previously introduced classification rules. The remaining events are divided into two types: first type, target object events. Second type, events similar to target object events, which are caused by small objects (stones with maximum edge length smaller than the critical edge length of target objects), which should be classified due to their size as non-target objects. Small objects usually lead to weak and limited vibration events in contrary to the target objects.

Rule V is developed to classify the target object events (first type) from the other (second type). It performs this task by estimating the number of remaining events (remaining events after the filtering process using Rule I to IV) within a specific sliding window. It checks whether the number of events within the sliding window is greater than experimentally defined threshold value. If this condition is fulfilled at any time point, the knowledge-based classifier provides a positive preliminary individual decision.

This classification rule is defined based on numerous experimental data sets in order to achieve the highest possible detection rate and accordingly the lowest possible falls alarms rate.

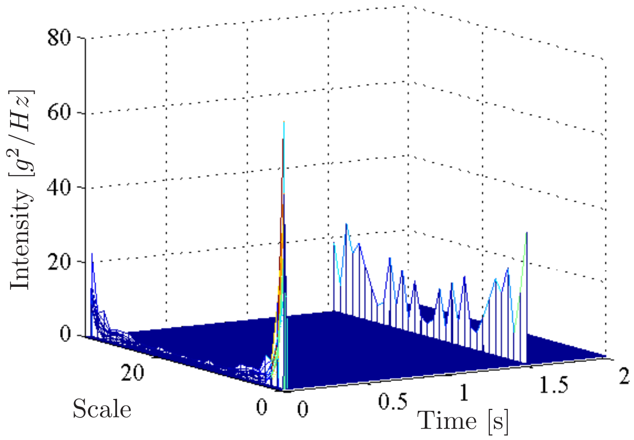

(a) The STFT spectrogram of an acceleration signal after applying rule I

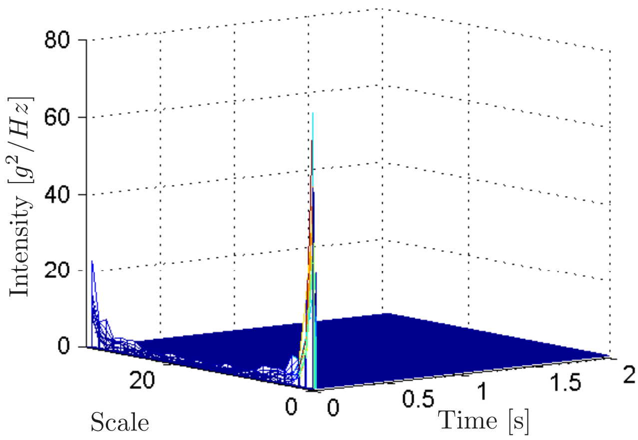

(b) The STFT spectrogram shown in Fig. 5.7(a) after applying rule IV

Fig. 5.7: Classification results of rule IV [ASS12]

5.3.3 Decision fusion process

A decision fusion process based on the analysis of experimental data is realized to combine the individual preliminary decisions to get a final decision for the acceleration module (target object presents (yes/no)). To fulfill this task, a rule-based decision fusion process is developed. The realized rules are described as follows:

- *Rule I*: At least two simultaneously positive individual decisions lead to a final decision of "positive: target object present". Consequently the parameter "Decision_A" is set to one and parameter "Decision_B" stills zero.
- *Rule II*: If at least four individual decisions are simultaneously positive, the parameter "Decision_B" is set to one.

The distinction of the decision paths (Decision_A, Decision_B) is necessary for the plausibility test by means of the weightometer module.

5.3.4 Implementation and results

The approach was tested using an experimental set of real industrial data. The results of this module are summarized in Table 5.1. The best individual detection accuracy is 54.5% (classifier 1). Classifiers 2 and 4 do not lead to false alarms for the tested data set. This result demonstrates a typical compromise: an increase in the detection rate leads to an increase in the false alarm rate (Table 5.1).

Table 5.1: Classification results of the modified acceleration module. The used test data set contains 33 target objects [ASS12].

Sensor/classifier	1	2	3	4	5
Results of each classifier					
Objects detected	18	14	17	15	12
Accuracy [%]	54.5	42.4	51.5	45.5	36.4
False alarms	1	0	1	0	3
Fusion results					
Objects detected			18		
Accuracy [%]			54.5		
False alarms			0		

The accuracy of the individual classifiers for the considered test data varies from 36.4% to 54.5%. At the same time the number of false alarms is relatively low (3 false alarms).

The preliminary individual decisions are unreliable due to their individuality. Although the combination of the preliminary decisions does not improve the final detection rate for the considered data set, it leads to highly reliable final decision over the individual decisions. This claim is approved through the zero false alarms rate which being achieved by the combination process.

It is necessary to mention that the detection rate of this module can be improved by tuning the classification rules of each classifier. However, the false alarms could be accordingly increased.

5.4 Weightometer module

The analysis of the weightometer signal and the acceleration signals shows that the weightometer signal can be used to avoid specific kind of false alarms, which could be caused by the acceleration module. For this reason, the weightometer module is developed in order to check the plausibility of the final decisions of the acceleration module to avoid this specific false alarms.

The specific false alarms of interest can occur when few quantity of overburden including many small objects (small stones) is excavated and discharged on the transport belt (Fig. 5.8). These objects cause strong excitation of the acceleration sensors in case of the direct impact against the front sides of the plates, where the acceleration sensors are mounted. The strong excitation can also occur if the objects are discharged on the transport belt with few overburden quantity and make direct impact against the transport belt. Such direct impacts lead to events in the acceleration signals similar to the target objects events (in feature space) and can not be distinguished from each other. Consequently, they lead to false alarms.

The analysis of the acceleration signals shows that some of these non-target objects lead to simultaneously false alarms by many acceleration sensors and can not be avoided by the introduced fusion process in the acceleration module.

Fig. 5.8: Non-target objects with few discharged overburden

Usually, the discharged target objects on the transport belt either with few or much quantity of overburden have a certain minimum weight. The weight of discharged small objects with few quantity of overburden that cause false alarms, do not exceed the minimum weight of target objects. Therefore such kind of false alarms could be neglected with the help of their corresponding weights. If the corresponding weight of any positive decision of the acceleration module does not exceed specific threshold value, then it is highly probable that this decision be a wrong one (false alarm). Therefore, this positive decision has to be canceled to avoid such kind of probable false alarms.

The load cells signals are added together to determine the total weight of the transported material. An experimentally defined sliding window is used to build the mean value of the total weight within the specified window. Two plausibility values are obtained by comparing the mean value with two experimentally defined threshold values. The plausibility values are fed to the fusion module to approve the plausibility of the acceleration module statements (Fig. 5.9).

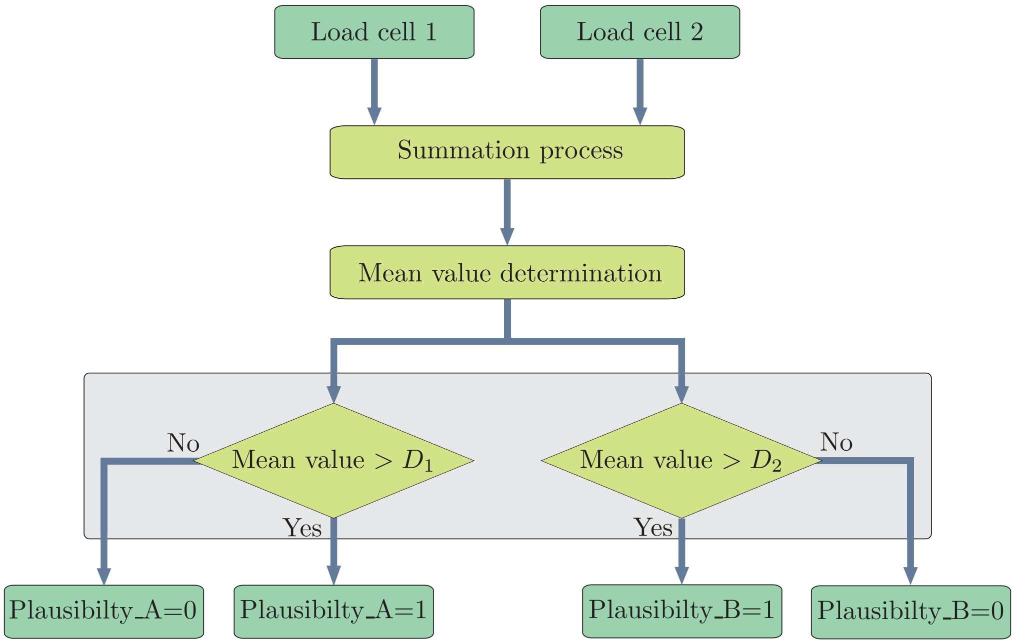

Fig. 5.9: Weightometer module [ASS12]

It is important to mention that the plausibility test could help to avoid many false alarms but it might be cancel few correct positive decisions. Thus, the detection rate might be slightly negatively affected.

5.5 Decision fusion module

The decision fusion process is performed to combine the output statements of the different modules (acceleration, laser, and weightometer module) to obtain a better inference/detection about the presence of the target objects over the individual decisions. In other words, the goal of the fusion process is to improve the detection and false alarms rates.

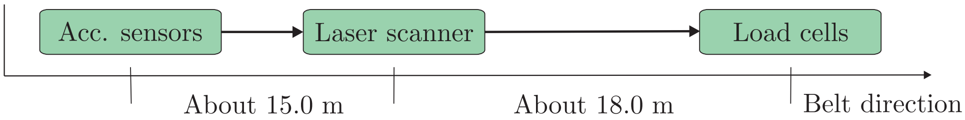

Fig. 5.10: Distance between different acceleration sensors, laser scanner, and load cells [ASS12]

Owing to the geometrical distribution of the used sensors (Fig. 4.1 and Fig. 5.10), the output statements of the different modules (acceleration, laser, and weightometer module) should be synchronized in order obtain the final decision. This synchronization process is performed by the decision fusion module (Fig. 5.11).

The evaluation process of the laser scanner module has shown that the positive statement (target object present) of this module is highly reliable. The tests results of laser scanner module showed that the degree of accuracy of its positive decisions is around 95%; i.e. the probability that a positive laser scanner decision to be a false alarm is extremely small (less than 5%). According to that, the positive decisions of this module are considered to be correct and do not need further assessment statements to approve their correctness to ensure the presence of target objects.

Acceleration module provides two output statements (Decision_A and Decision_B). If the value of the statement "Decision_A" is set to one, it is synchronized with plausibility value "Plausibilty_A" of the weightometer module in order to check the plausibility of the positive decision. If the corresponding plausibility value is also equal one, then the synchronized positive statement is considered as correct final decision (target object present). If the value of the statement "Decision_B" is set to one, it is synchronized with the plausibility value "Plausibilty_B" of the weightometer module in order to check the plausibility of this positive decision. If the corresponding plausibility value is also equal one, then the synchronized positive statement is considered as correct final decision (target object present). However, any decision does not fulfill the related plausibility test is considered to be a false alarm and be canceled (Fig. 5.11).

Positive decisions, which pass the plausibility tests are combined with the decision of the laser scanner module using an OR-logic to meet the final decision about the system state (target object present (yes/no)).

5.6 Implementation and results

The modified object detection system was tested using an experimental set of real industrial data. The used data set contains 50 target objects. The results of the preliminary application to the system are summarized in Table 5.2.

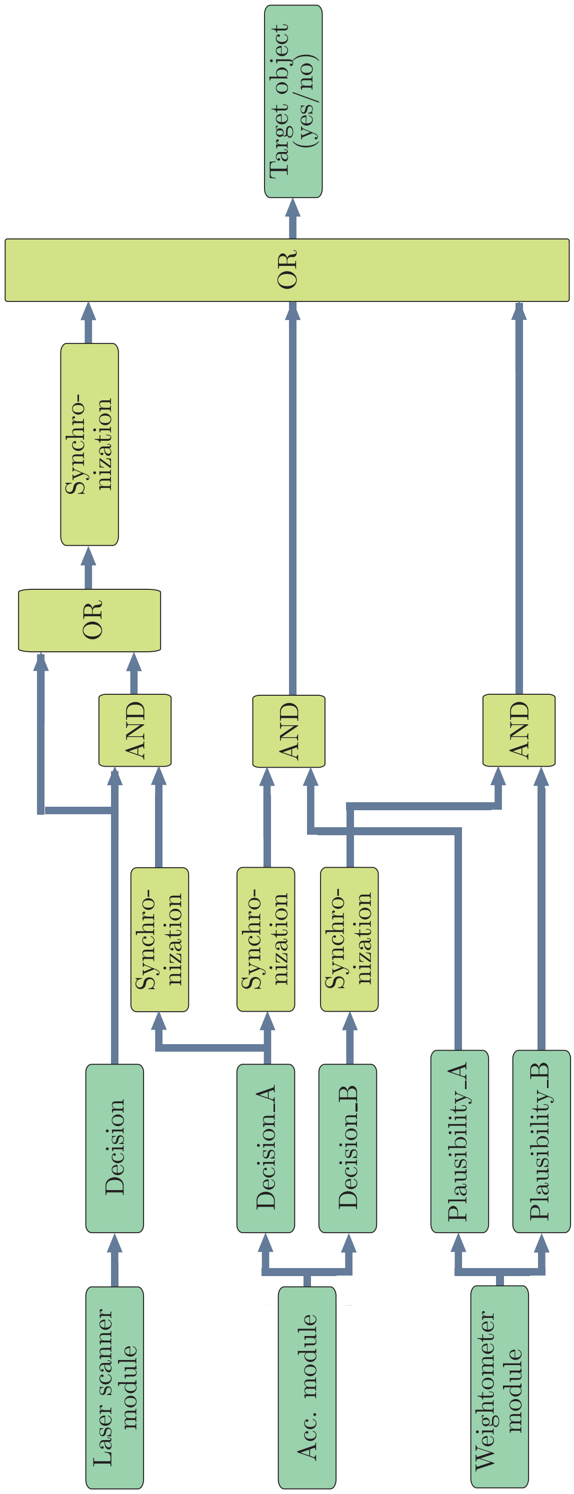

Fig. 5.11: Fusion process of the object detection system [ASS12]

Table 5.2: Classification results of the modified monitoring system. The used test data set contains 50 target objects.

Module	Acceleration					Laser scanner
Sensor/classifier	1	2	3	4	5	Laser scanner
Results of each classifier						
Objects detected	25	15	19	22	13	-
Accuracy [%]	50	30	38	44	26	-
False alarms	9	5	5	1	1	-
Results of each module						
Objects detected			22			44
Accuracy [%]			44			88
False alarms			2			1
Results of the overall system						
Objects detected			46			
Accuracy [%]			92			
False alarms			3			

The best individual detection rate of acceleration module classifiers is 50% through classifier 1, which leads to the highest false alarm rate as well (9 false alarms). On the other side, classifier 5 in acceleration module leads to the lowest detection and false alarms rates.

The accuracy of the system based on fused decisions of the acceleration sensor network is 44%. It can be seen from Table 5.2 that the fused detection rate of acceleration module (44%) is less than the detection rate of classifier 1 (50%). Even if the fusion process of the individual acceleration sensors does not improve the detection rate over the individual classifiers for the tested data set, false alarms rate is considerably improved (only two final false alarm in compare to 9 false of classifier 1). Consequently, the specific process of fusion leads to more reliable final positive decisions; more specifically, a reliability value of the final positive decision of about 91% according to the definition of reliability

$$Re = \frac{Nr.\ of\ detected\ objects}{Nr.\ of\ detected\ objects\ +\ Nr.\ of\ false\ alarms}. \tag{5.1}$$

Owing to the fusion accuracy of acceleration module for the tested data set, the individual classifiers (acceleration sensors) seem that they provide redundant informations about system state. This observation (redundancy) is might be right and valid for the tested data set. The experimental experiences showed that the detection rate of the various sensors is varied and depends on the operating conditions such as type of excavated material, excavation angle, and the volume of excavated material. Therefore the classifiers (sensors) which might be not useful for specific data set, they might obtain the best classification result for another data set (under different operating condition).

Laser scanner module leads to a detection rate of 88%. In addition, it leads to only one false alarm. The reliability of its final positive decision is about 98%. Owing to the highly reliability of laser scanner statement, no further support is needed to ensure the correctness of the positive decisions of laser scanner module. Consequently OR-logic is used to combine the decision statement of laser scanner module with the other decision statements.

As mentioned in Section 4.3.5 the detection rate of laser scanner module can be affected by the position of target objects above the transport belt in relation with the overburden.

The occurred false alarm is caused by several non-target objects laid close to each other above the overburden and they recognized as one object, which is classified as target object. The experimental experiences showed that the probability for such kind of false alarm is very low. Therefore, it could be concluded that the false alarm rate for laser scanner module is always low; i.e. the reliability of the positive decisions is always very high.

It should be noted that accuracy for individual classifiers can be increased by tuning the classification rules; the rate of the false alarms would also increase accordingly. During the development and depending on the system requirements, a compromise between detection accuracy and false alarms must be achieved.

The plausibility of the decision statements of acceleration module is approved with the help of weightometer module statements in order to avoid a specific kind of false alarms. Weightometer module does not affected the false alarms rate of the acceleration module in the considered test data because these two false alarms are belong to different kind of false alarm, which can not be avoided by weightometer module.

The approved acceleration module decisions are synchronized, and respectively fused with laser scanner decisions in order to obtain a single final decision about the presence of target objects. Fusion process is performed using the OR-logic, which leads to a detection rate of 92% of the tested target objects and to three false alarms along the used data set.

According to the final detection and false alarm rates, it can be concluded that modified multisensor-based monitoring system is successfully fulfilled the system requirements. Moreover, the first tests of the modified monitoring system on the standard hardware showed its ability to provide an online detection of target objects at the right time.

6 Summary, conclusion, and future work

A complex production process is investigated in this work to develop an advanced multisensor-based pattern recognition monitoring system. The objective of the designed monitoring system is to detect the target object in transported material to avoid resulting disturbances and failures during the continuous transportation process. The developed approach must provide an online detection of the target objects.

In the first chapter of this work, the research objectives are introduced and the investigated production system to be improved is described. After that, the previous researches on the investigated problem is introduced. The literature research showed that all previous works did not provide an effective solution for the investigated problem with satisfactory detection and false alarms rates.

In the second chapter, a brief theoretical background about pattern recognition and decision fusion techniques are given. The definition and the design steps of pattern recognition system are discussed in the first section. In the second section, the definition and importance of the decision fusion and fusion types are briefly introduced. The used feature extraction, classification, and decision fusion tools for the design of the targeted monitoring system are described in this chapter.

The novel decision fusion method “Basic Belief Fusion” (BBF) is developed and described in this work. The plausibility of BBF method is approved with the help of a standard fusion technique “Bayesian combination rule (BCR)” and artificial numerical examples. This method has been developed to be used to combine the individual decisions of the different realized detection modules in order to obtain a reliable final decision about the state of the monitored system. In fact, there are several known methods, which can be used to solve the fusion in this work, but the objective being to develop a new comparable method, which is based on different mathematical rules.

The designed multisensor-based pattern recognition monitoring system is introduced in the fourth chapter. Two different physical effects have been considered. These effects are measured using a laser scanner and five acceleration sensors. Laser scanner is mounted above the transportation belt and used to construct the surface topography of the transportation belt including the transported material. Acceleration sensors are mounted in the impact area along the transportation belt and used to measure the resulted vibration because of the discharged material (overburden, non-/target objects, etc.).

The proposed monitoring system consists of two detection module (acceleration and laser scanner module) and a decision fusion module. Two alternative approaches are developed for the acceleration module. The first approach uses a Short-Time

Fourier Transform (STFT) as a prefilter to extract relevant features from the acceleration signals. The features extracted from different sensor channels (the five acceleration signals) are first classified using Support Vector Machine (SVM)-based classifiers. A new decision fusion process is developed to combine individual decisions. This method is based on two SVM-classifiers levels and two rule-based filters. The second approach uses a Continuous Wavelet Transform (CWT) as a prefilter to extract relevant features from the acceleration signals. The features extracted from different sensor signals are subjected to further prefiltering processes before SVM-based classification. The individual decision functions are then combined in a decision fusion module. The classification system is trained and validated using real industrial data. The two approaches are tested using the same data and their performance and modeling complexity are compared. The CWT-SVM-based approach is chosen for the development of the overall monitoring system.

Within the laser scanner module, laser signal is subjected prefiltration, filtration, validation, and classification processes. The proposed module is designed, validated, and successfully tested using real industrial data. Decision fusion module is used to combine the obtained individual decisions of the two detection modules. Bayesian combination rule (BCR), BBF method, and OR-logic are used to perform the fusion task. According to the characteristics of the considered application, the OR-logic is chosen to perform the fusion task.

Owing to the online realization of the developed approach using the standard available hardware, modification and simplification processes are performed in order to overcome the hardware limitations. These processes are described in the fifth chapter.

The modified monitoring system consists of four modules (acceleration, laser scanner, weightometer, and decision fusion module). Owing to the hardware realization ability of laser scanner module, no changes are performed on it.

The potential modifications are performed on the acceleration module. In this module the five acceleration channels are subjected to feature extraction process using STFT. The extracted features are individually subjected to a knowledge-based classification process followed by a rule-based decision fusion process. The developed rule-based fusion filter obtains two final decision statements for the overall acceleration module. The two decision statements are fed to the main fusion module to be combined with the other statements.

The integrated weightometer module is designed in order to avoid specific kind of false alarms, which could be caused by the acceleration module. The signals of the mounted load cells on the festoon are considered to determine the mean value weight of the transported material within a specific sliding window. The determined mean value is compared to experimentally defined threshold values to obtain two different plausibility statements.

The output statements of laser scanner, weightometer, and acceleration module are fed to the decision fusion module to be combined in order to obtain final reliable decision about the presence of target objects.

6.1 Scientific contributions

The scientific contributions of this work can be summarized as follows:

- A new multisensor-based pattern recognition monitoring system is developed. A complex production process is considered for the development purposes. This approach is based on the investigation of different physical effects and utilizes an appropriate preprocessing, feature extraction, classification, and decision fusion processes.

- The so called STFT-SVM-based approach presents a novel multisensor monitoring approach, which can be applied to monitor various complex systems. In this approach, different classification levels are realized in combination with two rule-based filters for the development of a new fusion technique in order to obtain a reliable high inference about the monitored system. The developed approach is an interested and important technique for pattern recognition applications according to the following aspects: First aspect is that only strong indicators are used in the training process of the first level SVM-classifiers (SVM I) in order to reduce the number of false alarms, which could be occurred by the non-target objects. The second aspect is that the classification levels two and three are not permanently in use. These two levels are activated (by rule-based filter I) under specific conditions to perform specific classification tasks for short selected parts of the acceleration signals. This aspect reduces the computational costs in comparison to the permanent classification by the different classification levels. Third aspect is that this concept could be generally used to solve various pattern recognition problems; depending on the problem considered, the appropriate feature extraction and classification tools could be used instead of STFT and SVM (such as CWT, DWT, ANN, k-NN, etc.).

- A novel fusion method “BBF” is developed. This method is comparable to BCR. The final decision using BBF method for specific fusion scenarios was more plausible than the final decision of BCR. The mathematical rules are one of the key difference between this novel method and other methods, which gives the flexibility to realize it for various applications. Moreover, the designed method can deal with uncertainty in the individual decisions, which assumed to be zero. Another important aspect for BBF method is that, it can provide final decisions with uncertainty degrees also when the uncertainty in the individual decision statements is assumed to be zero.

6.2 Conclusion

Experimental results and data analysis showed that the basic idea of the developed approach is an appropriate way to solve this complex production process. The idea based on the use of different physical effects, several sensors, and the individual evaluation of different sensor channels followed by a decision fusion process. The complexity of the monitoring task is due to the irregularities of the characteristics of the transported overburden including target objects, their irregularity behavior during the transportation process, and the impossibility to perform direct measurement of target objects.

In spite of the mentioned complexity, the testing processes using industrial test data approved the success of the developed monitoring approach in fulfillment the production system requirements. The simplification and modification processes on the designed monitoring system are performed in order to apply it in real time using standard industrial hardware. The testing results showed that the modified system being able to detect more than 90% of the target objects with a limited and very small number of false alarms.

6.3 Future work

The following points are suggested as future work:

- The developed decision fusion approach “BBF method” stills in its early development stages. It is only tested and approved based on a numerical examples and the industrial test data for the considered application in this work. As future work, the designed approach could be tested using various benchmark data and its fusion performance could be compared to the performance of the standard decision fusion techniques.
- The BBF method is designed to be able to model the hypotheses “uncertain” for the individual decision statements. In this work, this hypotheses is neglected and its degree of belief considered to be zero. The uncertainty could be considered and a degree of belief could be defined for this hypotheses. After that, it could be tested using various benchmark data to approve its fusion ability. Moreover, the fusion performance, the time cost, the complexity, etc. of the designed method could be studied and compared to Dempster-Shafer decision fusion technique for various applications and benchmark data.
- The STFT-SVM-based detection approach is novel approach and obtained better detection and false alarms rate than the individual decisions. The applicability of this approach for various complex pattern recognition problems could be tested in order to generalize it as an advanced pattern recognition tool for complex systems.

- The developed monitoring system and its modified version are fulfilled the system requirements. However, the performance of acceleration module was clearly lower than the performance of laser scanner module. The performance of this module could be improved by the appropriate placing of the acceleration sensors in the impact area along the transportation belt.

Bibliography

[Abe10] S. Abe, *Support Vector Machines for Pattern Classification*, S. Singh, Ed. London, England: Springer-Verlag London Limited, 2010.

[ABSC11] F. Al-Badour, M. Sunar, and L. Cheded, "Vibration analysis of rotating machinery using time-frequency analysis and wavelet techniques", *Mechanical Systems and Signal Processing*, vol. 25, no. 6, pp. 2083–2101, 2011.

[AD12] S. Asht and R. Dass, "Pattern recognition techniques: A review", *International Journal of Computer Science and Telecommunications*, vol. 3, no. 8, pp. 25–29, 2012.

[Add02] P. Addison, *The Illustrated Wavelet Transform Handbook: Introductory Theory and Applications in Science, Engineering, Medicine, and Finance*, S. Laurenson and J. Revill, Eds. Bristol, England: IOP Publishing, 2002.

[AnC09] G. Acuña and M. Curilem, "Comparison of neural networks and support vector machine dynamic models for state estimation in semiautogenous mills", in *MICAI 2009: Advances in Artificial Intelligence*, Ser. Lecture Notes in Computer Science, A. Aguirre, R. Borja, and C. García, Eds. Heidelberg, Germany: Springer Berlin Heidelberg, 2009, vol. 5845, pp. 478–487.

[ASA+12] W. Astuti, W. Sediono, A. Aibinu, R. Akmeliawati, and M. Salami, "Adaptive Short Time Fourier Transform (STFT) analysis of seismic electric signal (SES): A comparison of Hamming and rectangular window", in *Industrial Electronics and Applications (ISIEA), 2012 IEEE Symposium on*, Bandung, Indonesia, September 2012, pp. 372–377.

[ASS11] L. Al-Shrouf and D. Söffker, "Multi-classifier fusion method based on the reliability of indivdual classifiers statements", in *8th Int. Workshop on Structural Health Monitoring 2011*, F. Chang (Ed.), Stanford, USA, September 2011, pp. 127–134.

[ASS12] ——, "Merkmalsbasierte Multisensorik zur Objekt- und Steinerkennung", August 2012.

[ASSS13] L. Al-Shrouf, M. Saadawia, and D. Söffker, "Improved process monitoring and supervision based on a reliable multi-stage feature-based pattern recognition technique", *Information Sciences*, vol. 259, pp. 282–294, 2013.

[ASSSS10] L. Al-Shrouf, M. Saadawia, N. Szczepanski, and D. Söffker, "Multisensorfusionsbasierte Prozessüberwachung", in *Diagnose und Anlagenüberwachung AKIDA*, Ser. Berichtsband 8. Aachener Kolloquium für Instandhaltung, Aachen, Germany, November 2010, pp. 413–422.

[ASSSS11] ——, "Adaptive classification based on multisensoric decision fusion", in *8th Int. Workshop on Structural Health Monitoring 2011*, F. Chang (Ed.), Stanford, USA, September 2011, pp. 127–134.

[ASSSS12] ——, "Event detection using multisensor fusion and filtering techniques based on CWT and SVM", in *6th European Workshop on Structural Health Monitoring 2012*, C. Boller (Ed.), Dresden, Germany, July 2012, pp. 206–213.

[AV13] J. Armony and P. Vuilleumier, *The Cambridge Handbook of Human Affective Neuroscience*, Ser. The Cambridge Handbook of Human Affective Neuroscience. New York, USA: Cambridge University Press, 2013.

[BBST13] L. Batista, B. Badri, R. Sabourin, and M. Thomas, "A classifier fusion system for bearing fault diagnosis", *Expert Systems with Applications*, vol. 40, no. 17, pp. 6788–6797, 2013.

[BD12] T. Banerjee and S. Das, "Multi-sensor data fusion using support vector machine for motor fault detection", *Information Sciences*, vol. 217, pp. 96–107, 2012.

[BDS+10] S. Basu, N. Das, R. Sarkar, M. Kundu, M. Nasipuri, and D. Basu, "A novel framework for automatic sorting of postal documents with multi-script address blocks", *Pattern Recognition*, vol. 43, no. 10, pp. 3507–3521, 2010.

[Ber97] A. Berger, "The Improved Iterative Scaling Algorithm: A Gentle Introduction", Carnegie Mellon University, Pittsburgh, PA, USA, 1997.

[BGV92] B. Boser, I. Guyon, and V. Vapnik, "A training algorithm for optimal margin classifiers", in *Proceedings of the 5th Annual Workshop on Computational Learning Theory (COLT'92)*. D. Haussler (Ed.), Pittsburgh, PA, USA: ACM Press, July 1992, pp. 144–152.

[Bur98] C. Burges, "A tutorial on support vector machines for pattern recognition", *Data Mining and Knowledge Discovery*, vol. 2, pp. 121–167, 1998.

[BWR12] G. Bhatnagar, Q. Wu, and B. Raman, "Fractional dual tree complex wavelet transform and its application to biometric security during communication and transmission", *Future Generation Computer Systems*, vol. 28, no. 1, pp. 254–267, 2012.

[BWR13] ——, "Discrete fractional wavelet transform and its application to multiple encryption", *Information Sciences*, vol. 223, pp. 297–316, 2013.

[Can10] M. Canal, "Comparison of wavelet and short time Fourier transform methods in the analysis of EMG signals", *Journal of Medical Systems*, vol. 34, pp. 91–94, 2010.

[CDSM10] P. Chowdhury, S. Das, S. Samanta, and U. Mangai, "A survey of decision fusion and feature fusion strategies for pattern classification", *IETE Technical Review*, vol. 27, no. 4, pp. 293–307, 2010.

[CGYI11] N. Celik, R. Gagarin, H. Youn, and M. Iskander, "A noninvasive microwave sensor and signal processing technique for continuous monitoring of vital signs", *Antennas and Wireless Propagation Letters, IEEE*, vol. 10, pp. 286–289, 2011.

[Cha11] J. Chaudhari, "Design of artificial back propagation neural network for drug pattern recognition", *International Journal on Computer Science and Engineering (IJCSE)*, pp. 1–6, 2011.

[CKLS07] M. Cheriet, N. Kharma, C. Liu, and C. Suen, *Character Recognition Systems: A Guide for Students and Practitioners*, 1st ed. Hoboken, USA: John Wiley & Sons, Inc., 2007.

[CL11] C. Chang and C. Lin, "LIBSVM: A library for support vector machines", *ACM Transactions on Intelligent Systems and Technology*, vol. 2, pp. 1–27, 2011.

[CMXC12] L. Chen, X. Mao, Y. Xue, and L. Cheng, "Speech emotion recognition: Features and classification models", *Digital Signal Processing*, vol. 22, no. 6, pp. 1154–1160, 2012.

[CV95] C. Cortes and V. Vapnik, "Support vector networks", *Machine Learning*, vol. 20, no. 3, pp. 273–297, 1995.

[Das91] B. Dasarathy, "Decision fusion strategies in multisensor environments", *Systems, Man and Cybernetics, IEEE Transactions on*, vol. 21, no. 5, pp. 1140–1154, 1991.

[DRS+12] N. Das, J. Reddy, R. Sarkar, S. Basu, M. Kundu, M. Nasipuri, and D. Basu, "A statistical-topological feature combination for recognition of handwritten numerals", *Applied Soft Computing*, vol. 12, no. 8, pp. 2486–2495, 2012.

[Eas10] R. Easton, *Fourier Methods in Imaging*, 1st ed., M. Kriss, Ed. West Sussex, England: John Wiley & Sons, Ltd, 2010.

[Ert11] W. Ertel, *Introduction to Artificial Intelligence*, I. Mackie, Ed. Heidelberg, Germany: Springer Berlin Heidelberg, 2011.

[FCB06] M. Fauvel, J. Chanussot, and J. Benediktsson, "Decision fusion for the classification of urban remote sensing images", *Geoscience and Remote Sensing, IEEE Transactions on*, vol. 44, no. 10, pp. 2828–2838, 2006.

[FLC13] Z. Feng, M. Liang, and F. Chu, "Recent advances in time-frequency analysis methods for machinery fault diagnosis: A review with application examples", *Mechanical Systems and Signal Processing*, vol. 38, pp. 165–205, 2013.

[GE03] I. Guyon and I. Elisseeff, "An introduction to variable and feature selection", *Journal of Machine Learning Research*, vol. 3, pp. 1157–1182, 2003.

[GJN05] H. Guo, L. Jack, and A. Nandi, "Feature generation using genetic programming with application to fault classification", *Systems, Man, and Cybernetics, Part B: Cybernetics, IEEE Transactions on*, vol. 35, no. 1, pp. 89–99, 2005.

[GMGD13] S. Ghorai, A. Mukherjee, M. Gangadaran, and P. Dutta, "Automatic defect detection on hot-rolled flat steel products", *Instrumentation and Measurement, IEEE Transactions on*, vol. 62, no. 3, pp. 612–621, 2013.

[GT51] H. Gale and A. Tucker, "Linear programming and the theory of games", in *Activity Analysis of Production and Allocation*, Ser. Monograph, T. Koopmans, Ed. New York, USA: John Wiley & Sons, Inc., 1951, pp. 317–329.

[GY11] R. Gao and R. Yan, *Wavelets Theory and Applications for Manufacturing*, S. Elliot and A. Leigh, Eds. Secaucus, USA: Springer New York, 2011.

[Haa10] A. Haar, "Zur Theorie der orthogonalen Funktionensysteme", *Mathematische Annalen*, vol. 69, no. 3, pp. 331–371, 1910.

[Hay98] S. Haykin, *Neural Networks: A Comprehensive Foundation*, 2nd ed., Ser. International Edition. Upper Saddle River, NJ, USA: Prentice Hall PTR, 1998.

[HK05] J. Han and M. Kamber, *Data Mining: Concepts and Techniques*, 2nd ed., A. Stephan, Ed. San Francisco, USA: Morgan Kaufmann Publishers Inc., 2005.

[HL09] D. Hall and J. Llinas, *Handbook of Multisensor Data Fusion: Theory and Practice*, 2nd ed., Ser. The Electrical Engineering and Applied Signal Processing Series, D. L. Hall and J. Llinas, Eds. Boca Raton, USA: CRC Press, 2009.

[HSY12] M. Hariharan, R. Sindhu, and S. Yaacob, "Normal and hypoacoustic infant cry signal classification using time-frequency analysis and general regression neural network", *Computer Methods and Programs in Biomedicine*, vol. 108, no. 2, pp. 559–569, 2012.

[HVG11] D. Hammonda, P. Vandergheynst, and R. Gribonval, "Wavelets on graphs via spectral graph theory", *Applied and Computational Harmonic Analysis*, vol. 30, no. 2, pp. 129–150, 2011.

[HXWC09] C. Hong, C. Xiaojuan, X. Wei, and W. Cong, "Short-time Fourier transform based analysis to characterization of series arc fault", in *Power Electronics and Intelligent Transportation System (PEITS), 2009 2nd International Conference on.* Q. Luo and D. Zeng (Eds.), Shenzhen, China: Institute of Electrical and Electronics Engineers, Inc., December 2009, pp. 185–188.

[HYLW10] C. Huang, D. Yu, H. Guan, G. Li, and Q. Wu, "Feature extraction of frictional vibration based on CWT time-frequency image", in *Intelligent Control and Information Processing (ICICIP), 2010 International Conference on*, Dalian, China, August 2010, pp. 192–196.

[HZBF10] D. Huang, Z. Zhao, V. Bevilacqua, and J. Figueroa, Eds., *Advanced Intelligent Computing Theories and Applications - 6th International Conference on Intelligent Computing, ICIC 2010, Changsha, China, August 18-21, 2010, Proceedings*, Ser. LNCS sublibrary: Theoretical computer science and general issues, vol. 93. Heidelberg, Germany: Springer-Verlag Berlin Heidelberg, 2010.

[IDO10] Z. Iscan, Z. Dokur, and T. Ölmez, "Tumor detection by using zernike moments on segmented magnetic resonance brain images", *Expert Systems with Applications*, vol. 37, no. 3, pp. 2540–2549, 2010.

[IGL+11] I. Illán, J. Górriz, M. López, J. Ramirez, D. Salas-Gonzalez, F. Segovia, R. Chaves, and C. Puntonet, "Computer aided diagnosis of alzheimers disease using component based SVM", *Applied Soft Computing*, vol. 11, no. 2, pp. 2376–2382, 2011.

[Ise06] R. Isermann, *Fault-Diagnosis Systems: An Introduction from Fault Detection to Fault Tolerance*, 1st ed. Berlin, Germany: Springer, 2006.

[JFR07] A. Jain, P. Flynn, and A. Ross, *Handbook of Biometrics*, 1st ed. Springer Publishing Company, Incorporated, 2007.

[Kay07] R. Kay, "Fundamentals of the Dempster-Shafer theory and its applications to system safety and reliability modeling", *Reliability: Theory and Applications*, vol. 2, no. 3-4, pp. 173–185, 2007.

[KC03] D. Koks and S. Challa, "An introduction to Bayesian and Dempster-Shafer data fusion", Defence Science and Tech Org, Edinburgh, SA 5111, AUSTRALIA, Tech. Rep., July 2003.

[KC11] P. Konar and P. Chattopadhyay, "Bearing fault detection of induction motor using wavelet and support vector machines (SVMs)", *Applied Soft Computing*, vol. 11, no. 6, pp. 4203–4211, 2011.

[Kec05] V. Kecman, "Support vector machines - An introduction", in *Support vector machines: Theory and applications*, Ser. Studies in Fuzziness and Soft Computing, L. Wang, Ed. Heidelberg, Germany: Springer Berlin Heidelberg, 2005, vol. 177, pp. 1–47.

[Kul03] N. Kularatna, *Digital and Analogue Instrumentation Testing and Measurement*, Ser. Electrical Measurement series, A. Bailey, O. Jones, and A. Lynch, Eds. London, England: Institution of Engineering and Technology, 2003, vol. 11.

[Kun04] L. Kuncheva, *Combining Pattern Classifiers: Methods and Algorithms*. Hoboken, USA: John Wiley & Sons, Inc., 2004.

[LCZD05] G. Lv, H. Cheng, H. Zhai, and L. Dong, "Fault diagnosis of power transformer based on multi-layer svm classifier", *Electric Power Systems Research*, vol. 75, no. 1, pp. 9–15, 2005.

[LH13] W. Liu and J. Han, "The optimal Mexican hat wavelet filter denoising method based on cross-validation method", *Neurocomputing*, vol. 108, pp. 31–35, 2013.

[LKH09] S. Lee, H. Ko, and H. Hahn, *Multisensor Fusion and Integration for Intelligent Systems: An Edition of the Selected Papers from the IEEE International Conference on Multisensor Fusion and Integration for Inelligent Systems 2008*, 1st ed., Ser. Lecture Notes in Electrical Engineering. Heidelberg, Germany: Springer Berlin Heidelberg, 2009, vol. 35.

[LLK+99] J. Lee, S. Lee, I. Kim, H. Min, and S. Hong, "Comparison between short time fourier and wavelet transform for feature extraction of heart sound", in *Tencon 99. Proceedings of the IEEE Region 10 Conference*, Y. Kim (Ed.), Silla Cheju, Cheju Island, Korea, December 1999, pp. 1547–1550.

[LZY+13] S. Li, W. Zhou, Q. Yuan, S. Geng, and D. Cai, "Feature extraction and recognition of ictal EEG using EMD and SVM", *Computers in Biology and Medicine*, vol. 43, no. 7, pp. 807–816, 2013.

[LZZ11] H. Li, Y. Zhang, and H. Zheng, "Application of hermitian wavelet to crack fault detection in gearbox", *Mechanical Systems and Signal Processing*, vol. 25, no. 4, pp. 1353–1363, 2011.

[Mal08] S. Mallat, *A Wavelet Tour of Signal Processing: The Sparse Way*, 3rd ed. Burlington, USA: Academic Press, 2008.

[MF08] S. Marinai and H. Fujisawa, *Machine Learning in Document Analysis and Recognition*, 1st ed., Ser. Studies in Computational Intelligence. Heidelberg, Germany: Springer-Verlag Berlin Heidelberg, 2008, vol. 90.

[Mit07] H. Mitchell, *Multi-Sensor Data Fusion: An Introduction*, 1st ed. Heidelberg, Germany: Springer-Verlag Berlin Heidelberg, 2007.

[Mit10] T. Mitsa, *Temporal Data Mining*, 1st ed., V. Kumar, Ed. Boca Raton, USA: Chapman & Hall/CRC, 2010.

[MLN10] A. Metallinou, S. Lee, and S. Narayanan, "Decision level combination of multiple modalities for recognition and analysis of emotional expression", in *Acoustics Speech and Signal Processing (ICASSP), 2010 IEEE International Conference on*, Dallas, Texas, USA, March 2010, pp. 2462–2465.

[MMOM96] M. Misiti, Y. Misiti, G. Oppenheim, and J. Michel, *Wavelet Toolbox: For Use with Matlab*. The Math Works, Inc., 1996.

[MR05] O. Maimon and L. Rokach, *Data Mining and Knowledge Discovery Handbook*. Secaucus, USA: Springer-Verlag New York, Inc., 2005.

[MS13] V. Muralidharan and V. Sugumaran, "Feature extraction using wavelets and classification through decision tree algorithm for fault diagnosis of mono-block centrifugal pump", *Measurement*, vol. 46, no. 1, pp. 353–359, 2013.

[MW09] S. Maldonado and R. Weber, "A wrapper method for feature selection using support vector machines", *Information Sciences*, vol. 179, no. 13, pp. 2208–2217, 2009.

[NHYT07] G. Niu, T. Han, B. Yang, and A. Tan, "Multi-agent decision fusion for motor fault diagnosis", *Mechanical Systems and Signal Processing*, vol. 21, no. 3, pp. 1285–1299, 2007.

[Nie09] T. Nieß, "Automatic metal and stone detection on bucket-wheel excavators used in RWE power AGs opencast lignite mines", *World of Mining*, vol. 61, pp. 226–233, 2009.

[NTMB10] H. Nobuhara, D. Trieu, T. Maruyama, and B. Bede, "Max-plus algebra-based wavelet transforms and their FPGA implementation for image coding", *Information Sciences*, vol. 180, no. 17, pp. 3232–3247, 2010.

[NWS+08] G. Niu, A. Widodo, J. Son, B. Yang, D. Hwang, and D. Kang, "Decision level fusion based on wavelet decomposition for induction motor fault diagnosis using transient current signal", *Expert Systems with Applications*, vol. 35, no. 3, pp. 918–928, 2008.

[ODDA10] L. Oukhellou, A. Debiolles, T. Denaux, and P. Aknin, "Fault diagnosis in railway track circuits using Dempster-Shafer classifier fusion", *Engineering Applications of Artificial Intelligence*, vol. 23, no. 1, pp. 117–128, 2010.

[PK05] F. Petrich and U. Köhler, "Stone detection and stone excavation - results and current directions of work with regard to technical stone handling in lusatian opencast mines", *World of Mining*, vol. 57, pp. 412–420, 2005.

[Pol06] R. Polikar, "Ensemble based systems in decision making", *Circuits and Systems Magazine, IEEE*, vol. 6, no. 3, pp. 21–45, 2006.

[RLD+97] D. Rebya, S. Lekb, I. Dimopoulosc, J. Joachima, J. Laugac, and S. Aulagniera, "Artificial neural networks as a classification method in the behavioural sciences", *Behavioural Processes*, vol. 40, no. 1, pp. 35–43, 1997.

[RNJ06] A. Ross, K. Nandakumar, and A. Jain, *Handbook of Multibiometrics*, Ser. International Series on Biometrics. Secaucus, USA: Springer-Verlag New York, Inc., 2006.

[ROG99] M. Rychetsky, S. Ortmann, and M. Glesner, "Support vector approaches for engine knock detection", in *Neural Networks, 1999.*

IJCNN '99. International Joint Conference on, Washington, USA, July 1999, pp. 969–974.

[Rot12] S. Rothe, "Multi-Klassifikatorfusion basierend auf der Zuverlässigkeit individueller Klassifikatoren", Student work, University of Duisburg-Essen, Duisburg, Germany, April 2012.

[RR06] S. Rein and M. Reisslein, "Identifying the classical music composition of an unknown performance with wavelet dispersion vector and neural nets", *Information Sciences*, vol. 176, no. 12, pp. 1629–1655, 2006.

[Sch92] R. Schalkoff, *Pattern Recognition: Statistical, Structural, and Neural Approaches.* New York, USA: Wiley, 1992.

[SES+05] R. Supangat, N. Ertugrul, W. Soong, D. Gray, C. Hansen, and J. Grieger, "Broken rotor bar fault detection in induction motors using starting current analysis", in *Power Electronics and Applications, 2005 European Conference on*, Adelaide SA, Australia, Dresden, Germany 2005, pp. 1–10.

[SJYH11] J. Shin, S. Jung, G. Yoon, and D. Han, "A multi-classifier approach for WiFi-based positioning system", in *Electrical Engineering and Applied Computing*, Ser. Lecture Notes in Electrical Engineering, S.-I. Ao and L. Gelman, Eds. Dordrecht, Netherlands: Springer Dordrecht, 2011, vol. 90, pp. 135–147.

[SL00] C. Suen and L. Lam, "Multiple classifier combination methodologies for different output levels", in *Multiple Classifier Systems*, Ser. Lecture Notes in Computer Science. Heidelberg, Germany: Springer Berlin Heidelberg, 2000, vol. 1857, pp. 52–66.

[SLS12] Y. Shao, R. Lunetta, and J. Y. Stein, "Comparison of support vector machine, neural network, and CART algorithms for the land-cover classification using limited training data points", vol. 70, pp. 78–87, 2012.

[SMABTS07] N. Sánchez-M., A. Alonso-B., and M. Tombilla-S., "Filter methods for feature selection- A comparative study", in *Intelligent Data Engineering and Automated Learning IDEAL 2007*, Ser. Lecture Notes in Computer Science, H. Yin, P. Tino, E. Corchado, W. Byrne, and X. Yao, Eds. Heidelberg, Germany: Springer Berlin Heidelberg, 2007, vol. 4881, pp. 178–187.

[SMK01] S. Singh, N. A. Murshed, and W. G. Kropatsch, Eds., *Advances in Pattern Recognition - ICAPR 2001, Second International Conference*

Rio de Janeiro, Brazil, March 11-14, 2001, Proceedings, Ser. Lecture Notes in Computer Science, vol. 2013. Heidelberg, Germany: Springer-Verlag Berlin Heidelberg, 2001.

[SMS07] J. Saß, F. Matare, and T. Schubert, *Metallsuchgerät und Steinerfassungssystem, Bagger 258 und 261 Tagebau Garzweiler, Bagger 259, 260 und 290 Tagebau Hambach, Bagger 255 Tagebau Inden*, Siemens AG, April 2007.

[SS07] S. Singh and M. Singh, *Progress in Pattern Recognition*, Ser. Advances in Computer Vision and Pattern Recognition. London, England: Springer-Verlag London Limited, 2007.

[Ste00] J. Stein, *Digital Signal Processing: A Computer Science Perspective.* New York, USA: John Wiley & Sons, Inc., 2000.

[SW11] C. Sammut and G. Webb, *Encyclopedia of Machine Learning*, Ser. Springer reference. New York, USA: Springer New York, 2011.

[SXC07] H. Su, W. Xi, and K. Chong, "Vibration signal analysis for electrical fault detection of induction machine using neural networks", in *Information Technology Convergence, 2007. ISITC 2007. International Symposium on*, Jeonju, Korea, November 2007, pp. 188–192.

[Tan00] Y. Tang, *Wavelet Theory and Its Application to Pattern Recognition*, Ser. Series in Machine Perception and Artificial Intelligence. Farrer Road, Singapore: World Scientific Publishing Co. Pte. Ltd., 2000, vol. 36.

[TK08] S. Theodoridis and K. Koutroumbas, *Pattern Recognition*, 4th ed. London, England: Academic Press, 2008.

[TLS10] B. Tang, W. Liu, and T. Song, "Wind turbine fault diagnosis based on Morlet wavelet transformation and Wigner-Ville distribution", *Renewable Energy*, vol. 35, no. 12, pp. 2862–2866, 2010.

[Vap95] V. Vapnik, *The Nature of Statistical Learning Theory*, 2nd ed., M. Jordan and S. Lauritzen, Eds. New York, USA: Springer-Verlag New York, Inc., 1995.

[Vib13] Vibration Analysis Guide, , "Dictionary: Hamming window", 2013, last visited: September 27th 2013. [Online]. Available: http://www.vibrationanalysisguide.org/dictionary/gloss_hammingwindow1.htm

[VK95] M. Vetterli and J. Kovačevic, *Wavelets and Subband Coding.* Upper Saddle River, NJ, USA: Prentice-Hall, Inc., 1995.

[VLR+06] G. Vachtsevanos, F. Lewis, M. Roemer, A. Hess, and B. Wu, *Intelligent Fault Diagnosis and Prognosis for Engineering Systems.* New York, USA: Wiley, 2006.

[Win11] J. Winkler, “Algorithmenentwicklung zur Steuerung eines Förderprozesses”, Diploma thesis, University of Duisburg-Essen, Duisburg, Germany, March 2011.

[Wu12] S. Wu, *Data Fusion in Information Retrieval*, Ser. Adaptation, Learning, and Optimization. Heidelberg, Germany: Springer-Verlag Berlin Heidelberg, 2012, vol. 13.

[WWWL12] M. Weyrich, Y. Wang, J. Winkel, and M. Laurowski, “High speed vision based automatic inspection and path planning for processing conveyed objects”, *Procedia CIRP*, vol. 3, pp. 442–447, 2012.

[XKH11] M. Xia, F. Kong, and F. Hu, “An approach for bearing fault diagnosis based on PCA and multiple classifier fusion”, in *Information Technology and Artificial Intelligence Conference (ITAIC), 2011 6th IEEE Joint International*, vol. 1, Chongqing, China, August 2011, pp. 321–325.

[XKS92] L. Xu, A. Krzyzak, and C. Suen, “Methods of combining multiple classifiers and their applications to handwriting recognition”, *Systems, Man and Cybernetics, IEEE Transactions on*, vol. 22, no. 3, pp. 418–435, 1992.

[YGD09] S. Yella, S. Ghiamati, and M. Dougherty, “Condition monitoring of wooden railway sleepers using time-frequency techniques and pattern classification”, in *Systems, Man and Cybernetics, 2009. SMC 2009. IEEE International Conference on*, San Antonio, Texas, USA, October 2009, pp. 4164–4169.

[YKF94] R. Yager, J. Kacprzyk, and M. Fedrizzi, *Advances in the Dempster-Shafer Theory of Evidence*, Ser. Wiley Professional Computing. New York, USA: John Wiley & Sons, Inc., 1994.

[YS09] W. Yu and E. Sanchez, *Advances in Computational Intelligence.* Springer-Verlag Berlin Heidelberg, 2009, vol. 61.

[YSL+13] Q. Yin, L. Shen, M. Lu, X. Wang, and Z. Liu, “Selection of optimal window length using STFT for quantitative SNR analysis of LFM signal”, *Systems Engineering and Electronics, Journal of*, vol. 24, no. 1, pp. 26–35, 2013.

[YX10] D. Yuyuan and W. Xu, “Research on fault detection of high voltage inverter based on STFT”, in *Control and Decision Conference (CCDC), 2010 Chinese*, Xuzhou, China, May 2010, pp. 2229–2233.

[Zan12] E. Zanaty, “Support vector machines (SVMs) versus multilayer perception (MLP) in data classification”, *Egyptian Informatics Journal*, vol. 13, no. 3, pp. 177–183, 2012.

[ZX09] N. Zheng and J. Xue, *Statistical Learning and Pattern Analysis for Image and Video Processing*, Ser. Advances in Computer Vision and Pattern Recognition. London, England: Springer-Verlag London Limited, 2009.

The thesis is based on the results and development steps presented in the following previous publications :

[ASS11] L. Al-Shrouf and D. Söffker, "Multi-classifier fusion method based on the reliability of indivdual classifiers statements", in *8th Int. Workshop on Structural Health Monitoring 2011*, F. Chang (Ed.), Stanford, USA, September 2011, pp. 127–134.

[ASSS13] L. Al-Shrouf, M. Saadawia, and D. Söffker, "Improved process monitoring and supervision based on a reliable multi-stage feature-based pattern recognition technique", *Information Sciences*, vol. 259, pp. 282–294, 2013.

[ASSSS10] L. Al-Shrouf, M. Saadawia, N. Szczepanski, and D. Söffker, "Multisensorfusionsbasierte Prozessüberwachung", in *Diagnose und Anlagenüberwachung AKIDA*, Ser. Berichtsband 8. Aachener Kolloquium für Instandhaltung, Aachen, Germany, November 2010, pp. 413–422.

[ASSSS11] ——, "Adaptive classification based on multisensoric decision fusion", in *8th Int. Workshop on Structural Health Monitoring 2011*, F. Chang (Ed.), Stanford, USA, September 2011, pp. 127–134.

[ASSSS12] ——, "Event detection using multisensor fusion and filtering techniques based on CWT and SVM", in *6th European Workshop on Structural Health Monitoring 2012*, C. Boller (Ed.), Dresden, Germany, July 2012, pp. 206–213.

In the context of the research projects at the Chair of Dynamics and Control the following student theses have been supervised by Lou'i Al-Shrouf and Univ.-Prof. Dr.-Ing. Dirk Söffker. Development steps and results of the research projects and the student theses are integrated to each other and hence are also part of this thesis.

[Ras11] S. Raspopov, "Künstliche neuronale Netze in Python mit Schwerpunkt auf Modellbildung und Mustererkennung", Bachelor thesis, University of Duisburg-Essen, Duisburg, Germany, November 2011.

[Rot12] S. Rothe, "Multi-Klassifikatorfusion basierend auf der Zuverlässigkeit individueller Klassifikatoren", Student work, University of Duisburg-Essen, Duisburg, Germany, April 2012.

[Wda11] L. Wdaah, "Development and implementation of a monitoring system based on image processing", Master thesis, University of Duisburg-Essen, Duisburg, Germany, November 2011.

[Win11] J. Winkler, "Algorithmenentwicklung zur Steuerung eines Förderprozesses", Diploma thesis, University of Duisburg-Essen, Duisburg, Germany, March 2011.

[Win12] ——, "Optimierung technischer Systeme mit evolutionären Algorithmen in Python", Diploma thesis, University of Duisburg-Essen, Duisburg, Germany, March 2012.